



Cite this: *Energy Environ. Sci.*, 2014, 7, 3135

Received 27th April 2014
Accepted 4th August 2014

DOI: 10.1039/c4ee01303d

www.rsc.org/ees

Anion-exchange membranes in electrochemical energy systems†

John R. Varcoe,^{*a} Plamen Atanassov,^b Dario R. Dekel,^c Andrew M. Herring,^d Michael A. Hickner,^e Paul A. Kohl,^f Anthony R. Kucernak,^g William E. Mustain,^h Kitty Nijmeijer,ⁱ Keith Scott,^j Tongwen Xu^k and Lin Zhuang^l

This article provides an up-to-date perspective on the use of anion-exchange membranes in fuel cells, electrolyzers, redox flow batteries, reverse electrodialysis cells, and bioelectrochemical systems (e.g. microbial fuel cells). The aim is to highlight key concepts, misconceptions, the current state-of-the-art, technological and scientific limitations, and the future challenges (research priorities) related to the use of anion-exchange membranes in these energy technologies. All the references that the authors deemed relevant, and were available on the web by the manuscript submission date (30th April 2014), are included.

Broader context

Many electrochemical devices utilise ion-exchange membranes. Many systems such as fuel cells, electrolyzers and redox flow batteries have traditionally used proton-/cation-exchange membranes (that conduct positive charged ions such as H^+ or Na^+). Prior wisdom has led to the general perception that anion-exchange membranes (that conduct negatively charged ions) have too low conductivities and chemical stabilities (especially in high pH systems) for application in such technologies. However, over the last decade or so, developments have highlighted that these are not always significant problems and that anion-exchange membranes can have OH^- conductivities that are approaching the levels of H^+ conductivity observed in low pH proton-exchange membrane equivalents. This article reviews the key literature and thinking related to the use of anion-exchange membranes in a wide range of electrochemical and bioelectrochemical systems that utilise the full range of low to high pH environments.

Preamble

There is an increasing worldwide interest in the use of anion-exchange membranes (including in the alkaline anion forms), in electrochemical energy conversion and storage systems. This perspective stems from the “Anion-exchange membranes for energy generation technologies” workshop (University of Surrey, Guildford, UK, July 2013), involving leading researchers in the field,¹ that focussed on the use of AEMs in alkaline polymer electrolyte fuel cells (APEFCs),² alkaline polymer electrolyte electrolyzers (APEE),³ redox flow batteries (RFB),⁴ reverse electrodialysis (RED) cells,⁵ and bioelectrochemical systems including microbial fuel cells (MFCs)⁶ and enzymatic fuel cells.⁷

Conventions used in this perspective article

In this article the following terminology is defined:

- AEM is used to designate anion-exchange membranes in non-alkaline anion forms (e.g. containing Cl^- anions);
- AAEM used to designate anion-exchange membranes containing alkaline anions (i.e. OH^- , CO_3^{2-} and HCO_3^-);
- HEM is used to designate hydroxide-exchange membranes and should only be used where the AAEMs are totally separated from air (CO_2) and are exclusively in the OH^- form (with no

^aDepartment of Chemistry, University of Surrey, Guildford, GU2 7XH, UK. E-mail: j.varcoe@surrey.ac.uk; Tel: +44 (0)1483 686838

^bDepartment of Chemical and Nuclear Engineering, University of New Mexico, Albuquerque, NM, 87131-0001, USA

^cCellEra, Caesarea Business and Industrial Park, North Park, Bldg. 28, POBox 3173, Caesarea, 30889, Israel

^dDepartment of Chemical and Biological Engineering, Colorado School of Mines, Golden, CO, 80401, USA

^eDepartment of Materials Science and Engineering, The Pennsylvania State University, University Park, PA, 16802, USA

^fSchool of Chemical and Biomolecular Engineering, Georgia Institute of Technology, Atlanta, GA 30332-0100, USA

^gDepartment of Chemistry, Imperial College London, South Kensington, London, SW7 2AZ, UK

^hDepartment of Chemical & Biomolecular Engineering, University of Connecticut, Storrs, CT, 06269-3222, USA

ⁱMembrane Science and Technology, University of Twente, MESA+ Institute for Nanotechnology, P.O. Box 217, 7500 AE, Enschede, The Netherlands

^jSchool of Chemical Engineering and Advanced Materials, Faculty of Science, Agriculture and Engineering, Newcastle University, Newcastle upon Tyne, NE1 7RU, UK

^kSchool of Chemistry and Material Science, USTC-Yongji Membrane Center, University of Science and Technology of China, Hefei, 230026 P. R. China

^lDepartment of Chemistry, Wuhan University, Wuhan, 430072, P. R. China

† Electronic supplementary information (ESI) available: This gives the biographies for all authors of this perspective. See DOI: [10.1039/c4ee01303d](https://doi.org/10.1039/c4ee01303d)



traces of other alkaline anions such as CO_3^{2-}); this is not the case in most of the technologies discussed in the article (a possible exception being APEEs);

- AEI is used to designate an anion-exchange ionomer which are anion-exchange polymer electrolytes in either solution or dispersion form: *i.e.* anion-exchange analogues to the proton-exchange ionomers (*e.g.* Nafion® D-52x series) used in proton-exchange membrane fuel cells (PEMFCs). AEIs are used as polymer binders to introduce anion conductivity in the electrodes (catalyst layers).

- CEM is used to designate cation-exchange membranes in non-acidic form (*e.g.* containing Na^+ cations);

- PEM is used to designate proton-exchange membranes (*i.e.* CEMs specifically in the acidic H^+ cation form);

- IEM is used to designate a generic ion-exchange membrane (can be either CEM or AEM).

Note that in this review, all electrode potentials (E) are given as reduction potentials even if a reaction is written as an oxidation.

AEMs and AEIs for electrochemical systems

Summary of AEM chemistries used in such systems

AEMs and AEIs are polymer electrolytes that conduct anions, such as OH^- and Cl^- , as they contain positively charged [cationic] groups (typically) bound covalently to a polymer backbone. These cationic functional groups can be bound



Professor John Varcoe (Department of Chemistry, University of Surrey, UK) obtained both his 1st class BSc Chemistry degree (1995) and his Materials Chemistry PhD (1999) at the University of Exeter (UK). He was a postdoctoral researcher at the University of Surrey (1999–2006) before appointment as Lecturer (2006), Reader (2011) and Professor (2013). He is recipient of an UK EPSRC Leadership Fellowship (2010). His research interests are focused on polymer electrolytes for clean energy and water systems: more specifically, the development of chemically stable, conductive anion-exchange polymer electrolytes. He is also involved in the University's efforts on biological fuel cells.

er



Professor Michael Hickner (Associate Professor, Department of Materials Science and Engineering, Pennsylvania State University, USA) focuses his research on the relationships between chemical composition and materials performance in functional polymers to address needs in new energy and water purification applications. His research group has ongoing projects in polymer synthesis, fuel cells, batteries, water treatment membranes, and organic electronic materials. His work has been recognized by a Presidential Early Career Award for Scientists and Engineers from President Obama (2009). He has co-authored seven US and international patents and over 100 peer-reviewed publications with >5400 citations.



Dr Dario Dekel (Co-Founder and VP for R&D and Engineering, CellEra, Israel) received his MBA, MSc and PhD in Chemical Engineering from the Technion, Israel Institute of Technology. He was the chief scientist and top manager at Rafael Advanced Defense Systems, Israel, where he led the world's second largest Thermal Battery Plant. He left Rafael in 2007 to co-found CellEra, leading today a selected group of 14 scientists and engineers, developing the novel Alkaline Membrane Fuel Cell technology. He currently holds \$3M government research grants from Israel, USA and Europe. Dr Dekel holds 14 battery and fuel cell patents.



Professor Paul Kohl (Hercules Inc./Thomas L. Gossage Chair, Regents' Professor, Georgia Institute of Technology, USA) received a Chemistry PhD (University of Texas, 1978). He was then involved in new chemical processes for silicon and compound semiconductor devices at AT&T Bell Laboratories (1978–89). In 1989, he joined Georgia Tech's School of Chemical and Biomolecular Engineering. His research includes ionic conducting polymers, high energy density batteries, and new materials and processes for advanced interconnects for integrated circuits. He has 250 papers, is past Editor of JES and ESSL, past Director MARCO Interconnect Focus Center, and President of the Electrochemical Society (2014–15).



either *via* extended side chains (alkyl or aromatic types of varying lengths) or directly onto the backbone (often *via* CH₂ bridges); they can even be an integral part of the backbone.

The most common, technologically relevant backbones are: poly(arylene ethers) of various chemistries⁸ such as polysulfones [including cardo, phthalazinone, fluorenyl, and organic-inorganic hybrid types],⁹ poly(ether ketones),^{10,11} poly(ether imides),¹² poly(ether oxadiazoles),¹³ and poly(phenylene oxides) [PPO];¹⁴ polyphenylenes,¹⁵ perfluorinated types,^{16,17} polybenzimidazole (PBI) types including where the cationic groups are an intrinsic part of the polymer backbones,¹⁸ poly(epichlorohydrins) [PECH],¹⁹ unsaturated polypropylene²⁰ and polyethylene²¹ types [including those formed using ring opening metathesis polymerisation (ROMP)],²² those based on polystyrene and poly(vinylbenzyl chloride),²³ polyphosphazenes,²⁴ radiation-grafted types,²⁵ those synthesised using plasma techniques,²⁶ pore-filled types,²⁷ electrospun fibre types,²⁸ PTFE-reinforced types,^{26g,29} and those based on poly(vinyl alcohol) [PVA].^{19a,30}

The cationic head-group chemistries that have been studied (Scheme 1), most of which involve N-based groups, include:

(a) Quaternary ammoniums (QA) such as benzyl-trialkylammoniums [*benzyltrimethylammonium will be treated as the benchmark chemistry throughout this report*],^{2,31} alkyl-bound (benzene-ring-free) QAs,^{21a,b} and QAs based on bicyclic ammonium systems synthesised using 1,4-diazabicyclo[2.2.2]octane (DABCO) and 1-azabicyclo[2.2.2]octane (quinuclidine, ABCO) (to yield 4-aza-1-azoniabicyclo[2.2.2]octane,^{14b,25f,h,27g,32} and 1-azoniabicyclo[2.2.2]octane {quinuclidinium}^{19c,33} functional groups, respectively);

(b) Heterocyclic systems including imidazolium,^{10a,13,23a,25g,31,34} benzimidazolium,³⁵ PBI systems where the positive charges are on the backbone (with or without positive charges on the side-chains),^{18b,d,f,h,36} and pyridinium types (can only be used in electrochemical systems that do not involve high pH environments),^{26h,i,30i,37}

(c) Guanidinium systems;^{16c,38}

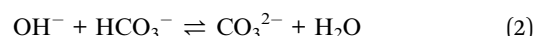
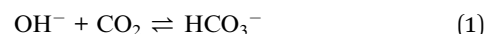
(d) P-based systems types including stabilised phosphoniums [*e.g.* tris(2,4,6-trimethoxyphenyl)phosphonium]^{11,14d,32a,39} and P-N systems such as phosphatranium^{16d} and tetrakis(dialkylamino)phosphonium⁴⁰ systems;

(e) Sulfonium types;⁴¹

(f) Metal-based systems where an attraction is the ability to have multiple positive charges per cationic group.⁴²

General comments on the characterisation of AEMs

Given that OH⁻ forms of AAEMs quickly convert to the less conductive CO₃²⁻ and even less conductive HCO₃⁻ forms when exposed to air (containing CO₂ – see eqn (1) and (2)), even for very short periods of time,^{25d,43} it is essential that CO₂ is totally excluded from experiments that are investigating the properties of AAEMs in the OH⁻ forms. This includes the determination of water uptakes, dimensional swelling on hydration, long-term stabilities, and conductivities [see specific comments in the below sections].



Additionally, when converting an AEM or AEI into a single anion form, it is vital to ensure complete ion-exchange. An IEM cannot be fully exchanged to the desired single ion form after only 1× immersion in a solution containing the target ion, even if a concentrated solution containing excess target ion is used: the use of only 1× immersion will leave a small amount of the original ion(s) in the material (ion-exchange involves partition equilibria). IEMs must be ion-exchange by immersion in multiple (at least 3) consecutive fresh replacements of the solution containing an excess of the desired ion. Traces of the original (or other contaminant) ions can have implications regarding the properties being measured.⁴⁴

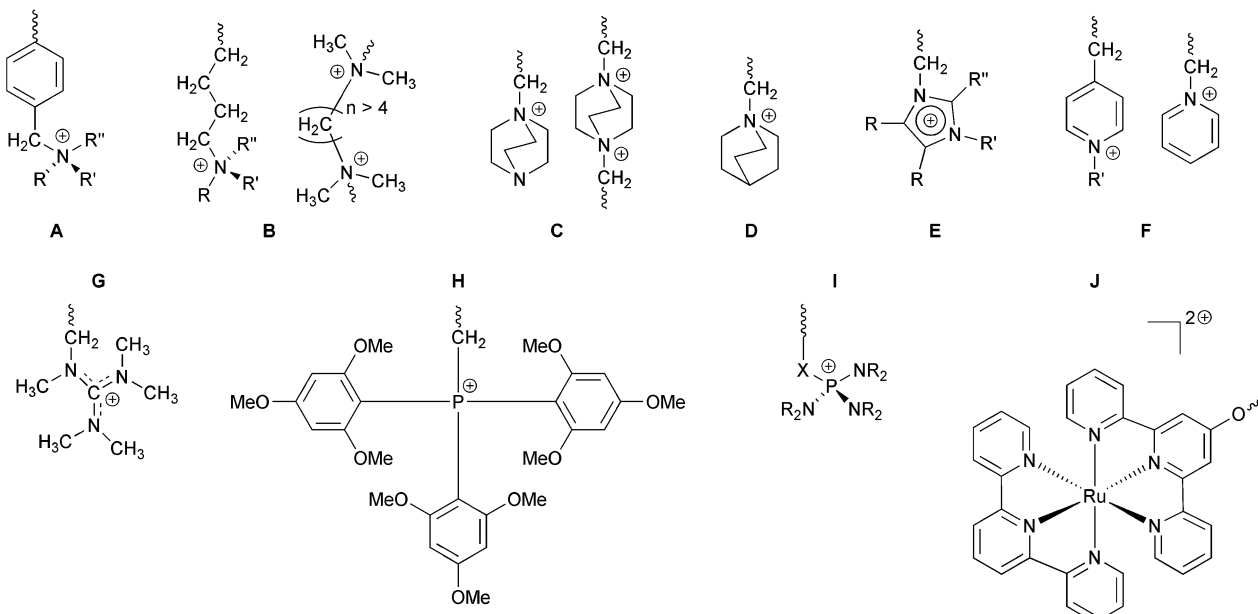


Professor Tongwen Xu (University of Science and Technology of China) received his BSc (1989) and MSc (1992) from Hefei University of Technology and his Chemical Engineering PhD (1995) from Tianjin University. He then studied polymer science at Nankai University (1997). He was visiting scientist at University of Tokyo (2000), Tokyo Institute of Technology (2001) and Gwangju Institute of Science and Technology (Brain Pool Program Korea award recipient). He has received a "New Century Excellent Talent" (2004) and an "Outstanding Youth Foundation" (2010) Chinese awards. His research interests cover membranes and related processes, particularly ion exchange membranes and controlled release.



Professor Lin Zhuang (Department of Chemistry, Wuhan University, China) earned his electrochemistry PhD (1998) at Wuhan University. He was then promoted to lecturer, associate professor (2001) and full professor (2003). He was a visiting scientist at Cornell (2004–05) and is an adjunct professor at Xiamen University. He is an editorial board member of *Science China: Chemistry*, *Acta Chimica Sinica*, and *Journal of Electrochemistry*. He was recipient of a National Science Fund for Distinguished Young Scholars. He was vice-chair of the physical electrochemical division of the International Society of Electrochemistry (2011–12) and China section chair of the Electrochemical Society (2010–11).





Scheme 1 Commonly encountered AAEM/AEI cationic head-groups (those containing N–H and P–H bonds are omitted): A = benzyltrimethylammonium (the benchmark benzyltrimethylammonium is where R, R', and R'' are methyl groups); B = alkyl-side-chain (benzene-free) quaternary ammonium (QA) and crosslinking diammonium groups (where the link chain is $>C4$ in length [preferably $>C6$ in length]); C = DABCO-based QA groups (more stable when only 1 N atom is quaternised [crosslinked systems where both Ns are quaternised are also of interest but are less stable in alkali]); D = quinuclidinium-based QA groups; E = imidazolium groups (where R = Me or H and R', R'' = alkyl or aryl groups [not H]); F = pyridinium groups; G = pentamethylguanidinium groups; H = alkali stabilised quaternary phosphonium groups; I = P–N systems (where X = $-SO_2-$ or $-NR'-$ groups and where R = alkyl, aryl, or unsaturated cyclic systems); and J is an exemplar metal containing cationic group.

One of the main properties that must be reported for each AEM/AEI produced is the ion-exchange capacity (IEC), which is the number of functional groups (molar equivalents, eq.) per unit mass of polymer. *In the first instance, it is highly recommended that the IEC of the Cl^- form of the AEM being studied is measured (the form typically produced on initial synthesis).*^{19e,31,45} This is so that the AEMs have not been exposed to either acids or bases that may cause high and low pH-derived degradations (even if such degradations are only slight) and to avoid significant CO_2 -derived interferences: both acid and bases are required for the use of the classical back-titration method of determining IECs of AAEMs.⁴⁶ Additionally when using Cl^- based titrations, methods are available to measure the total exchange capacities, quaternary-only-IEC and non-quaternary (e.g. tertiary) exchange capacities.⁴⁷ These techniques will be useful for AAEM degradation studies where QA groups may degrade into polymer-bound non-QA groups (such as tertiary amine groups). However, there can be discrepancies between IECs derived from titration experiments and other techniques such as those that use ion-selective electrodes or spectrophotometers.⁴⁸ NMR data can also be used to determine IECs with soluble AEMs and AEIs.^{49,50}

Perceived problems with the use of AAEMs

The two main perceived disadvantages of AAEMs are low stabilities in OH^- form (especially when the AAEMs are not fully hydrated)⁵¹ and low OH^- conductivities (compared to the H^+ conductivity of PEMs, especially [again] when the AAEMs are

not fully hydrated).^{19d,52,53} The former is going to be challenging problem to solve if the electrochemical system in question requires the conduction of OH^- anions (*i.e.* a strong nucleophile) as the polymer electrolytes contain positively charged cationic groups (*i.e.* good leaving groups!). Conductivity issues are not insurmountable with improved material and cell designs. While conductivities of *ca.* 10^{-1} S cm $^{-1}$ are needed for high current density cell outputs, operating electrochemical devices with membranes that have intrinsic conductivities of the order of 5×10^{-2} S cm $^{-1}$ is not out of the question. Conductivities of 10^{-2} S cm $^{-1}$ may, however, be too low for many applications.

The alkali stabilities of AAEMs. A primary concern with the use of AAEMs/AEI in electrochemical devices such as APEFCs and APEEs is their stabilities (especially of the cationic head-groups) in strongly alkaline environments (*e.g.* in the presence of nucleophilic OH^- ions). This alkali stability issue has dominated discussions such that radical-derived degradations (*e.g.* from the presence of highly destructive species such as OH radicals that originate from peroxy species generated from the $n = 2e^-$ oxygen reduction reaction [ORR]) have only been considered in a small number of reports.^{23a,54} This is a major long-term degradation issue with PEMs in PEMFCs.⁵⁵ The perception has been that AAEM/AEI degradation *via* attack by OH^- anions is so severe over short timeframes that radical-derived degradation cannot be studied until alkali stable AAEMs/AEIs have been developed. This assumption needs to be challenged especially as AAEMs/AEIs tend to be hydrocarbon or aromatic based, which have poor peroxide and oxidation stabilities.

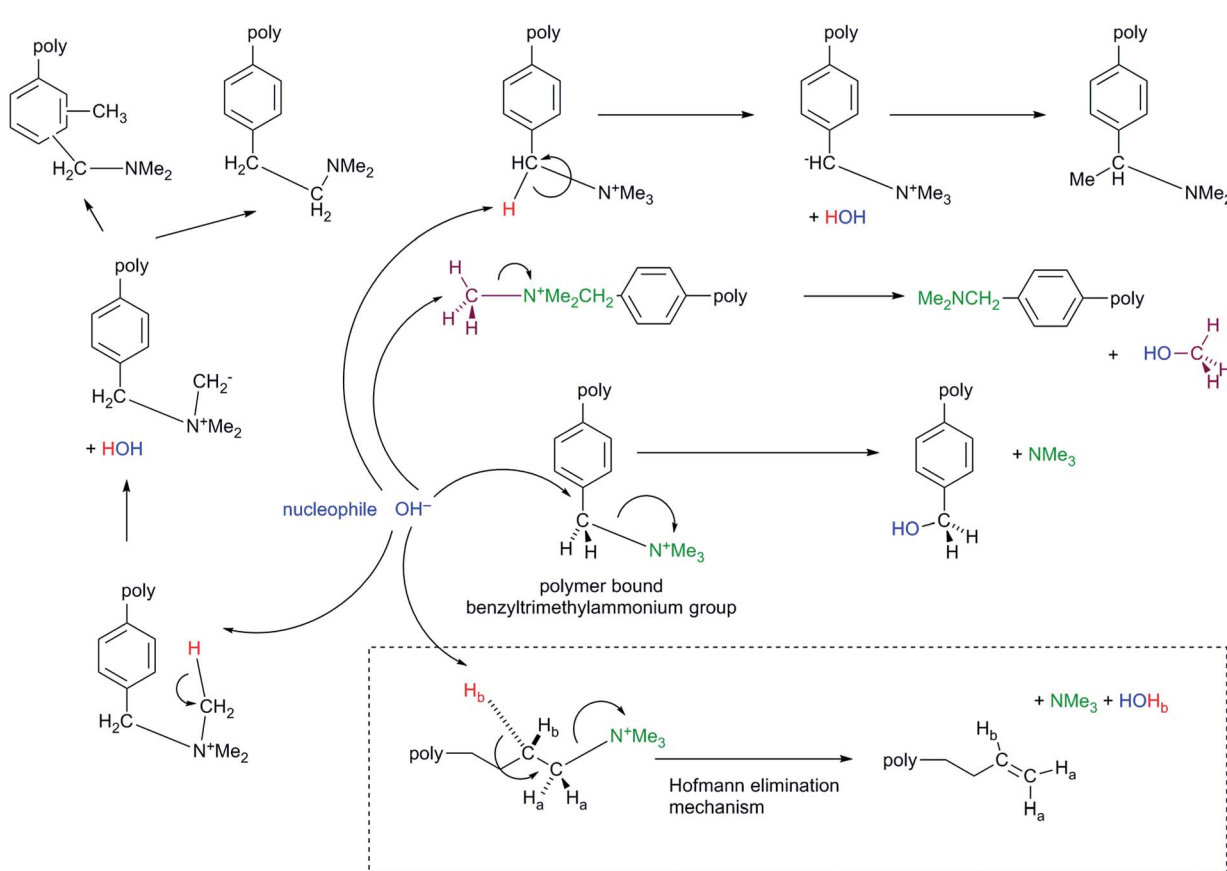


It is apparent in Scheme 2 that even simple benzyltrimethylammonium cationic functional groups (the most commonly encountered, Scheme 1A) can undergo a number of degradation processes in the presence of OH^- nucleophiles. The main degradation mechanism for benzyltrimethylammonium groups is *via* direct nucleophilic substitution (displacement). The formation of intermediate ylides ($>\text{C}^-\text{N}^+\text{R}_3$) have been detected *via* deuterium scrambling experiments and these can potentially lead to Sommelet-Hauser and Stevens rearrangements;^{51c} however, such ylide-derived mechanisms rarely end in a degradation event.^{51a} Hofmann elimination reactions cannot occur with benzyltrimethylammonium as there are no β -Hs present; this is not the case with benzyltriethylammonium groups,^{51b,56} which contain β -Hs [even though the $\text{R}-\text{N}^+(\text{CH}_2\text{CH}_3)_3$ OH^- groups may be more dissociated than $\text{R}-\text{N}^+(\text{CH}_3)_3$ OH^- groups]. As an aside, neopentyltrimethylammonium groups (on model small compounds, *i.e.* not polymer bound) contain a long alkyl chain but with no β -Hs: Hofmann elimination cannot occur, but the degradation of this cationic group appears to be even more complex with unidentified reaction products detected.^{51b}

Historically, due to concerns about facile Hofmann elimination reactions, QAs bound to longer alkyl chains were considered to be less stable than those bound to aromatic

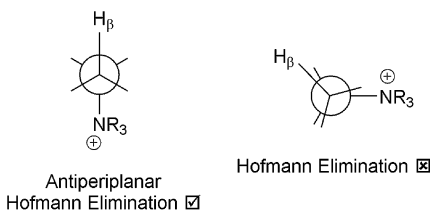
groups *via* $-\text{CH}_2-$ bridges.⁵⁶ However, more recent evidence suggests that this may not be the case and that QA groups that are tethered (or crosslinked) with N-bound alkyl chains that are >4 carbon atoms long (C4, see Scheme 1B) can have surprisingly good stabilities in alkali.^{13a,47a,57,58} A hypothesis is that the high electron density around the β -Hs in longer alkyl chains can inhibit Hofmann elimination reactions^{47a} and that steric shielding in the β -positions may also play a role in the surprising stability imparted by longer alkyl chains.^{57g}

The search for alkali stable AAEMs/AEIs is the primary driver for the study of alternative cationic head-group chemistries. An alternative QA system is where DABCO is used as the quaternisation agent (Scheme 1C). This system contains β -Hs but due to the rigid cage structure, the β -Hs and the N atoms do not form the anti-periplanar confirmation required for facile Hofmann Elimination to occur (Scheme 3).^{19e,59,60} It is suspected that AAEMs/AEIs containing 4-aza-1-azoniabicyclo[2.2.2]octane groups, where only 1 N of the DABCO reactant is quaternised, are more stable than $\text{R}-\text{N}^+\text{Me}_3$ analogues.^{32e,60} However, it is not easy to produce AAEMs/AEIs where only 1 \times N of the DABCO reagent reacts (although low temperatures may be helpful in this respect).⁵⁹ The tendency is for DABCO to react *via* both N atoms forming crosslinks, which will produce materials with low alkali stabilities.^{32e} This has led to the recent interest



Scheme 2 Degradation pathways for the reaction of OH^- nucleophiles with benzyltrimethylammonium cationic (anion-exchange) groups.⁵¹ The inset [dashed box] shows the additional Hofmann Elimination degradation mechanism that can occur with alkyl-bound QA groups (that possess β -H atoms).





Scheme 3 The antiperiplanar confirmation required for facile Hofmann elimination reactions.

in quinuclidinium-(1-azoniabicyclo[2.2.2]octane) systems (Scheme 1D), which is a DABCO analogue containing only 1 N atom.^{19c,33} However, quinuclidine is much harder to synthesise than DABCO (harder to “close the cage”) and this is reflected in the price: quinuclidine = US\$775 for 10 g *vs.* DABCO = US\$34 for 25 g (laboratory scale prices, not bulk commodity prices).⁶¹ Also, quinuclidine is highly toxic (*e.g.* Hazard statement H310 – Fatal in contact with skin).⁶² This must be taken into account if quinuclidinium-containing AAEMs/AEIs degrade and release any traces of quinuclidine.

Systems involving >1 N atoms and “resonance stabilisation” have been evaluated with the desire of developing alkali stable and conductive AAEMs/AEIs. Firstly, non-heterocyclic pentamethylguanidinium systems (made using 1,1,2,3,3-pentamethylguanidine) have been reported,³⁸ including perfluorinated AAEM examples.^{16c} However, more recent studies suggest that this system may not be as alkali stable as originally reported.^{38e} Polymer bound benzyltetramethylguanidinium (*i.e.* addition of a benzyl substituent) is reported to be more alkali stable than polymer bound pentamethylguanidinium groups.⁶³ However, other reports indicate that guanidiniums bound to the polymer backbone *via* phenyl groups may be more stable than those bound *via* benzyl groups and perfluorosulfone groups.^{16c,64} These prior reports indicate that new degradation pathways (*cf.* QA benchmarks) are available with this cationic head-group.

The other multiple N atom system that has been extensively reported is the heterocyclic imidazolium system (Scheme 4). This includes where imidazolium groups have been used to introduce covalent crosslinking into the system.⁶⁵ Imidazolium systems where R₂, R₄, and R₅ are all H atoms are unstable to

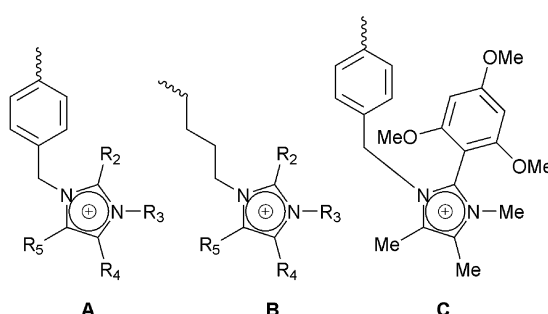
alkali.^{31,34c,34f,66} Polymer bound imidazolium groups with R₂ = H can degrade *via* imidazolium ring-opening in the presence of OH[–] ions.^{34f,67} Replacement of the protons at the C2 position (*e.g.* R₂ = Me or butyl group) increases the stability of the imidazolium group.^{34c,d,68} Different substituents at the N3 position (R₃ = butyl, isopropyl, amongst others) can also affect the alkali stability of the imidazolium group:^{68a,69} systems where R₃ = isopropyl or R₂ = R₃ = butyl groups are reported to be more stable options.

Yan *et al.* has recently reported an alkali stable PPO-bound imidazolium group [made using 1,4,5-trimethyl-2-(2,4,6-trimethoxyphenyl)imidazole] that contains no C–H bonds on the imidazolium ring and no C2 methyl group (Scheme 4C).^{34b} This sterically bulky functional group was at least as stable as QA benchmarks. This claimed alkali stability is also backed up by DFT measurements in another recent study by Long and Pivovar, which suggests that similar C2-substituted imidazoliums will have superior alkali stabilities.⁷⁰ Alkyl-2,3-dimethylimidazolium groups (R₂ and R₃ = Me) that are bound *via* long alkyl chains^{34k} may also be more alkali stable than benzyl-bound analogues: the latter undergo facile removal of the imidazolium rings *via* nucleophilic displacement reactions^{34c} (as well as degradation *via* imidazolium ring-opening).

However, contrary to the above, a study of small molecule imidazolium species by Price *et al.* suggests that adding steric hindrance at the C2 position is the least effective strategy;⁷¹ this study reports that 1,2,3-trimethylimidazolium cations appear to be particularly stable and this matches our experience in that the 1,2,3,4,5-pentamethylimidazolium cation appears to be reasonably stable in alkali. Furthermore, it has been reported that as you add more bulky cations, such as the 1,4,5-trimethyl-2-(2,4,6-trimethoxyphenyl)imidazole highlighted above, the anion transport switches from Arrhenius-type to Vogel–Tammann–Fulcher-type behaviour (*i.e.* the anions become less dissociated).⁷² Other studies that have looked into the alkali stability of various imidazolium-based ionic liquids, however, report that all 1,3-dialkylimidazolium protons (R₂, R₄, and R₅ = H) can undergo deuterium exchange (*i.e.* represent alkali stability weak spots) and that even C2 methyl groups (R₂ = –CH₃) can undergo deprotonation in base.⁷³ Further fundamental research into these and related systems is clearly still warranted.

The stabilised PBI system poly[2,2'-(*m*-mesitylene)-5,5'-bis(*N,N'*-dimethylbenzimidazolium)], where the cationic group is part of the polymer backbone, has recently been reported with promising alkali stabilities.^{18d} This research has led to the development of other PBI-type ionenes that contain sterically protected C2 groups and are soluble in aqueous alcohols but insoluble in pure water;⁷⁴ they are reported to have “unprecedented” hydroxide stabilities.

Regarding P-based systems, phosphonium AAEMs/AEIs are also common in the recent literature. Yan *et al.* first reported an alkali-stabilised polymer-bound phosphonium system made using tris(2,4,6-trimethoxyphenyl)phosphine as the quaternising agent (Scheme 1H) where the additional methoxy groups are electron donating and provide additional steric hindrance.^{11,14d,32a,39,66} This stabilisation is important as simple



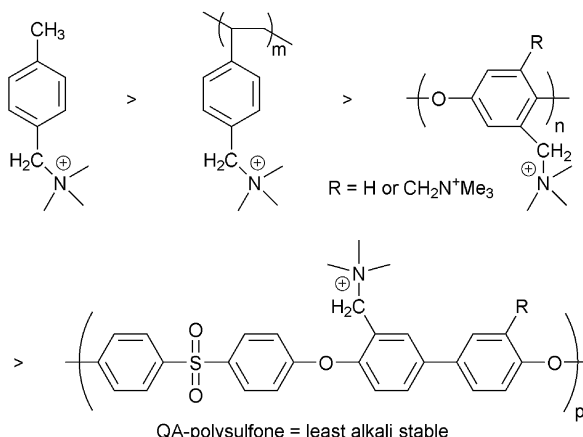
Scheme 4 Imidazolium-based cationic head-group chemistry: A = benzyl-bound imidazolium groups; B = alkyl-bound imidazolium groups; and C the alkali stabilised imidazolium group reported by Yan *et al.*^{34b}



trialkylphosphonium and triphenylphosphonium analogues (e.g. small molecule benzyltriphenylphosphonium cations) will degrade in aqueous OH^- solutions at room temperature in only a few hours; the thermodynamic driving force being the formation of phosphine oxide *via* the Cahours–Hofmann reaction (especially in the presence of organics).^{73,75} However, recent spectroscopic studies suggest this bulky (high molecular weight) head-group still degrades in alkali.⁶⁶ Initial results with the P–N tetrakis(dialkylamino)phosphonium system [poly-(Me)N–P⁺–(N(Me)Cy)₃ where Cy = cyclohexane] first reported by Coates *et al.* suggests that this type of cationic head-group chemistry may be stable to alkali⁴⁰ as indicated by early reports on small molecule studies.⁷⁶

Prior thinking was that the alkali stability of the cationic head-groups could be treated separately to the chemical stability of the polymeric backbone (e.g. once an alkali stable head-group is found it can be attached to whatever polymer backbone is required and the polymer backbone and head-group will remain alkali stable). However, recent results suggest a much more complex situation with a symbiosis between the stability of the head-groups and the polymer backbone. For example, polysulfone itself is stable when exposed to aqueous alkali but is destabilised and degrades in high pH environments when QA groups are attached to the polymer backbone (*via* $-\text{CH}_2-$ linkages): the polymer backbone becomes partially hydrophilic, allowing close approach of the OH^- anions.⁷⁷ The electron withdrawing sulfone linkage has a profound negative influence on the stabilities of the resulting AAEMs.⁷⁸ The hydrophobicity of unfunctionalised plastics lends significant resistance to alkali and it therefore stands to reason that more OH^- uptake into the polymer structure will induce greater degradation. The degradation of AAEM backbones in alkali have been observed for other systems.^{15b,33b,34f} The alkali stabilities of the following backbones containing pendent trimethylammonium cationic groups appear to decrease in the following order (Scheme 5): polystyrene > PPO > polysulfone (and all were less stable than the model small molecule p-methylbenzyltrimethylammonium).⁷⁷ Note that with polysulfone AAEMs, strategies are now being developed to move the QA group away from the polysulfone backbone, where an additional benzyl group is located between the QA group and the backbone.⁷⁹ Backbone stability may also be enhanced if phase segregated systems are developed (see later). The development of cationic side-chains containing multiple positive charges may help due to the ability to widely disperse the cationic side chains along the polymer backbone (charged groups placed further apart from each other without changing the IEC).⁸⁰ Therefore, when evaluating the alkali stabilities of new AAEMs/AEIs, the head-group and backbone must be evaluated together in combination.

Another problem with evaluating the *ex situ* alkali stabilities of different AAEMs/AEIs with different chemistries is the broad range of different methodologies used throughout the literature. A common approach is to evaluate the change of ionic conductivity of the materials with increasing immersion times in aqueous alkali. This can be a useful measure of alkali stability but there is a risk of false positives: if the degraded membranes exhibit ionic conductivity, then the original AAEM/



Scheme 5 The relative alkali stability of various polymer backbones when containing pendent trimethylammonium groups.⁷⁷

AEI may appear more alkali stable than it really is. A more useful measure of alkali stability is the measurement of IEC with increasing immersion times in aqueous alkali. This will be even more useful if changes in both quaternary IEC and non-quaternary exchange capacities are studied (see earlier discussion on IECs by titration). However, the authors recommend that such secondary measurements of alkali stability (changes in ionic conductivity and IEC) are *always supplemented with multiple spectroscopic measurements* (e.g. NMR,^{30f,33b,34c,66,69,77,81} IR,^{34k,82} and Raman^{31,34c}).

Clearly as more alkali stable AAEMs/AEIs are developed, *ex situ* accelerated test protocols must be developed, *i.e.* immersion in concentrated alkali at high temperatures [e.g. aqueous KOH (6 mol dm⁻³) at 80–90 °C] with/without addition of peroxy/radical-based degradation agents. However, it must be kept in mind that if the aqueous alkali is too concentrated, viscosity effects may come into play and interfere with the stability measurements (e.g. diffusion of OH^- nucleophiles towards the cationic groups is retarded). Data from accelerated degradation studies conducted inside NMR spectrometers (with soluble AAEMs/AEIs) will allow the simple and quick production of useful stability data (including an idea of the degradation mechanism that is operating).⁷⁷ All of these *ex situ* stability measurements must be validated/benchmarked against *in situ* real-world and accelerated durability tests (in the spirit of DOE protocols for PEMFCs).⁵⁵

It should also be kept in mind that the AAEMs/AEIs inside APEFCs are in an environment in the absence of excess metal (e.g. Na^+ or K^+) hydroxide species. Therefore, *ex situ* stability data at high temperatures with the AAEMs/AEIs in OH^- forms in the absence of additional/excess NaOH or KOH species is also useful (e.g. an OH^- form AAEM submerged in deionised water at 90 °C). The challenge here will be to ensure the AAEMs/AEIs remain in the OH^- form (*i.e.* CO_2 is totally excluded from all stages of the experiments [not easy to achieve]) as the AAEMs/AEIs will be more stable in the HCO_3^- and CO_3^{2-} anion forms. Warder titration methods^{43b} will be useful as these measure the relative contents of OH^- , CO_3^{2-} and HCO_3^- anions in the polymer electrolyte materials with time (example data given in



Fig. 1 for an AAEM [originally in the OH^- form] that is exposed to air); control experiments can be run alongside the degradation experiments where additional AAEMs/AEIs samples, originally in the OH^- forms and kept in the same environment as the primary degradation samples, are monitored for a reduction in OH^- content and an increase in $\text{CO}_3^{2-}/\text{HCO}_3^-$ content.

However, despite all of the studies into the different chemistries, the benzyltrimethylammonium hydroxide group may be stable enough for some applications (even those that contain alkali environments) as long as the benzyltrimethylammonium head-groups are kept fully hydrated (the OH^- anion is less nucleophilic when it possesses a full hydration shell).^{51d} This is more true for the use of this cationic group in the AAEMs but less true for use in the AEIs that are exposed to gas flows (much more difficult to maintain the AEIs in the fully hydrated state). Tailoring the hydrophobicity of the cationic group's environment may well have an impact.⁵⁶ The challenge for applications such as APEFCs, where it is difficult to keep the polymer electrolyte components fully hydrated (unlike in APEEs), is to develop AAEMs and (especially) AEIs that are stable (and conductive) in the presence of OH^- when less than fully hydrated.

AAEM conductivities. The most commonly cited reasons for the lower conductivities of AAEMs/HEMs *vs.* PEMs are:

(a) The lower mobility of OH^- (and $\text{HCO}_3^-/\text{CO}_3^{2-}$) *vs.* H^+ (see Table 1);⁸⁴

(b) The lower levels of dissociation of the ammonium hydroxide groups (*cf.* the highly acidic $\text{R}-\text{SO}_3\text{H}$ groups in PEMs).

With regards to (a) above, the intrinsically lower mobilities are traditionally offset by using AEMs with higher IECs compared to PEMs because ionic conductivity \propto ion mobility \times ion concentration. AEMs typically possess IECs much higher than 1.1 meq. g^{-1} (*cf.* Nafion®-11x series of PEMs = 0.91–0.98 meq. g^{-1})⁸⁵ apart from the state-of-the-art phase segregated systems discussed in detail later. This can lead to problems with high water uptakes and dimensional swelling (hydrated *vs.* dehydrated) and this leads to AEMs with lower mechanical

Table 1 Select ion mobilities (μ) at infinite dilution in H_2O at 298.15 K

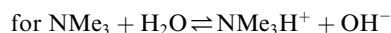
Ion	Mobility (μ) $\times 10^{-8}$ $\text{m}^2 \text{s}^{-1} \text{V}^{-1}$	Relative mobility ^a (relative to K^+)	Ref.
H^+	36.23	4.75	87 and 88
OH^-	20.64	2.71	87 and 88
CO_3^{2-}	7.46	0.98	87 and 88
HCO_3^-	4.61	0.60	87
Na^+	5.19	0.68	88
Cl^-	7.91	1.04	88
K^+	7.62	1.00	88

^a Calculated from the mobility data to the left and in general agreement with the relative mobility data presented in ref. 89.

strengths and a difficulty in maintaining the *in situ* integrity of membrane electrode assemblies (MEAs) containing AEMs (especially for APEFCs that use gas feeds [the MEAs are not in continuous contact with aqueous solutions/water]).⁸⁶

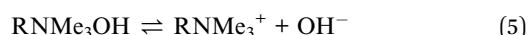
Regarding (b) above and “lower levels of dissociation”, it is often stated that “trimethylamine is a weak base” as it has a $\text{p}K_b$ value (in aqueous solutions) of only *ca.* 4.2 ($\text{p}K_a \approx 14 - \text{p}K_b = 9.8$ for the conjugate trimethylammonium $[\text{Me}_3\text{N}^+\text{H}]$ cation).⁸⁸

$$K_b = \frac{a(\text{NMe}_3\text{H}^+) \times a(\text{OH}^-)}{a(\text{NMe}_3)} \quad (3)$$



$$K_a = \frac{a(\text{H}^+) \times a(\text{NMe}_3)}{a(\text{NMe}_3\text{H}^+)} \quad \text{for } \text{NMe}_3\text{H}^+ \rightleftharpoons \text{H}^+ + \text{NMe}_3 \quad (4)$$

where $\text{p}K_a = -\log(K_a)$, $\text{p}K_b = -\log(K_b)$, K_b is the relevant base dissociation constant, K_a is the dissociation constant for the conjugate acid trimethylammonium ($= 1.6 \times 10^{-10}$), and $a(X)$ are the activities (activity coefficient corrected concentrations) of the various species in solution. However these are not the relevant equilibria to consider for QA hydroxides such as benzyltrimethylammonium hydroxide: these contain no N–H bonds! Take the simplest exemplar tetramethylammonium hydroxide (which has never been isolated in anhydrous form): NMe_4OH is a very strong base (used industrially for the anisotropic etching of silicon) and has a conjugate acid $\text{p}K_a > 13$.⁹⁰ Similarly, benzyltrimethylammonium hydroxide (also known as Triton B) is also a strong base and has been used as the catalyst in various base catalysed organic reactions.⁹¹ The relevant equilibrium is more analogous to aqueous alkali metal hydroxides (*e.g.* aqueous KOH):



Indeed, AEMs in the OH^- (*and* F^-) forms appear to be completely dissociated at high hydration levels (in CO_2 -free conditions) unlike AEMs in the I^- , Cl^- , Br^- , and HCO_3^- forms and the OH^- ions conduct mainly *via* structure diffusion (approaching half the conductivities of H^+ in PEMs).⁹² Therefore, concerns over the low levels of dissociation of OH^- for N–H bond free QA hydroxide groups (in AAEMs) are generally overstated.

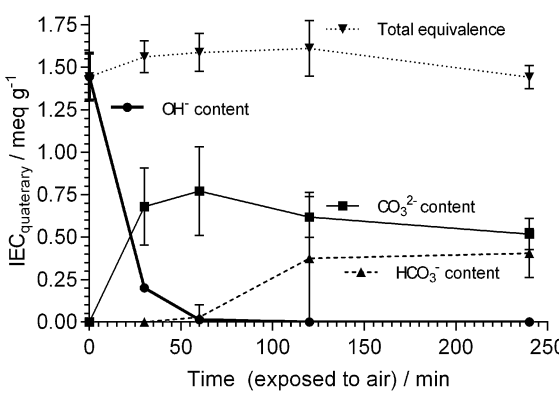


Fig. 1 IECs (quaternary) of different alkali anions for a benzyltrimethylammonium-type ETFE-radiation-grafted AAEM (80 μm thick) that was initially exchanged to the OH^- form and then directly exposed to air. IECs determined using Warder titration methods.^{43b,83} Error bars are sample standard deviations ($n = 3$ repeats).



As the AAEMs quickly convert to less conductive $\text{CO}_3^{2-}/\text{HCO}_3^-$ forms when exposed to CO_2 (*i.e.* air, recall Fig. 1),^{25d,43,93} it is essential that CO_2 (air) is totally excluded from conductivity determinations of OH^- form AAEMs. It is clear from the literature that this is rarely the case and that different laboratories use different set-ups probably with different levels of CO_2 exclusion. This creates problems with regard to inter-laboratory comparisons of OH^- conductivities. Most groups are likely underestimating the OH^- conductivities of their AAEMs/AEIs due to [difficult to obtain] incomplete CO_2 exclusion (*i.e.* they are measuring the conductivities of mixed alkali [$\text{OH}^-/\text{HCO}_3^-/\text{CO}_3^{2-}$] anion forms). *Therefore to aid inter-laboratory comparisons, we make the recommendation that HCO_3^- conductivities are always reported for AAEMs/AEIs alongside conductivity data in other anion forms, such as Cl^- and OH^- (the water uptake of the material in each of the anion forms must also be measured to understand the conductivity changes in the material).* The rationale is the AAEMs remain predominantly in the HCO_3^- form in the presence of air (CO_2) and that the OH^- conductivities can be estimated from the measured HCO_3^- conductivities.^{31,53} However, caution is required with such estimates as OH^- conductivities for AAEMs containing benzyltrimethylammonium cations have been measured to be higher than the size of the cation would normally indicate.⁹³ There is also the added complication with materials of a hydrophobic nature as ion-exchange is often incomplete and small amounts of residual anions can have profound effects on the mobility of the ion that you think you are studying.⁴⁴

It should also be kept in mind that the conductivities of most relevance to electrochemical devices are the through plane conductivities as the ions move from one electrode to the other through the thickness of the AAEM. The measurement of in-plane conductivities (typically using 4-probe techniques) can sometimes lead to an overestimation of the ionic conductivities (*i.e.* conductivities are often anisotropic) with a bias towards the conductivities across the surface layers of the membranes (sometimes the most functionalised parts).⁹⁴ However, we acknowledge that the measurement of through-plane conductivities can be tricky (difficult to isolate the membrane resistance from the electrode interfacial resistance when the membrane thicknesses are smaller than the dimensions of the electrodes) and that in-plane measurements have their place as they are often much more repeatable (and yield results that are less likely to be misinterpreted).

In devices where the AEMs/AEIs are not in continuous contact with liquid water (*e.g.* APEFCs) it is essential that they can conduct at lower relative humidities (RH). This will be a big challenge as the conductivities (and chemical stabilities) of AAEMs drop off much more rapidly with RH than with PEMFCs.^{19d,52} Hence, measurements in liquid water are not always relevant because fuel cell developers want ionic conductivities reported with the membranes in water vapour (reviewers often push that conductivity measurements where the membranes are immersed in liquid water should be reported). These are much harder to conduct especially when the measurement of the OH^- conductivities of AAEMs/AEIs in $\text{RH} \leq 100\%$ atmospheres is desired (the use of glove boxes with CO_2 -free atmospheres are essential).^{15a}

Fundamental studies (including modelling studies) related to anion conductivity, the effect of water contents and transport, and the effect of CO_2 on the properties of AAEMs have been undertaken.^{19d,46a,95} These should continue in order to understand what is required to maintain high conductivities under lower humidity environments (low water content per exchange group) and the effect of the presence of CO_2 on AAEM conductivity (see APEFC section later). For fundamental studies, it is often useful to normalise conductivities to other factors such as, water contents,⁵⁰ IECs^{39b} and mobilities.^{46a} Additional experiments such as the measurement of NMR T_1 and T_2 relaxation times for water in AAEMs can also be useful.⁴⁹ Short water relaxation times can lead to improved AAEM conductivity (even with lower IECs) as they indicate more close interaction between the water molecules and the solid polymer. Too high water uptake (often *via* excessively high IEC) can mean that much of the H_2O is inactive (not interacting with polymer) and is actually diluting the conductive species (leading to a lowering of the conductivity).

Various strategies have been proposed to enhance the conductivities of AAEMs without employing excessively high IECs and water uptakes (dimensional swelling). The development of phase-segregated AAEMs, containing hydrophobic phases interspersed with hydrophilic ionic channels and clusters (*à la Nafion®*), is rapidly becoming the *de facto* strategy for developing the high conductivity AAEMs with low IECs and water uptakes (see next section). It should be noted that phase separation is not always essential for high AAEM/AEI conductivities.²⁰ Covalent crosslinking is an alternative strategy, which can additionally reduce gas crossover but may also lead to less desirable attributes such as insolubility, reduced flexibility and brittleness (leading to poor membrane processability), and even a loss of conductivity (if it interferes with phase segregation).^{10d,13a,14b,d,25a,96} Other strategies include ionic crosslinking,^{10b} maximising the van der Waals interactions (to minimise swelling without the use of crosslinks),^{14d} using 1,2,3-triazoles to link the QA groups to the polymer backbone,⁹⁷ and enhancing the number of positive charges on the side-chains.^{42d,80}

Phase segregated AEMs⁹⁸

A realistic strategy to enhance the ionic conductivity of AAEMs is to improve the effective mobility of OH^- rather than increasing the IEC (to avoid excessive water uptakes and dimensional swelling on hydration).^{2e} As shown in Table 1, the mobility of OH^- in dilute KOH solution is actually rather high and is only inferior to that of H^+ but much superior to that of other ions. However, in AAEMs, the motion of OH^- can be retarded by the polymer framework where the effective mobility of OH^- is often much lower than that in dilute solutions. This is a common drawback of polymer electrolytes including Nafion® (where the effective mobility of H^+ is only about 20% of that in dilute acids).

The conduction of ions, such as H^+ or OH^- , relies on the presence of water so the structure of hydrophilic domains in a polymer electrolyte is the predominant factor for ion



conduction. It is believed that the outstanding ionic conductivity of Nafion® is attributed to its phase segregation morphological structure.⁹⁹ Specifically, the presence of both a highly hydrophobic fluorocarbon polymer backbone and flexible side chains (that contain the ionic groups) drives the formation of a hydrophilic/hydrophobic phase separation structure, where ion-containing hydrophilic domains overlap and form interconnected ionic channels. Although the nominal IEC of Nafion® is only *ca.* 0.92 meq. g⁻¹, the localised H⁺ concentration in the ionic channels is much greater, which significantly increases the efficiency of H⁺ hopping conduction.

Since the OH⁻ conduction operates *via* a similar mechanism to H⁺ conduction,¹⁰⁰ a phase segregated (self-assembled) structure is expected to improve ion conduction in AAEMs.⁹⁸ However, the formation of phase segregated structures in AEMs is more challenging as most AEMs are based on hydrocarbon backbones with lower hydrophobicities compared to fluorocarbon-based AEMs. The hydrophobicities are often even lower again as the cationic groups are commonly connected to the hydrocarbon backbones *via* short links (often -CH₂-), *e.g.* the quaternisation used to form QA polysulfone AAEMs markedly changes the alkali stability and hydrophobicity of the polysulfone backbone (relatively hydrophobic when unmodified). Elongating the length of the link between the polymer backbone and the cationic functional groups should, in principle, assist in the formation of phase segregation structures. However, this requires an entire change in material synthesis methods as a significant number of AEMs reported in the literature are prepared using a polymer modification protocol; for example, a commercially available polymer (such as polysulfone) is functionalised with a reactive group (commonly -CH₂Cl formed using some form of chloromethylation reaction [often using highly carcinogenic reagents such as chloromethylether]) and then further reacted (with reagents such as trimethylamine) to yield the final AEM containing polymer bound cations (Scheme 6a).¹⁰¹ This typical process is not easily adapted to yield Nafion®-like pendent cations (*i.e.* a QA attached to the polymer backbone through a long side chain).

Phase segregated morphologies generally exist in block (Scheme 6b/d/e/g) and graft copolymers (Scheme 6f),^{46a,102} which results from the enthalpy associated with the demixing of incompatible segments.¹⁰³ Regarding the development of copolymers, it is clear from the literature that the formation of phase segregated morphologies is much more successful for block copolymers compared to random copolymers (if comparable systems are compared).^{14a,49,104} For example, the phase separated morphology of a polysulfone block copolymer (IEC = 1.9 meq. g⁻¹, high $\lambda = 32$ value [λ values give the number of water molecules per cationic head-group] has been reported to give a very high hydroxide conductivity of 144 mS cm⁻² at 80 °C (over 3 times higher than an IEC = 1.9 meq. g⁻¹ random copolymer benchmark).^{104e} Coughlin *et al.* have shown that block copolymers can yield well defined lamella phase separation morphologies.^{23b} Such high level organisation is, however, not mandatory given that perfluoro QA AEMs can also phase separate (just like perfluorosulfonic acid [PFSA] PEMs like Nafion®).^{16a} QA-functionalised poly(hexyl methacrylate)-block-

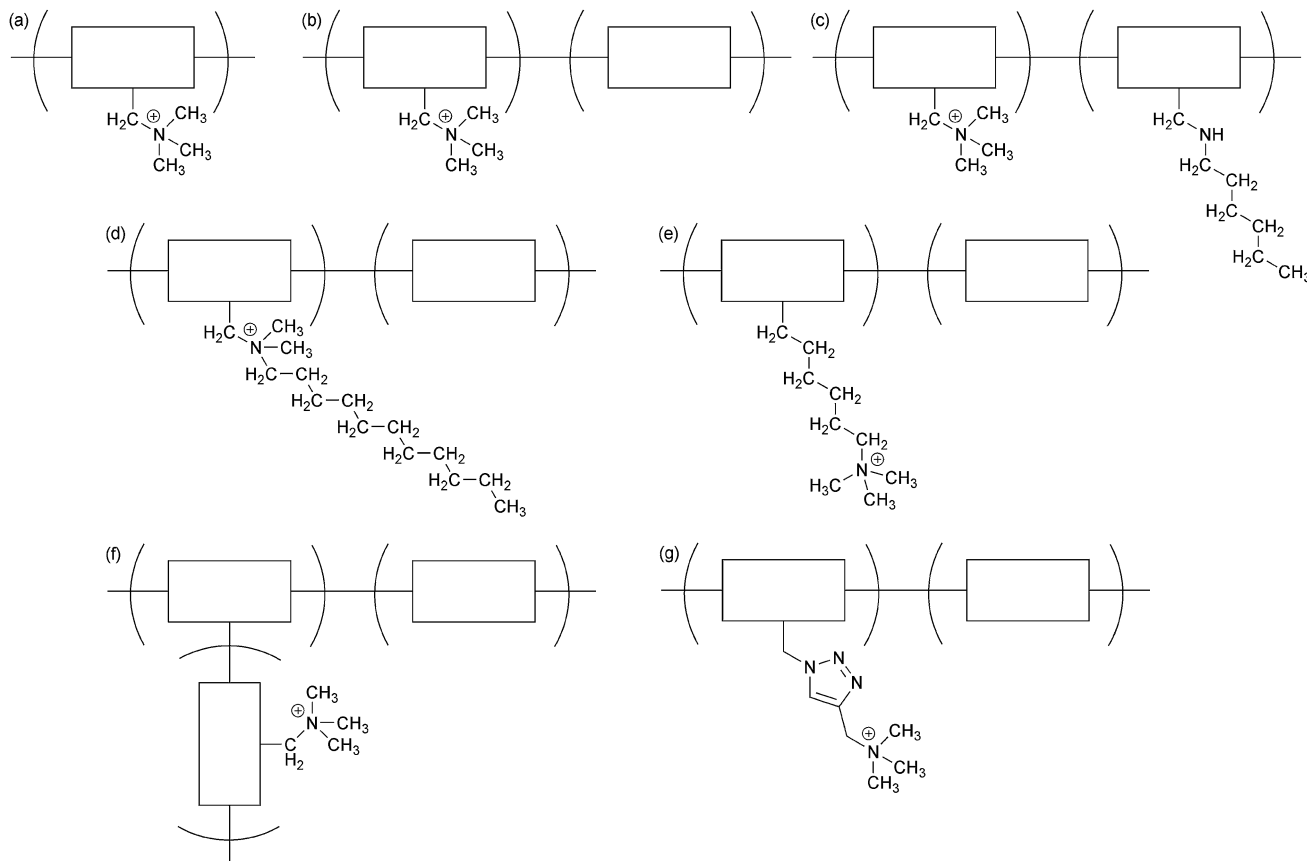
poly(styrene)-block-poly(hexyl methacrylate) systems have also been shown to possess a highly developed phase separation (using SAXS and TEM techniques) and this yielded relatively high OH⁻ ion diffusion coefficients (comparable to PEM benchmarks).¹⁰⁵ However, due to the insufficient mechanical strengths, such olefin types can only serve as models to assess the effects of molecular architecture on performances.

Beyer *et al.* reported strongly self-segregating covalently crosslinked triblock copolymers with high conductivities (120 mS cm⁻¹ at 60 °C for the fully hydrated sample with IEC = 1.7 meq. g⁻¹ and $\lambda = 72$).¹⁰⁶ Similarly, Bai *et al.* have reported conductivities >100 mS cm⁻¹ at 60 °C and >120 mS cm⁻¹ at 80 °C for QA-PPO/polysulfone/QA-PPO triblock AAEM (IEC > 1.83 meq. g⁻¹, fully hydrated but with a much lower $\lambda = 16$).¹⁰⁷ Coates *et al.* have also developed block copolymers but with additional crosslinking (*via* the cationic groups) and this yielded AAEMs with equally exceptional OH⁻ conductivities (up to 110 mS cm⁻¹ at 50 °C).^{21c} Guiver *et al.* produced polysulfone block copolymer AAEMs with higher OH⁻ conductivities at lower λ values, water uptakes, and dimensional swelling compared to a non-block copolymer QA polysulfone benchmark AAEM.¹⁰⁸ Li *et al.* developed another class of block copolymer where the QA group was separated from the polymer chain by a triazole group (Scheme 6g).⁹⁷ The triazole formation stemmed from the use of Cu(i) catalysed “click chemistry”. This produced AAEMs with excellent conductivities at room temperature when fully hydrated: an IEC = 1.8 meq. g⁻¹ AAEM gave a OH⁻ conductivity of 62 mS cm⁻¹ (and an interestingly high CO₃²⁻ conductivity of 31 mS cm⁻¹). However, the addition of triazole links increased the water uptakes (*cf.* triazole-free examples).

Binder *et al.* have also developed “comb shaped” block copolymers where the QA groups contained a long hydrocarbon tails (Scheme 6d).¹⁰⁹ AAEMs with OH⁻ conductivities up to 35 mS cm⁻¹ (room temperature, fully hydrated, IEC = 1.9 meq. g⁻¹) were reported. Even more interestingly, the water contents, λ , appeared to be independent to IEC ($\lambda = 5.2\text{--}5.9$ over the IEC range 1.1–1.9 meq. g⁻¹); these were much lower than a benchmark block copolymer AAEM where the QA was a polymer bound trimethylammonium (IEC = 1.4 meq. g⁻¹, $\lambda = 10.4$, OH⁻ conductivity = 5 mS cm⁻¹). Hickner *et al.* also investigated “comb shaped” AEIs for APEFCs where an increasing number of long alkyl chains (C6, C10 and C16 in length) were attached to the QA groups.⁵⁰ Higher performances were obtained with the 1 × C16 AEI (IEC = 1.65–1.71 meq. g⁻¹, 21 mS cm⁻¹ at room temperature in water) but this AEI had less *in situ* durability compared to a different 1 × C6 example (IEC = 2.75–2.82 meq. g⁻¹, 43 mS cm⁻¹). The AEIs with multiple long alkyl chains on the QA groups exhibited lower conductivities and water uptakes compared to AEIs of similar IECs that contain only a single long QA alkyl chain. Hickner *et al.* also showed that introducing crosslinking into comb shaped AEMs can enhance their stability towards alkali.¹¹⁰

Recent studies by Xu *et al.* investigated graft copolymers (Scheme 6f) for AAEMs, which displayed superior fuel cell related properties.^{102c} Dimethyl-PPO-based copolymers with poly(vinylbenzyl trimethylammonium) grafts were synthesized *via* atom transfer radical polymerization (ATRP).¹¹¹ AAEMs with





Scheme 6 General strategies for the development of phase segregated AEMs (b–g) compared to a benchmark homopolymer system (a). The rectangles represent a polymer block.

OH^- conductivities up to 100 mS cm^{-1} at 80°C were produced with high graft densities and optimised graft lengths (IEC = 2.0 meq. g⁻¹). Knauss *et al.* have also produced a PPO block copolymer AAEM but where the hydrophobic blocks contained additional phenyl side-groups (not aliphatic hydrocarbon side chains). A high OH^- conductivity of 84 mS cm^{-1} was obtained with an IEC = 1.3 meq. g⁻¹ AAEM.^{14a} Importantly, this conductivity was produced with the AAEM in a RH = 95% environment (rather than the normally encountered fully hydrated condition where the AAEM is fully immersed in water).

Recently, Zhuang *et al.* reported a new and simple method for achieving highly efficient phase segregation in a polysulfone AEM.¹¹² Instead of elongating the cation-polymer links or adding hydrophobic chains to the QA groups, long hydrophobic side chains were directly attached to polymer backbone at positions that are separated from the cationic functional group (Scheme 6c). This polysulfone phase segregated AEM was designated *a*QAPS. This structure is not categorised as a block copolymer, but rather a “polysurfactant” where the hydrophilic cationic head-groups (e.g. QA) are linked through the polymer backbone but the long hydrophobic tails are freely dispersed. This concept was inspired by the structure of Gemini-type surfactants, where enhanced ensemble effects are seen when properly tying up two single surfactant molecules.¹¹³ The effect of phase segregation of the *a*QAPS design was identified using

TEM and SAXS data (Fig. 2). The TEM image of the QAPS polysulfone copolymer benchmark, where there was no hydrocarbon side chain on the hydrophobic blocks (analogous to Scheme 6b), was uniform (Fig. 2a), which indicates the lack of clear phase segregation. However, the hydrophilic domains in the *a*QAPS system (dark zones in Fig. 2b, dyed using I^- before TEM measurement) were clustered and separated from the hydrophobic polymer framework (light background in Fig. 2b). This strong phase segregation resulted in a long-distance structural ordering, as indicated by the SAXS pattern (Fig. 2c).

As a consequence of the phase segregation, the ionic conductivity of *a*QAPS was 35 mS cm^{-1} at 20°C and $>100 \text{ mS cm}^{-1}$ at 80°C (Fig. 3) in comparison to non-phase-segregated QAPS (15 mS cm^{-1} at 20°C and 35 mS cm^{-1} at 80°C). *These are very high conductivities for such a low IEC AAEM (1 meq. g⁻¹).* The ionic conductivity of *a*QAPS(OH^-) at room temperature was *ca.* 57% of that of Nafion® (very close to the mobility ratio between OH^- and H^+ in diluted solutions). This indicates that the ionic channels in *a*QAPS are as efficient as that in Nafion® (*i.e.* the difference in ionic conductivity being just the mobility difference between OH^- and H^+). However, at temperatures that are more relevant to fuel cell operation (60 – 80°C), the IEC normalised ionic conductivity of *a*QAPS(OH^-) was as high as that of Nafion®(H^+). This shows that the OH^- conduction can be as fast as that of H^+ at elevated temperatures, provided the ionic

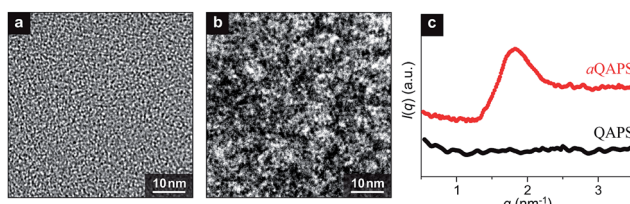


Fig. 2 TEM images of polysulfone-based AEMs: (a) QAPS [Scheme 6b] and (b) aQAPS [Scheme 6c]. (c) The resulting SAXS patterns.¹¹²

channels in the AAEM are optimised. This significant finding demonstrates that OH^- conductivities in AAEMs are not intrinsically inferior those of H^+ in PEMs.

The need for AEIs in electrochemical systems

Before the discussions move onto application specific items, the subject of the need for solubilised/dispersible AEIs needs to be introduced. To maximise the catalyst utilisation (optimal tri-phase interface [gas diffusion + ionic conduction + electronic conduction pathways available to a maximum amount of catalyst surface]) and introduce the required level of ionic conduction and hydrophobicity into the electrodes of low pH electrochemical devices such as PEMFCs, Nafion® dispersions (e.g. D-521/D520) are commercially available, scientifically well known, and widely used as acidic ionomers.^{99,114} For AEM/AAEM containing systems, the availability of commercial-grade AEIs is more restricted and less optimised for application in electrochemical applications. The usage of Nafion® CEM ionomers with AAEMs in APEFCs is a non-ideal situation.¹¹⁵ Both Tokuyama¹¹⁶ and Fumatech have developed AEIs.¹¹⁷ Other researchers have developed their own concepts or solubilised the materials used to make the AAEMs themselves (where possible).^{15c,28b,118} However, it is important to keep in mind that if production of an AEI technology is to be scaled up (for commercialisation) then it is vital that the AEI is supplied most desirably in an aqueous-based form (dispersion or solution). This is for safety considerations: the presence of both organic solvents and large quantities of finely divided (nano) catalysts in the scaled up manufacture of MEAs present will present a significant hazard.¹¹⁹

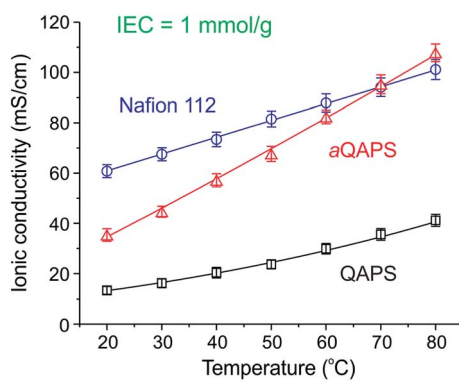


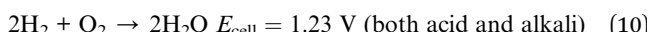
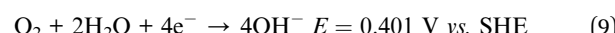
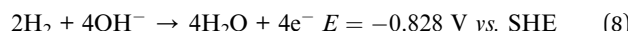
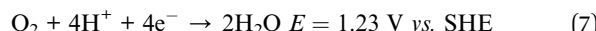
Fig. 3 IEC normalised conductivities of Nafion®, aQAPS, and QAPS.¹¹²

AAEMs in (chemical) fuel cells²

$\text{H}_2/\text{air}(\text{O}_2)$ alkaline polymer electrolyte fuel cells (APEFCs)

AAEMs and AEIs are used in APEFC technology.² In the literature this class of fuel cell is also called Alkaline Membrane Fuel Cell (AMFC), Anion Exchange Membrane Fuel Cell (AEMFC), or Solid Alkaline Fuel Cells (SAFC). In principle APEFCs are similar to PEMFCs, with the main difference that the solid membrane is an AAEM instead of a PEM. With an AAEM in an APEFC, the OH^- is being transported from the cathode to the anode, opposite to the H^+ conduction direction in a PEMFC. The schematic diagram in Fig. 4 illustrates the main differences between the PEMFC and the APEFC. In the case of a PEMFC, the H^+ cations conduct through a solid PEM from the anode to the cathode, while in the case of an APEFC the OH^- anions (or other alkali anions – see later) are transported through a solid AAEM from the cathode to the anode. The use of solid electrolytes also prevents electrolyte seepage, which is a risk with traditional alkaline fuel cells (AFCs) that use aqueous Na/KOH electrolytes.

The ORR¹²¹ and hydrogen oxidation reaction (HOR) for a PEMFC (HOR = eqn (6) and ORR = eqn (7)) are compared to an APEFC (HOR = eqn (8) and ORR = eqn (9)) below [recall, all E values are given as reduction potentials even if a reaction is written as an oxidation]:



Although the overall reaction (eqn (10)) is the same for both types of fuel cells, the following differences in both technologies are very important:

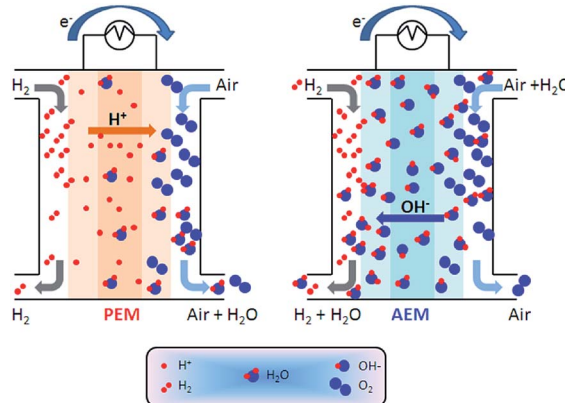


Fig. 4 Schematic comparison of a proton exchange membrane fuel cell (PEMFC, left) and an alkaline polymer electrolyte fuel cell (APEFC, right) that are supplied with H_2 and air.¹²⁰



(a) Water is generated at cathode side of PEMFCs but is generated at the anode in APEFCs;

(b) While there is no need for water as a direct reactant in PEMFCs, *water is a reactant in APEFCs as it is consumed in the cathode reaction.*¹²²

In principle, the advantages of APEFCs over PEMFCs are related to the alkaline pH cell environment of the APEFCs:

(a) Enhanced ORR catalysis, allowing for the use of less expensive, Pt-free catalysts such as those based on inorganic oxides including perovskites, spinels and MnO_x , as well as those based on Fe, Co, Ag, and doped graphene (among others);¹²³

(b) Extended range of (available) cell and stack materials such as cheap, easily stamped metal (*e.g.* Ni and uncoated stainless steel bipolar plates);

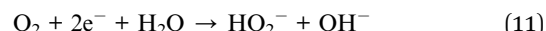
(c) A wider choice of fuels in addition to pure H_2 (*e.g.* hydrazine hydrate and “dirty” H_2 including H_2 containing traces of ammonia – see later sections).

The most critical concerns for APEFC technology are the low conductivities and the relatively poor stabilities of the AAEMs that were developed in the first years of the APEFC development.^{2,124} However, as discussed above, significant advances have been made in recent years that have promoted APEFC development.

Electrocatalysts for H_2 -based APEFCs. The reader should first refer to the paper by Gasteiger *et al.* if they require detailed discussion on the issues and considerations of benchmarking fuel cell catalysts (including non-Pt types).¹²⁵ With the latest advances in conductive and alkali stable AAEM for fuel cells, the need for the research into developing suitable catalysts has increased in priority. While retaining the advantages of PEMFCs (*e.g.* all solid state), APEFC technology opens the door for the use of non-precious and cheaper catalysts,^{123,126} which yields the potential for overcoming the high fuel cell cost barrier. However, the field of electrocatalysts for both the cathode and anode in APEFCs is only now being explored in detail.¹²⁷ With the development and application of non-Pt catalysts, their stabilities also need to be considered.¹²⁸ Moreover, little has been done with real APEFCs containing catalysts others than Pt.

Oxygen reduction reaction (ORR) catalysts.¹²⁹ The ORR overpotentials in APEFCs are similar to those in PEMFCs, (*i.e.* the cathode overpotential loss remains an important factor limiting the efficiency and performance of an APEFC).¹³⁰ However, switching to an alkaline medium (as in APEFCs) allows for the use of either a low level usage of Pt-group metal (PGM) catalysts or a broad range of non-PGM catalysts with ORR activities similar to that of Pt. Jiang *et al.* reported that the ORR activity of a Pd coated Ag/C catalyst in alkaline medium was three times higher than the corresponding activities on the Pt/C (measured using *ex situ* rotating disk electrode tests).¹³¹ Piana *et al.* reported that the specific current of Acta’s Hypermec™ K18 (Pd-based) catalyst¹³² is about 3× higher than Pt/C and its Tafel slope is also lower; the latter is also observed with other non-Pt catalysts.¹³³ He *et al.* reported that the kinetic current density of a non-PGM catalyst based on $\text{CuFe-N}_x/\text{C}$ was comparable, or even higher, than a commercial Pt/C catalyst.¹³⁴ The development of non-PGM ORR catalysts that are designed specifically for use in APEFCs now requires further research in

order to make this a real affordable technology. Carbon-free catalysts should be considered, as carbons are active for the peroxide generating ($n = 2\text{e}^-$) ORR in alkali:



Alternatively, catalysts that are active in reduction of peroxide at low overpotentials (bi-functional catalyst) are also deemed advantageous for alkaline systems.¹²³

Hydrogen oxidation reaction (HOR) catalysts. Whereas research on ORR catalysts in alkali has now begun, studies on the HOR catalysts for APEFCs constitute a relatively unexplored field. The kinetics of the HOR on Pt catalysts in PEMFCs (at low pH) is so fast that the cell voltage losses at the anode are usually considered negligible.¹³⁵ This is not the case in APEFCs and the anode performance is often much poorer than the cathode performance (with Pt catalysts in each).^{127b,130,136}

In one of the very few studies investigating HOR activities of platinum in both acidic and alkaline media, Sheng *et al.* found that in alkaline electrolyte the HOR kinetics are several orders of magnitude slower than in acid electrolyte.¹³⁰ More recently, this finding has been confirmed and quantified by Rheinländer *et al.* who reported that ultra-low loadings Pt in aqueous KOH (1 mol dm^{-3}) might exhibit prohibitively large losses of 140 mV at 40 mA cm^{-2} .¹³⁷ Moreover, when looking for non-Pt HOR catalysts, it was found that Pd-based catalysts exhibit 5 to 10× lower activity than Pt in alkaline medium.¹³⁷ However, a recently reported PdIr/C catalyst showed a HOR activity comparable to Pt/C.¹³⁸

Rare studies investigating non-PGM catalysts for HOR in H_2/O_2 APEFCs have been carried out by Zhuang *et al.*^{127a,c} The authors reported that by decorating Ni nanoparticles with Cr, they succeeded to tune the electronic surface of Ni, making it possible to operate in the anodes of APEFCs. They reported a single preliminary test in real APEFCs, showing a maximum peak power of 50 mW cm^{-2} at a cell temperature of 60 °C (Ni-based anode and Ag-based cathode). Although the power densities were still low, these are the first published reports on APEFCs that used non-Pt catalysts for both the HOR (anode) and the ORR (cathode) in a single cell, hence they demonstrate the potential of the APEFCs. A more recent *ex situ* experimental and theoretical study by Yan *et al.* indicates that CoNiMo catalysts hold promise for use as a HOR catalyst in APEFCs with the potential to outperform Pt-catalysts (when at high loadings).¹³⁹ All of these fundamental HOR studies strongly emphasise the need for alternative, inexpensive HOR-catalysts for the successful development of the technology. This is a major research priority.

In all cases reported, however, the stability (and durability) of the non-Pt HOR catalyst has been a major limiting factor. All authors of published works suggest morphological changes in the process of catalyst operation as a major source of instability of the interface. The challenge in practical non-Pt HOR design is that no catalyst has been shown to be active at comparable rates in both the HOR and hydrogen evolution reaction (HER). The search for a true breakthrough continues!



The effect of AEI-bound cationic groups on the electrode reactions. To recap, more research is required to increase the fundamental understanding of electrocatalysts in alkaline medium, especially as little research has been conducted into effective catalysts that are specifically developed for use in APEFCs. For *ex situ* experiments, it is important that experiments are conducted with all-solid-state cells (*i.e.* not using aqueous electrolytes containing spectator ions such as K^+ and excess OH^-). This will yield more fuel cell relevant electrochemical activities and often reveals electrochemical features that were obscured in experiments in aqueous electrolytes.¹⁴⁰

As the AEIs will be in intimate contact with the catalysts, another consideration is the influence of the cationic functional groups on the electrochemical activities of the catalysts; this will vary for each catalyst/AEI-cationic-group combination. Recent *ex situ* electrochemical studies have investigated the effect of fully dissolved cationic small molecules (not bound to polymers) on bulk polycrystalline¹⁴¹ and Pt/C ORR catalysts [1 mmol dm^{-3} cationic molecules dissolved in aqueous KOH (1 mol dm^{-3})].¹⁴² Even though these studies are not directly comparable to the *in situ* situation in APEFCs (*i.e.* Nafion® [cation-exchange] ionomer dispersion were used in the formulation of the catalyst inks [rather than using AEIs as a binder] and cationic molecules were fully dissolved in aqueous KOH electrolytes with excess spectator ions), the studies have provided some useful indicators of issues that need to be considered:

(a) Unlike with acid electrolytes,¹⁴³ Cl^- anions (the anion present in all of the experiments) did not have a major effect on the ORR on Pt (1 mmol dm^{-3} Cl^- concentrations tested);

(b) Benzene-ring-free QA cations (*e.g.* tetramethylammonium) have a low impact on the ORR on Pt, whereas benzene-ring-analogues (*e.g.* benzyltrimethylammonium) lead to impeded ORR performances;

(c) Imidazolium cations (*e.g.* benzyl-3-methylimidazolium) lead to severe reductions in the ORR performance of Pt; these cations also change the mechanism so the level of undesirable (peroxide generating) $n = 2e^-$ ORR increases (eqn (11));

(d) Pt catalysts oxidise the organic cations at high potentials and the degradation products may also have an impact of the ORR performances (degradation of organic components at the anode may also have an effect on the HOR). This also suggests that research needs to be conducted into the electrochemical stability of the cationic head-groups bounds to the AEIs that are in contact with the catalysts (especially at higher cathode potentials). In this respect, Pt (that tends to catalyse a broad range of things very efficiently) may well be the worst choice of catalyst;

(e) As expected,¹⁴⁴ polycrystalline (bulk) Pt gave higher specific activities (electrochemically active surface area normalised current densities) and exchange current densities than Pt/C nanocatalysts (comparisons with each cation additive).

Similarly, a study by Shao *et al.* investigated the effect of 1-methylimidazole and triethylamine (but not charged imidazolium and quaternary ammonium species) on the ORR and HOR on Pt/C in aqueous KOH.¹⁴⁵ Similarly, Konopka *et al.* looked at the effect on the ORR of polycrystalline Pt of 1,1,3,3-tetramethylguanidinium cations.¹⁴⁶

Other studies have looked at the effect of AEIs themselves on the performances of various catalysts towards various reactions at high pH (where Nafion® ionomer is not present). These experiments are closer to the conditions in APEFCs. These studies involved AEIs such a commercial QA types (Tokuyama AS-4)¹⁴⁵⁻¹⁴⁷ in-house synthesised polysulfone-imidazolium types,¹⁴⁵ and a phosphonium type.^{123d} A more recent study investigated the effect of polymer backbone of QA-AEIs on the performance of an iron-cyanamide-derived catalyst.¹⁴⁸ The poly(phenylene) and Nafion®-based AEIs led to higher performances compared to the polysulfone AEI. For another example, the use of AS-4 and the imidazolium AEI both reduced the ORR mass activity on Pt/C compared to the use of Nafion® ionomer.¹⁴⁵ However, the HOR mass activities were increased with the use of AEIs compared to Nafion® (with the imidazolium AEI yielding the best HOR performance). Lemke *et al.* looked at the use of AS-4 as the AEI with Ag-nanowire ORR catalysts.¹⁴⁷ The presence and loading of the AEI was observed to have an effect on both the catalyst activity and the number of e^- per O_2 reduction ($n = 2$ [eqn (11)] *vs.* $n = 4$ [eqn (9)]). Yan *et al.* concluded that phosphonium cationic groups poison Ag ORR catalysts much less when polymer bound (as part of the AEI) compared to when part of dissolved small molecules.^{123d}

Note: these prior studies did not compare AEIs containing different head-groups but the same polymer backbone (and IEC). The next stage of this series of investigations should consider the ORR and HOR kinetics on fuel cell catalysts when bound using AEIs containing different cationic head-groups (QA *vs.* imidazolium *etc.*) in Nafion®-ionomer-free systems (and without addition of fully solubilised cationic molecules). An AEI concept is now available that would facilitate such a study that uses a selection of bulk producible AEIs containing different cationic head-groups (but with the same IEC and polymer backbone chemistry).¹⁴⁹

The issue of CO_2 in the air supplies (“carbonation”). One of the desires of the AAEM community is to operate under ambient conditions (*i.e.* with air supplies without prior CO_2 removal). Such operation is problematic at the APEFC cathode where ORR occurs (eqn (9)) as OH^- is extremely reactive with CO_2 , first forming bicarbonate (eqn (1)) and then carbonate (eqn (2)). Historically, CO_3^{2-} anions have been thought of as a poison in traditional AFCs that use aqueous KOH as the electrolyte since K_2CO_3 has low solubility in water at room temperature (risk the formation of precipitates in various parts of the AFC including the electrodes).¹⁵⁰ Even with the introduction of APEFCs, where the CO_3^{2-} and HCO_3^- species cannot precipitate (the positive charge is part of the already solid electrolyte and there are no mobile [*e.g.* metal] cations present), the reactions in eqn (1)/(2)/(9) can still be problematic.

The trace CO_3^{2-}/HCO_3^- anions, generated at the cathode from the reaction of the CO_2 in the air supply and the OH^- anions present in the electrolytes, diffuse away and accumulate at the anode side of the MEA. This sets-up an undesirable pH gradient where the anode side of the MEA has a lower effective pH (higher concentration of CO_3^{2-}/HCO_3^- species) than the cathode side (retains a higher OH^- content than the anode side);¹⁵¹ thermodynamically (cell voltage wise) it is better to have



a lower pH at the cathode and a higher pH at the anode. However, experimental and modelling studies^{43,152} show that the $\text{CO}_3^{2-}/\text{HCO}_3^-$ contents in the AAEMs and AEI can be purged from the anode (“self-purging” and CO_2 release) with the rapid and continuous generation of the OH^- anions at the cathode *at high current densities*. This self-purging can actually be exploited if AEMs with suspected low stabilities to high concentrations of OH^- [as in the commonly encountered aqueous KOH (0.5–1 mol dm^{-3}) ion-exchange solutions] are to be tested in APEFCs: the AAEMs and AEIs can be initially converted to the CO_3^{2-} forms, installed in the fuel cell, and then activated at high currents (*in situ* conversion of the AAEM and AEI into the OH^- forms).¹⁵²

In fact, the situation may be even more complex: while APEFC performances drop when the cathode supply is switched from O_2 to air, there is evidence that APEFC performances can actually increase when CO_2 is deliberately added to an O_2 cathode supply (at higher CO_2 concentrations than those found in air).¹⁵³ This intriguing effect certainly warrants more detailed study. There is also a feeling in the APEFC community along with some anecdotal evidence that being able to *raise the APEFC operating temperatures to > 80 °C* may well increase the tolerance of these systems to CO_2 in the air supplies (reduce the performance gap between APEFC operation with air compared to O_2). Again, this needs to be rigorously investigated, especially when development of AAEMs/AEIs that are stable in the OH^- forms at temperatures of >80 °C for long periods of time has been achieved.

H₂-based APEFC performances. Recent developments in highly conductive AAEMs have contributed to the growing interest in APEFC technology. The last decade or so has seen the first reports of APEFC performances. A number of these reports give performances high enough to show that the potential of APEFCs needs to be seriously considered for practical application. Table 2 summarises key APEFC results reported in the literature (with H_2/O_2 and H_2/air systems). As can be seen, maximum power densities of up to 823 mW cm^{-2} have been reported with O_2 supplied cathodes and 500 mW cm^{-2} for air supplied cathodes. Open circuit voltages (OCV) are routinely >1.0 V and OCVs as high as 1.1 V have been reported.

One of the best indicators of the potential of this technology comes from the industrial sector. After all, there are commercial (fuel cell relevant) AAEMs available including those by Tokuyama, Solvay and Fumatech.¹⁵⁴ Tokuyama showed a maximum peak power of 450 mW cm^{-2} and 340 mW cm^{-2} for H_2/O_2 and H_2/air (CO_2 free) respectively at 50 °C.^{43b} Even though those results were obtained with Pt/C catalysts (0.5 mg_{Pt} cm^{-2}), they show a power high enough for practical applications (such as backup power for stationary applications including in the telecoms industry). At same time, Kim reported interesting results with his polyphenylene based membranes.¹⁵⁵ With 3 mg cm^{-2} Pt black catalyst in both the anode and cathode, a maximum power density of 577 mW cm^{-2} (at 1 A cm^{-2}) and 450 mW cm^{-2} (at ≈ 0.8 A cm^{-2}) at 80 °C with H_2/O_2 and H_2/air conditions respectively. This power density is very similar to that achieved and reported by Yanagi and Fukuta.^{43b}

Although these Pt-based APEFCs already exhibit performances that are good enough for practical fuel cell application, the need for these performances (or better) with alternative and inexpensive catalysts is paramount. One of the very few results presented on H_2 -based APEFCs with non-Pt catalysts was recently obtained at CellEra (an Israeli company developing AMFCs).^{127b} Using dry H_2 and CO_2 filtered ambient air, Dekel reported a peak power density of 700 mW cm^{-2} (at 1.5 A cm^{-2}) with 3 bar_g/1 bar_g H_2/air at 80 °C with an APEFC containing a Pt anode catalyst, and a peak power density of 500 mW cm^{-2} (at 1.6 A cm^{-2}) with 3 bar_g/1 bar_g H_2/air at 80 °C with an entirely non-Pt (confidential catalysts) APEFC.^{127b} This data also demonstrates that AAEMs can withstand considerable pressure differentials between the anode and cathode (CellEra have data that shows this to be true with 3 bar differentials). Tokuyama also report that their A201 AEM has a burst strength of 0.4 MPa.¹⁵⁹

Performances of APEFCs can be increased with the use of active water management,¹⁶⁰ *i.e.* control of anode RHs with different anode RHs used at different current densities (lower anode RH at high current densities to prevent anode flooding – recall the anode is where the H_2O is electro-generated). Water management and APEFC performances should increase with the use of thinner AAEMs.¹⁶¹ However, our experience to date is that AAEMs that are thinner than *ca.* 30 μm (*e.g.* Tokuyama A901 is *ca.* 10 μm in thickness)^{116b} does not always lead to the expected increases in performance (even with well optimised APEFC systems). This mystery needs to be investigated further. A major *in situ* problem with the use of AAEMs and AEIs is when they are exposed to low RH environments in APEFCs: the conductivities significantly drop even with only small drops in RH (*i.e.* AAEMs and AEIs are much more sensitive to drops in humidity than PEMs and H⁺-conducting ionomers).⁵² The alkali stabilities of the AAEM and AEIs also decrease dramatically with lower hydration levels (OH^- is stronger nucleophile when not fully hydrated). AEI degradation occurs mostly in the cathode catalyst layer as this is where most dehydration occurs; it appears to be hard to keep the cathode AEI hydrated even when more than enough H_2O is transported back from anode and the cathode gas supply is fully hydrated.

In summary, extremely rapid and promising achievements in H_2 APEFC technology have been shown. Based on the above described (recent) results that have been obtained with first prototypes, it seems that APEFC technology is not just a future promise, but a present reality. APEFCs development has been rapid in the past five or so years where experimental work is now being followed up with detailed theoretical and modelling studies.^{43a,161,162} This technology promises to solve the cost barriers (of PEMFCs), which is one of the main “pain-points” of fuel cell technology. While H_2/air APEFC cells and stacks have achieved practical performances (for a few applications such as back-up power), there are still development challenges, which must be addressed to enable the large-scale introduction of APEFCs. These mainly include:

(a) AAEMs and AEIs with improved stabilities and conductivities at higher temperatures and especially when exposed to lower RH environments;



Table 2 Select literature data that present peak power densities measured with laboratory-scale H₂-based APEFCs

Peak power density achieved/ mW cm _{geo} ⁻²	Current density/ mA cm _{geo} ⁻² (voltage/V) at peak power	Gas supplies anode/cathode (back pressure)	AAEM	Cell temperature/°C	Catalyst type and loading/mg cm _{geo} ⁻²		References
					Anode	Cathode	
77	158 (0.49)	H ₂ /air	"Perfluorinated piperazinium"	70	Pt	0.5	156
70	170 (0.41)	H ₂ /O ₂	QA polysulfone	70	Pt/C	0.4	2n
180	400 (0.45)	H ₂ /O ₂ (1 bar _g)	QA polystyrene copolymer	70	Pt/C	0.4	157
≈ 90	≈ 170 (0.53)	H ₂ /O ₂ (2 bar _g)	QA polyphenylene	80	Pt	2	15c
≈ 40	≈ 60 (0.67)	H ₂ /air (2 bar _g)					
138	≈ 280 (0.49)	H ₂ /O ₂ (2.5 bar _g)	Stabilised phosphonium	50	Pt	0.2	39f
196	≈ 380 (0.52)	H ₂ /O ₂ (2.5 bar _g)	polysulfone	80		0.5	0.5
28	60 (0.47)	H ₂ /air	Crosslinked QA polysulfone	60	Pt/C	0.5	57f
30	≈ 65 (0.46)	H ₂ /air	Crosslinked QA polysulfone	60	Pt/C	0.5	57e
230	600 (0.38)	H ₂ /O ₂	QA radiation-grafted ETFE	50	Pt/C	0.5	158
50	100 (0.50)	H ₂ /O ₂ (1.3 bar _g)	QA polysulfone	60	Ni-Cr	5	127c
823	≈ 1800 (0.46)	H ₂ /O ₂	QA radiation-grafted low density polyethylene	60	Pt/C	0.4	25e
506	≈ 1000 (0.51)	H ₂ /air (1 bar _g)		60	Pt/C	0.4	0.4

(b) Pt-free highly efficient catalysts, especially for the HOR. Advances related the above two issues will assure rapid entrance of APEFCs into existing market opportunities.

AAEM fuel cells fuelled with C-based fuel alcohols^{2d,l,o,163}

There are several drivers for the use of alcohol fuels in AAEM-based fuel cells (primarily for portable power applications):

(a) Alcohols are liquid fuels with high volumetric energy densities (Table 3), even when compared to cryogenic H₂(l);

(b) The maximum theoretical efficiencies are widely stated to be high when based on the higher heating value (>97% for alcohols compared to 83% for H₂ and 91% for NaBH₄). However, please consider that these numbers can be misleading and not practical as only free energy in and free energy out (*i.e.* exergy) matters;

(c) Because alcohol oxidation is generally more facile in high pH environments¹⁶⁴ and can be structure insensitive,¹⁶⁵ there is a large repertoire of potentially cheaper and more abundant anode catalysts that can be used.

(d) A larger range of ORR catalysts increases the odds of finding alcohol tolerant options (including M_xO_y types);^{123f,132,166}

(e) The conductive ions (OH⁻) move through the AAEM in a direction (cathode → anode) that is contrary to alcohol crossover (anode → cathode). This may mitigate against alcohol (and alcohol electro-oxidation product) crossover, especially at higher currents. Alcohol oxidation at the cathode can lower the cathode potential and/or poison the cathode catalyst. This is different to the situation in PEM-based Direct Alcohol Fuel Cells (DAFC) where the H⁺ ions move from anode → cathode thereby enhancing alcohol crossover (due to electro-osmotic drag). This is serious when materials such as Nafion are used (with high methanol permeabilities of >10⁻⁶ cm² s⁻¹ and methanol uptakes).¹⁶⁷ Well designed and engineered systems, where the alcohol concentration in the anode catalyst layers is low (due to efficient and rapid oxidation), suffer less from alcohol crossover effects;

(f) In AAEM-DAFCs, H₂O is consumed in the cathode catalyst layers (recall eqn (9)) and electro-generated at the anode where there is already a liquid reactant supply present (the reverse situation to PEM-DAFCs). This change in water balance may be beneficial in reducing flooding at the cathode: there is electro-osmotic drag of a large number of H₂O molecules (>19) per H⁺ when aqueous alcohol solutions are supplied to the anode in PEM-DAFCs (a significant problem).¹⁶⁸ However, modelling suggests that insufficient H₂O transports through the AAEM (to the cathode) to sustain high currents in AAEM-DMFCs (Direct Methanol Fuel Cell).¹⁶⁹ Related to this, Smart Fuel Cells (Germany) has a patent for a "fuel cell combination", where the cathode of a PEM-DMFC is located next to the cathode of an AAEM-DMFC. This is to efficiently utilise, in the AAEM-DMFC cell, the large quantities of H₂O transported through the membrane (anode → cathode) of a PEM-DMFC cell.¹⁷⁰

(g) A small amount of alcohol penetrating into the membranes may protect the membranes (particularly hydrocarbon types) against peroxide attack.¹⁷¹ The presence of alcohols may also assist with the "cold start-up" of DAFCs (*i.e.* starting up the fuel cell from sub-zero temperatures).¹⁷²

Methanol, ethanol, ethylene glycol, and glycerol are the more common alcohols to have been tested in AAEM-based fuel cells; however, higher alcohols such as the propanols have also been considered for electro-oxidation in alkali.¹⁷³ The oxidation reactions (in alkali) for methanol, ethanol, ethylene glycol, and glycerol are given in eqn (12)–(16):

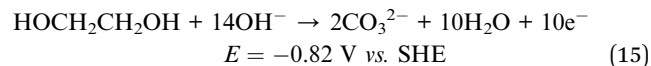
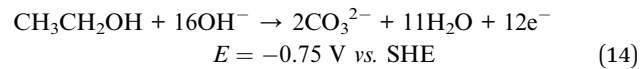
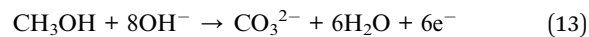
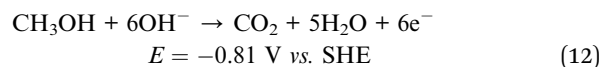


Table 3 Select properties of commonly encountered fuel options used in fuel cells

Fuel option	Specific energy density/kW h kg ⁻¹	Density at 20 °C/g cm ⁻³	Volumetric energy density/kW h dm ⁻³	E_{cell}^a /V	n^b
H ₂ (l)	33	Gas	2.37 (0.53 ^c)	1.23	2e ⁻
Methanol CH ₃ OH (l)	6.1	0.79	4.8	1.21	6e ⁻
Ethanol CH ₃ CH ₂ OH (l)	8.0	0.79	6.3	1.15	12e ⁻
Propan-1-ol CH ₃ CH ₂ CH ₂ OH (l)	9.1	0.81	7.4	1.13	18e ⁻
Propan-2-ol CH ₃ CH(OH)CH ₃ (l)	9.0	0.79	7.1	1.12	18e ⁻
Ethylene glycol HOCH ₂ CH ₂ OH (l)	5.2	1.11	5.8	1.22	10e ⁻
Glycerol HOCH ₂ CH(OH)CH ₂ OH (l)	5.0	1.26	6.4	1.09	14e ⁻
Formate HCOO ⁻ (s)	0.9	Solid	—	1.45	2e ⁻
Hydrazine N ₂ H ₄ (l)	5.4	1.00	5.4	1.62	4e ⁻
Ammonia (l)	3.3	Gas	3–5 ^d	1.17	3e ⁻
Ammonia borane H ₃ N:BH ₃ (s)	8.4	Solid	—	1.62	6e ⁻
Sodium borohydride NaBH ₄ (s)	9.3	Solid (1.07 ^e)	(10 ^e)	1.64	8e ⁻
Typical gasoline (l)	12.8	0.71–0.77	9.5	—	—

^a Maximum thermodynamic cell potential at 25 °C on oxidation in a cell with O₂ as the oxidant. ^b The number of e⁻ per fuel molecule obtained on full oxidation. ^c Gaseous H₂ at 200 bar. ^d Depending on the conditions. ^e For a solution of 500 g NaBH₄ in 1 dm³ solution at 25 °C. (l) = liquid and (s) = solid.



Alcohol oxidation (assuming full electro-oxidation) produces CO₂ leading to significant concentrations of CO₃²⁻/HCO₃⁻ in the anodes of the AAEM-based DAFCs. The resulting pH gradient (high pH cathode → low pH anode) will produce thermodynamically derived voltage losses.¹⁵¹ It has been calculated that a pH difference of 6.1 would exist across the AAEM at 20 °C corresponding to a thermodynamic voltage loss of *ca.* 360 mV, which drops to a pH difference of 4.1 (voltage loss of *ca.* 290 mV) at 80 °C. Such voltage losses can be offset with the improved kinetics at temperatures ≥ 80 °C (especially if alcohol crossover is suppressed).

As will be evident from the below discussions, acceptable power performances are only obtained when large amounts of Na/KOH are added to the aqueous alcohol fuel supplies. Assuming full oxidation of the alcohols, the presence of such additional quantities of additional OH⁻ will lead to CO₃²⁻ being the predominant product (rather than CO₂):⁵⁸ hence eqn (13)–(16) are written as such. As the point of using AAEMs/AEIs in fuel cells was to eliminate the use of aqueous Na/KOH, it must be questioned if the use of AAEMs is needed when the addition of Na/KOH to the fuel supplies cannot be avoided.¹⁷⁴ After all, methanol has been used as a fuel in AFCs in the past. The review by Koscher and Kordesch details historic work involving alkaline methanol-air systems with liquid caustic electrolytes.¹⁷⁵

AAEM-based DMFCs. Methanol is the simplest alcohol (a C1 alcohol with no C–C bonds to break) that has been evaluated in AAEM-based fuel cells.¹⁷⁶ This includes being used as a fuel in a microfabricated passive AAEM-containing fuel cell.¹⁷⁷ Despite this chemical simplicity, the power densities obtained with C2+ alcohols such as ethanol and glycerol are similar to those obtained with methanol (see later). The 6e⁻ methanol oxidation reaction (MOR) mechanism is still more complex compared to the 2e⁻ HOR and the rate determining step is thought to be the

oxidation of the –CHO intermediate species.²¹ Bi-functional catalysts such as PtRu, that are required as anode catalysts in PEM-DMFCs for the removal of strongly bound Pt–CO intermediates (facilitated by the presence of adjacent Ru–OH sites), may not be required (at least in such high amounts) for AAEM-DAFC anodes due to the high concentration of OH⁻ anions present.¹⁷⁸ High concentrations of CO₃²⁻/HCO₃⁻ species at the anode catalysts in AAEM-DMFCs may or may not interfere with the MOR (this needs to be studied in more detail).^{179,180} Along similar lines to the studies that are looking into the effect of AEI ionomers (or model small molecules) on the ORR on various catalysts, it has been reported that benzyltrimethylammonium has a stronger negative affect towards the MOR on Pt/C in aqueous KOH (0.1 mol dm⁻³ containing 0.05 mol dm⁻³ methanol) compared to tetramethylammonium over the additive concentration range 1–120 mmol dm⁻³.¹⁸¹ Again, the effect of the AEI being used on the MOR for the catalyst being considered for application needs to be evaluated.

Alongside the many studies with Pt-based catalysts,¹⁸² Pd^{183,184} and Au¹⁸⁵ catalysts have also been considered for MOR in alkali. However, due to cost, the big push has been towards the development of non-PGM catalysts. Ni-based catalysts are a commonly encountered option.¹⁸⁶ Spinner *et al.* have studied NiO-based catalysts for MOR in alkali. They found that activities were higher in aqueous CO₃²⁻ electrolyte compared to aqueous OH⁻ electrolytes.¹⁸⁰ Minteer *et al.* have reported that the inclusion of magnetic composites into Ni-based electrocatalysts can boost MOR in alkali.¹⁸⁷ Perovskite-based MOR catalysts have also been considered.¹⁸⁸

As well as the conductive species opposing methanol crossover in AAEM-DMFCs, there have been many studies into finding AAEMs with low methanol (and other alcohol) permeabilities.^{10f,65,189} High methanol diffusion through the anode AEI is, however, desirable.¹⁹⁰ Many of these studies mention an *ex situ* “selectivity” or “DMFC performance” parameter, which is the ratio of 2 intrinsic properties:^{10f,65,102b,191} ionic conductivity to



methanol permeability ($= \sigma/P_{\text{MeOH}}$). An ideal AAEM will have a high ionic conductivity and low methanol permeability yielding a high performance parameter. However, caution is required with this parameter as an AAEM with a high performance parameter value but with a very low ionic conductivity will not be suitable for application (*i.e.* a low conductivity material with an extremely low methanol permeability). Obviously there will be analogous *ex situ* performance parameters for the other fuel options detailed below.

Without the addition of metal OH^- (MOH) salts to the methanol anode supply, the performances of AAEM-DMFCs are generally poor with typical peak power densities of $<20 \text{ mW cm}^{-2}$ (even with reactant pressurisation).^{115,174,192} The chances of 6/8 OH^- anions diffusing/migrating through the hydrated components of the anode AEI at the same time (to a localised site on the catalyst surface) to allow rapid oxidation of a single methanol molecule is deemed very low in the absence of an additional source of OH^- ions. This is different to PEM-DMFCs where the $6 \times \text{H}^+$ (generated on oxidation of a methanol molecule) have to transport away from the anode catalyst surface sites. Despite this, Benziger *et al.* report a reasonable methanol (2 mol dm^{-3} and OH^- -free)/ O_2 AAEM-DMFC performance with a peak power density of 31 mW cm^{-2} ($\text{OCV} = 0.84 \text{ V}$) at room temperature using an imidazolium-PEEK AAEM (95 μm thickness and $\text{IEC} = 2.0 \text{ meq. g}^{-1}$) and AEI and Pt catalysts with loadings of $0.5 \text{ mg}_{\text{Pt}} \text{ cm}^{-2}$ (the catalyst coated membrane [CCM] method was used).^{19a} Analytical modelling of AAEM-DMFCs suggests that MOH-free performances can be improved when the anode side faces upwards due to more facile removal of the CO_2 bubbles (higher temperatures also facilitate CO_2 bubble removal).¹⁹³

The performances are generally higher when MOH is added to the aqueous methanol fuel supplies. The main contributor to this improved performance is an improved anode potential ($>300 \text{ mV}$ reduction in anode overpotential is possible). Katzfuß *et al.* obtained a peak power density of 132 mW cm^{-2} ($\text{OCV} \text{ ca. } 0.9 \text{ V}$) in AAEM-DMFCs at 80°C containing both an in-house synthesised DABCO-crosslinked PPO AAEM (10 μm thick, $\text{IEC} = 1 \text{ meq. g}^{-1}$, 80% degree of crosslinking) or a Tokuyama A201 AAEM (28 μm thick);^{14b} the fuel cells contained an Acta 4010 (6% $\text{Pd}/\text{CeO}_2/\text{C}$) anode catalyst, and Acta 3020 (4% FeCo/C) cathode catalyst and were supplied with aqueous methanol (4 mol dm^{-3}) containing KOH (5 mol dm^{-3}) at the anode and dry O_2 at the cathode. The same group obtained a similar performance (120 mW cm^{-2}) under the same test conditions using a 4 component DABCO-crosslinked PBI-polysulfone membrane that was more stable to alkali than the prior DABCO-crosslinked PPO AAEM.¹⁹⁴ Prakash *et al.* reported a methanol/ O_2 AAEM-DMFC containing Tokuyama's A201 AAEM and AS-4 AEI that yielded a higher peak power density of 168 mW cm^{-2} ($\text{OCV} = 0.9 \text{ V}$) at 90°C when supplied with an aqueous methanol (1 mol dm^{-3}) anode feed containing KOH (2 mol dm^{-3}).^{116a} However, these performances were obtained using PtRu (HiSpec 6000) anode and Pt (HiSpec 1000) cathode catalysts (cell optimised with a teflonised cathode and non-teflonized anode).

AAEM-based direct ethanol fuel cells (DEFC).^{2a,195} Unlike with PEM-based systems, the performances of AAEM-DEFCs are

as high with ethanol as they are with methanol. The interest in ethanol stems from its low toxicity (in moderation!), its higher boiling point (*cf.* methanol), and its high volumetric energy density. The use of lignocellulosic bioethanol may be a potentially "carbon-neutral" fuel option (*i.e.* next generation bioethanol that is not derived from food-based crops).¹⁹⁶ However, ethanol (C/O ratio = 2) contains a C-C bond that needs to be broken if full 12e^- oxidation to $\text{CO}_2/\text{CO}_3^{2-}$ is to be achieved. Partial ethanol oxidation (EOR) to [toxic] acetaldehyde (2e^- oxidation) and acetic acid/acetate (4e^- oxidation) predominates at temperatures of $<100^\circ\text{C}$ and this lowers the efficiencies of the DEFC (less e^- from each ethanol molecule than the maximum possible).¹⁹⁷ This is a major challenge for DEFCs. However, without full oxidation of alcohols (to $\text{CO}_2/\text{CO}_3^{2-}$), the degradation of fuel cell performance is thought to be less of a problem when using AAEMs;^{2a} full oxidation would involve adsorbed CO, which is an intermediate of full alcohol oxidation and a major Pt catalyst poison. It is generally believed that there is a higher chance of achieving full ethanol oxidation in alkaline systems compared to acid systems, although the formation of CO_3^{2-} instead of/as well as CO_2 can make product analysis more difficult with techniques such as DEMS.¹⁹⁸

As such, there has been a lot of research into more active EOR catalysts for use in alkali media.¹⁹⁹ As can be expected, Pt-based catalysts have been considered.^{182c,200} Pd and Pd alloy catalysts are of increasing prevalence in the literature as non-Pt options where C-C bond breakage has been reported (under conditions such as lower NaOH concentrations).^{164b,183,201} It is believed that the sites of the Pd where there are adsorbed OH (OH_{ads}) species are the catalytic active sites rather than the Pd atoms themselves.²⁰² However, the *in situ* durability testing (500 h) of Pd/C anode catalysts in AAEM-DEFCs show that the performance losses observed are due to the growth in Pd particle size (the performance of the Fe-Co cathode catalyst used remained constant).²⁰³ Oxide supported Pd catalysts have also been considered where Pd-NiO was reported to be a good option for EOR.^{204,205} It is believed that the formation of OH_{ads} on the metal oxide can transform carbonaceous species to CO_2 at lower potentials (releasing Pd sites for further reaction).²⁰⁶ PdAu (90 : 10) catalyst yielded a higher AAEM-DEFC performance compared to PdAu catalysts with other ratios and Pd- and Au-only benchmark catalysts. The presence of gold oxide/hydroxyl species is thought to be important.²⁰⁷ Datta *et al.* reported that PdAuNi catalyst produced improved AAEM-DEFC performances compared to Pd-, PdNi, and Pd-Au benchmarks;²⁰⁸ this catalyst also produced higher yields of acetate and CO_3^{2-} (*cf.* acetaldehyde) compared to the other catalysts. Zhao *et al.* have reported a PdIrNi high performance EOR catalyst for AAEM-DEFCs.²⁰⁹ This catalyst performed much better compared to Pd, PdNi and PdIr benchmarks. PdRu has also been studied (see later).²¹⁰ Li and He report that *in situ* reduction of Pd-layers on Ni foam gave higher AAEM-DEFC performances compared to conventional brushed Pd/Ni-foam anodes (164 mW cm^{-2} compared to 81 mW cm^{-2} at 60°C when tested in comparable ethanol- O_2 fuel cells containing a Tokuyama A201 AAEM).²¹¹ Au- and Ni-base catalysts (Pt- and Pd-free) have also been considered as catalysts for EOR in alkali.^{129,212} As an example,



RuNi catalysts have been reported to produce $8\text{--}9\text{e}^-$ per ethanol molecule on average (mixture of H_3COO^- and CO_3^{2-} as products).²¹³

Sun *et al.* considered the use of an alkali-doped PBI membrane (APM) for use in AAEM-DEFCs.²¹⁴ An *et al.* compared a CEM (Nafion®-211), an AEM (Tokuyama A201), and an APM in DEFCs.²¹⁵ They concluded that AAEM had the best conductivity and mechanical properties and the lowest Na^+ permeability, the CEM has the lowest ethanol permeability and the APM had the best thermal stability but the poorest species permeability. Overall the AAEM case was considered to have the best balance of characteristics for application in DEFCs but the thermal stability of the AAEMs need improvement.

In 2009, Bianchini *et al.* reported a AAEM-DEFC that gave a peak power density of 170 mW cm^{-2} at $80\text{ }^\circ\text{C}$ with the selective production of acetate when fuelled with ethanol (10% mass) in aqueous KOH (2 mol dm^{-3}) and with an active supply of O_2 to the cathode;²¹⁶ the DEFC utilised an anode containing a PdNiZn/C catalysts on Ni foam, an Acta Hypermec™ K-14 cathode, and a Tokuyama A201 AAEM. The performance dropped to a still respectable 58 mW cm^{-2} in a passive (air-breathing) AAEM-DEFC at $20\text{ }^\circ\text{C}$. More recently Chen *et al.* have reported a peak power density of 176 mW cm^{-2} ($\text{OCV} > 0.8\text{ V}$) in a AAEM-DEFC at $80\text{ }^\circ\text{C}$ when fuelled with ethanol (3 mol dm^{-3}) in aqueous KOH (3 mol dm^{-3}) and supplied with dry O_2 at the cathode;²¹⁰ the fuel cell utilised a CCM containing a Tokuyama A201 AAEM, a $\text{Pd}_3\text{Ru/C}$ anode catalyst on Ni foam (with a Nafion® ionomer binder), and a MnO_2 nanotube cathode catalyst (with Tokuyama AS-4 AEI). The enhancement of performance over the use of a benchmark Pd/C anode catalyst was attributed to the formation of RuO_xH_y at low potentials and weak CO adsorption.

Zhao *et al.* reported an AAEM-DEFC peak power performance of 185 mW cm^{-2} at a lower $60\text{ }^\circ\text{C}$ temperature using a Acta “non-Pt anode catalyst” supplied with ethanol (3 mol dm^{-3}) in aqueous KOH (5 mol dm^{-3}) and a $\text{Pd}_3\text{Au/CNT}$ catalyst supplied with O_2 supply at the cathode;²¹⁷ the DEFC contained a Tokuyama A201 AAEM and Tokuyama A3 was used as the AEI. The performance was higher than those obtained when using a Pd/CNT or a Au/CNT cathode catalysts. The Pd_3Au catalyst where the Pd and Au were physically mixed gave better performances than the alloyed and core-shell analogues. This performance was still lower than Zhao *et al.*’s alkaline-acid DEFC concept where a peak power performance of 360 mW cm^{-2} at $60\text{ }^\circ\text{C}$ was obtained with a Nafion-212 CEM, a PdNi/C-Ni-foam anode, and a Pt/C (60% mass) cathode catalyst (Nafion ionomers used at both electrodes);²¹⁸ the fuel supply was ethanol (3 mol dm^{-3}) in aqueous NaOH (5 mol dm^{-3}) and cathode supply was H_2O_2 (4 mol dm^{-3}) in aqueous sulfuric acid (1 mol dm^{-3}).

AAEM-based directly ethylene glycol fuel cells (DEGFC). Ethylene glycol (EG) is a low toxicity fuel option in AAEM-based fuel cells where the molecules contain a single C-C bond as with ethanol but where the C/O ratio = 1 rather than 2.^{18c,219} *Ex situ* studies show that the EG oxidation activities in OH^- and CO_3^{2-} containing aqueous electrolytes (EG oxidation activity in $\text{OH}^- >$ in CO_3^{2-}) are superior to the activities seen with methanol in

OH^- electrolyte.²²⁰ EG oxidation activities are also generally higher than seen with other polyhydric alcohols in alkali (EG > glycerol > methanol > erythritol > xylitol).¹⁷¹ As with ethanol, the full oxidation of EG molecules is rare and a variety of side products are commonly observed: glycolate, glyoxalate, oxalate, formate, glycol aldehyde and glyoxal.^{219c,221} However, full oxidation of EG to $\text{CO}_2/\text{CO}_3^{2-}$ appears to be easier than with ethanol due to the lower C/O ratio, especially when application-relevant concentrations of the alcohol fuels are used.^{220,222} For Pt, the partial oxidation pathway to oxalate is non-poisoning, but the pathway to C1 species (CO and CO_3^{2-}) is poisoning due to the adsorption of CO on the catalyst surface.²²⁰ Adding Bi and Ni to the Pt anode catalyst decreases the level of C-C bond breaking and directs the reaction to the oxalate pathway (yielding higher activities).^{219c} Pd/C catalysts that have been stabilised with the addition of various oxides (*e.g.* Pd– $\text{Mn}_3\text{O}_4/\text{C}$) have been shown to give good EG oxidation activities.²⁰⁴ A PdIn₃ catalyst (synthesised using the sacrificial support method) has been reported with a very high EG oxidation mass activity.²²³ In addition, cathode catalysts are available that are tolerant to EG (*e.g.* perovskite types or Ag).^{171,219b}

Zhao *et al.* have recently reported a AAEM-based DEGFC that yielded a peak power density of 112 mW cm^{-2} at $90\text{ }^\circ\text{C}$ when supplied with O_2 at the cathode and EG (1 mol dm^{-3}) dissolved in aqueous KOH (7 mol dm^{-3}) at the anode.^{18c} The fuel cell contained an APM, PdNi/C/Ni-foam anode catalyst, an Acta Hypermec™ non-PGM cathode catalyst. The peak power density dropped to 90 mW cm^{-2} when air was used instead of O_2 at the cathode.

AAEM-based direct glycerol fuel cells. Highly viscous and non-toxic glycerol (C3 with a C/O ratio = 1) has also been studied as a fuel in alkaline AAEM-based fuel cells.^{184,224} This interest partially stems from glycerol being an unwanted side product from the production of biodiesels.²²⁵ Full oxidation of glycerol has been achieved using enzyme cascades in an enzymatic fuel cell.²²⁶ However, in alkali, as with ethanol and EG, glycerol tends to be only partially oxidised leading to the production a wide variety of products: *e.g.* glyceraldehyde, glycerate, glycerone (dihydroxyacetone), formate, glycolate, hydroxyppyravate, oxalate, tartronate, and mesoxalate.²²⁷ Then again, as glycerol contains $3 \times$ -OH groups, it is a recognised feedstock for the production of a range of value-added chemicals and AAEM-based direct glycerol fuel cells may be useful for cogeneration of energy and such chemicals.^{224e,228} An AAEM-based direct glycerol fuel cell has been recently shown to selectively generate tartronate.^{224a}

Glycerol can have higher *ex situ* activities on Au electrodes in alkali compared to other alcohols (methanol, ethanol, and ethylene glycol) and higher than on Pt.²²⁹ There is spectroscopic evidence that full oxidation to $\text{CO}_2/\text{CO}_3^{2-}$ may be achieved on polycrystalline Au in alkali.²³⁰ A recent study into Pd_xBi catalysts (synthesised using the sacrificial support method) reports that Pd_4Bi displays the highest activity towards glycerol oxidation.²³¹ This report shows that the catalyst is selective towards production of aldehydes and ketones at low potentials, hydroxyppyravate at medium potentials, and CO_2 at high potentials in the forward voltammetric sweeps. However, the



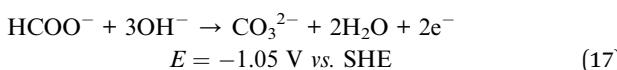
catalyst is history dependent and carboxylates are selectively produced on the reverse voltammetric sweep. Glycerol oxidation mass activities are also high on PdIn catalysts.²²³

The power densities of glycerol fuelled fuel cells are generally <200 mW cm $^{-2}$ and with low Faradic efficiencies (due to incomplete oxidation to CO₂/CO₃²⁻). However, there are reports of power densities of 265 mW cm $^{-2}$ being obtained.²³² There are even reports that glycerol can self-polymerise inside the fuel cell. Li *et al.* obtained 184 mW cm $^{-2}$ at 80 °C with an AAEM-based glycerol/O₂ fuel cell containing a Tokuyama AAEM and AEI, a Pt/C anode, and an Acta Hypermec™ non-PGM cathode;^{224c} the anode was supplied with an aqueous solution containing crude glycerol (1 mol dm $^{-3}$) and KOH (6 mol dm $^{-3}$) at 30 psi back pressure. The use of crude glycerol (88% mass glycerol, a by-product of soy-bean biodiesel production) did not produce a drop in performance compared to much more expensive high purity glycerol (99.8%). The Pt/C anode catalyst clearly had stability in the presence of the impurities of the crude glycerol (*e.g.* methanol, fatty acids [*e.g.* soaps], transesterification catalyst residues, and element such as K, Ca, Mg, Hg, P, S, As *etc.*).

Non-alcohol C-based fuels

Formate [HC(=O)O⁻],²³³ glucose (C₆H₁₂O₆),²³⁴ and urea [H₂NC(=O)NH₂] and urine²³⁵ have also been studied as alternative C-based fuels in AAEM-containing fuel cells. Dimethylether has also been studied in fuel cells containing Nafion® CEMs but where performances were highest when the dimethylether was dissolved in aqueous alkaline anolytes (*cf.* acid anolytes).²³⁶ The power densities achieved with glucose-fuelled AAEM-based fuel cells are currently below 50 mW cm $^{-2}$. For example, Zhao *et al.* achieved a peak power density of 38 mW cm $^{-2}$ at 60 °C when supplying a fuel cell containing a Tokuyama A201 AAEM (PdNi anode and Acta Hypermec™ K14 cathode catalysts) with aqueous glucose (0.5 mol dm $^{-3}$) containing added KOH (7 mol dm $^{-3}$). Obviously, there is a wide range of reaction pathways that are possible that will produce a variety of electrochemical intermediates and products. 24e⁻ would be needed for the full oxidation of glucose, which is highly unlikely to occur. Glutonate ($n = 2$ e⁻ reaction) is the most common product in alkali.^{234d} The urea (urine) fuel cells containing alkaline polymer electrolyte materials produced peak power densities of <15 mW cm $^{-2}$;²³⁵ however, as with many of the fuels mentioned above, this fuel cell concept is in a very early stage of development.

AAEM-based direct formate fuel cells (ADFFC). The interest in ADFFCs stems from the low (highly negative) anode potential of the formate oxidation reaction (compared to methanol and ethanol *etc.*):



Zhao *et al.* achieved a peak power density in an alkaline direct formate fuel cell (ADFFC) at 80 °C of 130 mW cm $^{-2}$ with aqueous potassium formate (5 mol dm $^{-3}$) as the fuel and when

using a Pd/C anode catalyst, commercial Acta Hypermec™ K14 cathode catalyst, QA polysulfone AAEM and AEI, and dry O₂ supply to the cathode;^{233a} this raised to >250 mW cm $^{-2}$ with the addition of KOH (1 mol dm $^{-3}$) to the fuel supply. Haan *et al.* achieved a peak power density of 267 mW cm $^{-2}$ at 60 °C in a ADFFC with a fuel supply consisting of HCOO⁻K⁺ (1 mol dm $^{-3}$) in aqueous KOH (2 mol dm $^{-3}$), a catalyst coated Tokuyama A201 AAEM (Pd black anode catalyst, Pt black cathode catalyst, and Tokuyama AS-4 AEI), and a humidified O₂ cathode supply;^{233b} the performance again decreased when the KOH was removed from the fuel supply (157 mW cm $^{-2}$).

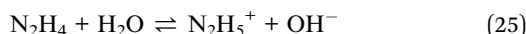
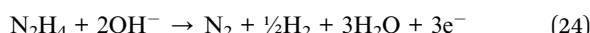
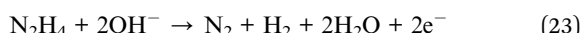
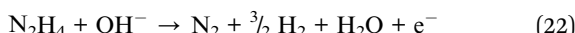
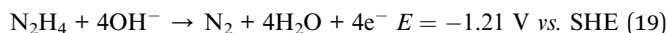
AAEM fuel cells supplied with N-based fuels²³⁷

Hydrazine and hydrazine hydrate.^{2p} Hydrazine (H₂N-NH₂) is a high volumetric energy density liquid fuel (at room temperature and atmospheric pressure) that contains 12.6% mass hydrogen. N₂H₄ has also been used in the 1960s in traditional AFCs including those that provided electric power in space satellites.²³⁸ As early as 1972, the Government Industrial Research Institute, Panasonic, and Daihatsu (all in Japan) produced an experimental N₂H₄-air AFC vehicle.²³⁹ Hence, N₂H₄ has been proposed for use in AAEM-based direct hydrazine fuel cells (DHFCs).^{29e,104e,118e,240} However, anhydrous N₂H₄ is highly toxic (mutagenic/carcinogenic) and very unstable (a rocket fuel). Technologies have been developed for practical application where N₂H₄ is chemically fixed to storage materials such as polymers that contain carbonyl bonds [forming less toxic hydrazone (>C=N-NH₂) and hydrazide (-C(=O)-NH-NH₂) functional groups]. The N₂H₄ can be released on addition of solvents when required.²⁴¹

Hydrazine hydrate (N₂H₄·H₂O) is, however, considered stable enough to be viable as a fuel for AAEM-DHFCs.²⁴² N₂H₄·H₂O is an industrially used chemical reagent (20 ktons per year distributed in Japan) and it is less volatile than alcohols (so air emissions will be potentially lower). It has a freezing temperature of -50 °C (so it can be easily used in cold climates) and it has a flame point of 74 °C (at 1 atm). Hence, at aqueous concentrations of <60%, N₂H₄·H₂O is not flammable. The carcinogenic risk of N₂H₄·H₂O (class 2B by International Agency for Research on Cancer) is equivalent to petroleum so the careful handling of the fuel is no more than currently accepted guidelines for petroleum.

The full (4e⁻) electro-oxidation of N₂H₄/N₂H₄·H₂O results in the generation of harmless N₂ and H₂O products (eqn (19) – the complete cell reaction is given by eqn (20) [along with the ORR given in eqn (9)]], while H₂ and NH₃ are produced on partial oxidation (eqn (21)–(24)).²⁴³ It has also been proposed that the use of high pH conditions suppresses undesirable hydrolysis reactions (eqn (25)).²⁴⁴ Unlike with the B-containing fuel vectors (see below), no product (BO₂⁻) accumulation occurs at the anode that requires spent fuel treatment, as all products are gaseous. The potential of the N₂H₄/O₂ cell reaction is larger than the width of potential window of stability of water (on Pt) and so there is a risk of the HER occurring (eqn (26)). Despite this, OCV values in the range 0.8–1.0 V are typically observed.



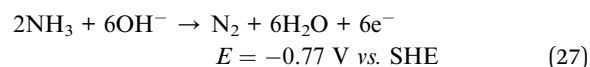


A variety of metal catalysts have been studied for use as anode catalysts for $\text{N}_2\text{H}_4/\text{N}_2\text{H}_4 \cdot \text{H}_2\text{O}$ oxidation in DHFCs (Ni, Co, Fe, Cu, Ag, Au, and Pt).²⁴⁵ Ni-based^{242,246} and Co-based^{29e,118c} catalysts appear most promising (Co catalysts have also been examined in the cathodes). For example, Sakamoto *et al.* used a combinatorial electrochemistry approach with 79 catalyst candidates and report that $\text{Ni}_{0.87}\text{Zn}_{0.13}$, $\text{Ni}_{0.9}\text{La}_{0.1}$, $\text{Ni}_{0.8}\text{Zn}_{0.1}\text{La}_{0.1}$, and $\text{Ni}_{0.6}\text{Fe}_{0.2}\text{Mn}_{0.2}$ catalysts have $\text{N}_2\text{H}_4 \cdot \text{H}_2\text{O}$ oxidation activities that are more active than a Ni/C reference catalyst.^{242a} Cu-based catalysts have also been proposed for use at the anode of DHFCs.²⁴⁷ For example, a totally irreversible and diffusion-controlled oxidation of N_2H_4 is reported on Cu-nanocubes on graphene paper with N_2 and H_2O as the reaction products.²⁴⁸ The *in situ* formed copper hydroxide/oxide layers surface layers on the Cu catalysts are thought to enhance the activity and durability of the electrocatalyst. Selectivity to N_2 and H_2O as sole products of hydrazine oxidation, as opposed to forming NH_3 (eqn (21)), is of critical importance in practical DHFC development.^{242,246} *The promise of such fuel cells as a “clean energy technology” will easily be compromised by a single digit ppm of NH_3 in the exhaust of a DHFC vehicle.*

DHFC are liquid fuel fed fuel cells with a highly reactive fuel. As a result, the fuel crossover is a natural concern of all designs. The requirement for no hydrazine oxidation on the cathode is a very strong one. As with other types of AAEM-based fuel cells, non-PGM catalysts, such as Ag, can be used in the cathodes and can have low N_2H_4 oxidation activities (mitigating against fuel crossover effects).²⁴¹

Peak power densities of over 600 mW cm^{-2} have been achieved by Daihatsu Motor Co. Ltd. (Japan) in an AAEM-DHFC at 80°C containing a QA-polyolefin AAEM with Ni anodes and Copolypyrrole/C cathodes (supplied with humidified O_2) and a fuel supply of an aqueous solution of N_2H_4 (5% vol) containing KOH (1 mol dm^{-3}).²⁴³ As a comparison involving the use of H_2O_2 at the cathode and a Nafion®-117 PEM, a PEM-DHFC performance of $>1000 \text{ mW cm}^{-2}$ has been achieved at 80°C (PtNi/C anode and Au/C cathode).²⁴⁹ Performances can be increased on increasing NaOH concentration in the anode fuel supply up to concentrations of 4 mol dm^{-3} (reduced anode overpotentials).²⁴⁴ However, concentrations higher than these reduce performances as viscosity increases and this causes mass transport voltage losses at the cathode.

Ammonia and ammonium carbonate. Ammonia (17.6% mass hydrogen content) has also been studied as an alternative fuel for AAEM-containing fuel cells.²⁵⁰ The complete electrochemical oxidation of NH_3 (3e⁻ needed to oxidise each NH_3) and the related overall reaction (in alkali) are given by:



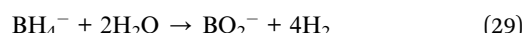
Power densities with NH_3 have been low to date ($<15 \text{ mW cm}^{-2}$) with OCVs $< 1.0 \text{ V}$; these values are lower compared to the historic use of KOH as an aqueous electrolyte (*ca.* 50 mW cm^{-2}).²³⁷ $(\text{NH}_4)_2\text{CO}_3$ has also been considered for use in AAEM-based fuel cells but power densities were $<1 \text{ mW cm}^{-2}$.²⁵¹

A major problem is the very sluggish ammonia oxidation reaction in alkali.²⁵² Only PtIr, PtRu, and PtRh catalysts show a reasonable ability to oxidise NH_3 with the least serious affinity towards the surface poison N_{ads} . There can be recovery from such N_{ads} surface poisoning of Pt with H_2 treatment of the anode.^{250c} The presence of Pt(100) surfaces appears to be important.^{252a,f,g} Reactive azides species may also be generated as intermediates.^{252h} Oxygenated (O_{ads} and OH_{ads}) can form on the catalyst surface with the presence of water and this (along with N_{ads}) also inhibits the catalytic performance.²⁵³ Interestingly, NH_3 oxidation reaction is remarkably different on Pt when studied in non-aqueous media (the formation of surface oxygenated species is prevented) yielding N_2 as the dominant product and allowing the Pt to remain continuously active.²⁵³ This study also shows that Pd becomes highly active towards NH_3 oxidation in non-aqueous media (a low activity is seen with Pd in aqueous KOH due to severe surface passivation).

APEFCs fuelled with H_2 that is produced from NH_3 reformation may have technological promise. AFCs can tolerate NH_3 (several %) in the H_2 fuel.²⁵⁴ However, PEMFCs are poisoned by traces (1–2 ppm) of NH_3 and performances decay (reversible but only after several days of operation with pure H_2).²⁵⁵ the PEMs themselves will slowly convert to the NH_4^+ forms lowering conductivity and water contents.²⁵⁶ Hence, using H_2 derived from NH_3 in PEMFCs would require prohibitively expensive scrubbing of the reformed H_2 supplies.

AAEM fuel cells fuelled with B-based fuels

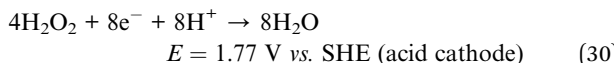
Alkaline direct borohydride fuel cells.²⁵⁷ Sodium borohydride (NaBH_4) is well known reducing agent in organic chemistry and a potential H_2 storage material (contains 10.6% by mass hydrogen). It is stable in concentrated aqueous alkali ($t_{1/2} = 430 \text{ d}$ at $\text{pH} = 14$) but hydrolyses in acidic and neutral pH environments yielding metaborate and H_2 :



where BO_2^- is the empirical formula (Na/KBO_2 typically contain cyclic $\text{B}_3\text{O}_6^{3-}$ anions). BH_4^- is being investigated as a fuel in direct borohydride fuel cells (DBHFC). This includes mixed reactant systems.²⁵⁸ A BH_4^-/O_2 fuel cell has a high theoretical

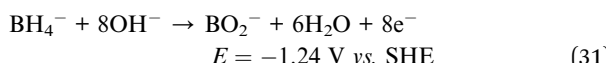


energy density of 9.3 kW h kg⁻¹ as it can release a maximum of 8e⁻ per BH₄⁻. DBHFCs are of particular interest to the defence industry for the portable power needs of the military and to power vehicles (e.g. underwater vehicles) where the use of H₂O₂ liquid oxidants have also been proposed (a BH₄⁻/H₂O₂ fuel cell has a theoretical energy density of 17 kW h kg⁻¹).²⁵⁹



Traditionally, the absence of AAEMs with adequate properties has meant that research efforts have traditionally focused on using CEMs in the DBHFCs (in Na⁺ form when exposed to aqueous solutions containing NaBH₄ and NaOH); this includes radiation-grafted CEMs.²⁶⁰ This configuration leads to the build-up of NaOH at the cathode over extended operational times with a concomitant and undesirable reduction of pH at the anode (in the absence of an engineering solution that resupplies NaOH to the anode from the cathode). However, CEM-DBHFCs can yield reasonable fuel efficiencies due to minimised BH₄⁻ crossover (CEMs are perselective towards positive charged ions).

Replacement of the CEM with an AAEM allows a balance:

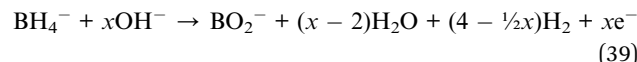
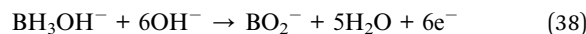
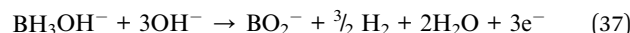
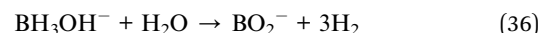


where the OH⁻ anions are produced at the cathode (eqn (9)) and consumed at the anode (eqn (31)). For both CEM- and AAEM-based systems, metaborate (not a major environmental pollutant) accumulates in the fuel supply; it can, however, be removed and converted back to BH₄⁻ but this is an energy intensive process. Higher BH₄⁻ crossover rates are also now observed with the use of AAEMs and this also limits the selection of cathode catalysts in AAEM-DBHFCs: Pt, Ag and Au cathode catalysts cannot really be used in systems with appreciable BH₄⁻ crossover as they are active towards BH₄⁻ oxidation. MnO_x-based ORR catalysts may be useful as they appear inactive to BH₄⁻ oxidation.²⁶¹ Operation at high current densities may mitigate against BH₄⁻ crossover to an extent due to a higher flux of OH⁻ anions being transported from the cathode → anode and consumption of the BH₄⁻ in the anode catalyst layers (lowering the localised concentration of BH₄⁻ concentration near the AAEM). The chemical stability of AAEMs is also critical as they are exposed to high concentrations of BH₄⁻ and OH⁻: a typical anode supply contains $\geq 6 \text{ mol dm}^{-3}$ OH⁻ (to ensure adequate BH₄⁻ stability). AAEM stability will be even more critical if peroxide is used as an oxidant ($E_{\text{cell}} = 2.1 \text{ V}$ with HO₂⁻/OH⁻ cathode supply):



The hydrolysis reaction is a serious problem in DBHFCs and is catalysed on many metals. This inevitably limits the selection of an anode catalyst. The BH₄⁻ oxidation and hydrolysis side reactions will happen in parallel to varying extents (as a

function of temperature, concentration, catalyst and anode potential *etc.*):



The formal reduction potential for the 8e⁻ BH₄⁻/BO₂⁻ redox couple is >300 mV negative to the formal potential of the HER (eqn (26)). It should therefore not be a surprise that the reduction of H₂O is thermodynamically favourable (a 1.64 V cell potential is wider than the potential window of stability for H₂O on Pt). Operating DBHFCs at high current densities (lower cell potential and higher anode potentials) will help to minimise parasitic HER. There are reports that the addition of small quantities of thiourea acts as a hydrolysis inhibitor.²⁶²

All of these factors reduce the number of e⁻ that are extracted from each BH₄⁻ molecule (reduces fuel efficiency). The HER is especially problematic in fuel cell stacks²⁶³ as H₂ evolution in the early cells of the stack can affect the operation of cells farthest away from the inlet (*i.e.* losses occur due to uneven fuel distributions). The evolution of H₂ gas must also be controlled unless it is desired to produce H₂ for oxidation at the anode of a PEMFC (an indirect DBHFC).²⁶⁴ Therefore, $n < 8\text{e}^-$ oxidation of BH₄⁻ is generally unavoidable and OCVs will not approach the theoretical maximum (due to a mixed potentials from the presence of both BH₄⁻/BO₂⁻ and H₂O/H₂ redox couples).

Pt, Pt-alloys, Ag, Au, Zn, Ni, Pd, Os, Cu, and hydrogen storage alloy based catalysts have all been studied for BH₄⁻ oxidation.²⁵⁷ The common claim that Au catalysts oxidise BH₄⁻ *via* 8e⁻ without competing hydrolysis reactions may not be universally true, while Pt can actually achieve near full BH₄⁻ oxidation (*e.g.* at low anode potentials),²⁶⁵ however, studies with Au and Pt may be complicated by catalyst poisoning by BH₄⁻ oxidation intermediates (possibly BH₃OH⁻).²⁶⁶ Ag-based catalysts are less active and the presence of oxidised surface oxide species appears to be a prerequisite for borohydride oxidation.²⁶⁷ Pd-based catalysts can achieve higher peak power densities and reduce the rate of H₂ evolution.²⁶⁸ The need for a rational design of binary anode catalysts, such as Au₂Cu(111), has been identified.²⁶⁹

In general for AAEM-based DBHFCs, peak power densities up to 250 mW cm⁻² are reported (OCVs values tend to be in the range 0.8–1.0 V).^{262b,270} Huang *et al.* argue that the use of KBH₄ can give improved performances over NaBH₄ in AAEM-DBHFCs (lower KBH₄ permeability and higher KOH-conductivity in the PVA AAEMs).^{270a} The highest AAEM-based DBHFC performance reported to date is by Zhang *et al.* who achieved 321 mW cm⁻²

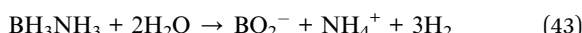
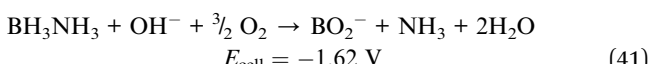
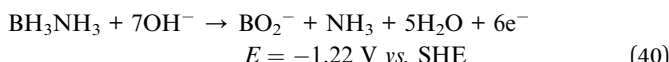


(at 700 mA cm⁻²) at 40 °C in a BH₄⁻/O₂ fuel cell [anode supply = NaBH₄ (1 mol dm⁻³) in aqueous NaOH (3 mol dm⁻³) and Pt/C catalysts used in both electrodes, AAEM = a guanidinium-poly(silsesquioxane)-PTFE composite (IEC = 1.14 meq. g⁻¹ and 65 mS cm⁻¹ at 60 °C)].²⁷¹

For comparison, Miley *et al.* achieved 680 mW cm⁻² (OCV of 1.95 V) in a Nafion®-based NaBH₄/H₂O₂ DBHFC stack at 60 °C with a Pd anode catalyst and an Au cathode catalyst (anode = 18% mass NaBH₄ in alkali and cathode = 17% mass H₂O₂ in acid).²⁷² The concept of using an alkali anode and an acid cathode is a recurring theme²⁷³ but may not be relevant to AAEM-containing DBHFCs. Liu *et al.* have achieved 663 mW cm⁻² at 65 °C in a BH₄⁻/O₂ (*i.e.* non-peroxide) DBHFC containing a porous polymer fibre membrane (PFM) separator and using aqueous KBH₄ (0.8 mol dm⁻³)/KOH (6 mol dm⁻³) as the fuel feed [CoO cathode catalyst and LiNiO₃ anode catalyst];²⁷⁴ the performance dropped to (a still respectable) 390 mW cm⁻² when Nafion® NRE-212 was used instead of the PFM.

Mixed N and B fuel options. Another proposed concept involved the use of an alkaline mixed BH₄⁻ + N₂H₄ anode feed where a fuel cell containing AAEM (from Asahi Kasei Corporation) outperformed a CEM-containing analogue.²⁷⁵ The performance of the AAEM-containing fuel cells increased with increasing hydrazine content and the cell supplied with hydrazine only aqueous feed (15% mass hydrazine in 10% mass NaOH) produced the highest performance (92 mW cm⁻² with dry O₂ cathode supply).

Alkaline direct ammonia borane (AB = H₃B ← NH₃) fuel cells have also been proposed.^{250b,276} AB (also known as borazane) is a water soluble white crystalline solid containing 19.5% mass hydrogen (AB is a proposed hydrogen storage material), which is stable at high pHs.²⁷⁷ Au and Ag catalysts again look promising for AB oxidation in alkali (MnO₂ catalysts appear unaffected by AB so again has promise as a cathode catalyst).^{276e,278} The reactions (and side-reactions) involved in the oxidation of AB in alkali (and for an overall AB-AFC) are given below:



The latter non-electrochemical reaction (eqn (43)) is thermodynamically spontaneous and so it is important that catalysts that are active for AB oxidation but not AB hydrolysis. An AB-AFC is less efficient than a BH₄⁻-AFC due to the lower number of e⁻ extracted per fuel molecule (6 [or 3 if eqn (42) is operating] *vs.* 8), despite similar E_{cell} values. Lu *et al.* first reported an AAEM-based fuel cell fuelled with AB,^{276e} which concluded that the 3e⁻ process (eqn (42)) was predominant (along with some capacity loss *via* hydrolysis). More recently Xu *et al.*^{276c} reported that a direct AB fuel cell containing a

Tokuyama AEI (IEC = 2 meq. g⁻¹) and a Tokuyama 27 μm thick AAEM (IEC = 1.8 meq. g⁻¹) achieved an OCV of 0.9 V and a peak power density of >110 mW cm⁻² at 45 °C [Pt-based anode and cathodes, anode feed containing AB (0.5 mol dm⁻³) in aqueous NaOH (2 mol dm⁻³), humidified cathode feed]; however, H₂ evolution was still a problem. In reality, and as expected from the discussion above, the BH₃ component of AB is more easily oxidised than the NH₃ component. Considering AB is expensive to produce (or regenerate from BO₂⁻), this fuel may only be suitable for niche applications.

Finally, other B-based fuel options exist but have not been considered as a fuel option in AAEM-based fuel cells. This includes the volatile liquid borazine [(BH)₃(NH)₃, a cyclic molecule that is isoelectronic and isostructural with benzene]. Borazine is normally a trace PEMFC poison when AB is being used as a H₂ storage material and it can also polymerise into polyborazylene “gums”.

The operation of carbonate-cycle APEFCs

Impacts and promise for carbonate anions. As discussed earlier, a pressing issue facing the implementation of AAEMs and AEIs for a whole host of applications are their chemical stability in highly alkaline (OH⁻) media. Most researchers have responded to this limitation by designing speciality membranes. Additionally, operation with air supplies to the cathode is desired, which is problematic due to the potential for carbonate formation in the electrolyte (eqn (1) and (2)).

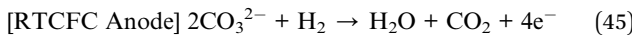
Even though there is growing awareness that CO₃²⁻ does not generally have such a serious deleterious effect on APEFC performance,^{9e,152,279} HCO₃⁻, however, has a strong negative effect.^{43a,116a,280} HCO₃⁻ has a much larger hydration radius than OH⁻ (*ca.* 4 *vs.* 3 Å respectively) with the same valence,²⁸¹ which significantly reduces conductivity and device performance in the presence of CO₂.⁹³ On the other hand, CO₃²⁻ anions have double the valence of OH⁻, which means that despite its larger hydration radius,^{281b} there will be lesser effect on AAEM conductivity.¹⁵² In addition, even commercial AEMs (that were not developed specifically for highly alkaline environments, such as that found in APEFCs), and those that are not stable in the presence of aqueous OH⁻ (such as a number of phosphonium exemplars), are far more stable in HCO₃⁻/CO₃²⁻ compared to OH⁻ environments/forms.^{9e,75,279b}

All of this suggests the possibility of an alternative high impact (disruptive) approach: to abandon OH⁻ anions altogether and transition to low temperature devices that use CO₃²⁻ conduction (cycles). The deliberate utilisation of CO₃²⁻ in low temperature electrochemical systems has only been investigated since 2006, with the lion's share of the effort concentrated on the development of a room temperature carbonate fuel cells (RTCFC).²⁸² However, there has been a recent but slow increase in the amount of work being conducted to investigate alkaline electrochemical devices that purposefully utilise CO₃²⁻ anions for energy generation (fuel cells), to facilitate new chemical synthesis pathways, and for CO₂ separation.^{279,283}

Selective carbonate formation at the cathode. For the traditional ORR at the cathode (eqn (9)), it has been reported that the



presence of CO_2 and $\text{CO}_3^{2-}/\text{HCO}_3^-$ does not noticeably impact on the intrinsic electrochemical kinetics;^{279b,284} however, there may be a negative impact on mass transport near the electrode surface (that leads to reduced device performance). The loss of performance has also been echoed in CO_3^{2-} -intended devices; generally low current densities have been observed compared to OH^- -based devices. This is hindered by the near non-existence of CO_3^{2-} -focused materials development in the literature. For example, only one catalyst ($\text{Ca}_2\text{Ru}_2\text{O}_7$) has been reported in the literature that can produce CO_3^{2-} anions through a direct electrochemical reduction with high selectivity (eqn (44) rather than the reaction in eqn (9) that generates OH^- ions):^{283c,d}



Such catalysts, including when doped with Bi, exhibit intriguing behaviour in the presence of CO_3^{2-} in aqueous alkali.²⁸⁵ However, $\text{Ca}_2\text{Ru}_2\text{O}_7$ catalyst still has many issues. Most notably, it is hard to synthesise and it has a CO_2 adsorption strength that is too large (leads to an optimum CO_2 concentration at the cathode of 10% mol, which yields a very low CO_2 activity in the cell).

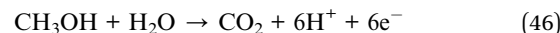
The direct formation of CO_3^{2-} in these devices is important since the competing indirect pathway (*i.e.* involving the chemical reaction between CO_2 and electrochemically generated OH^-) still involves OH^- desorption (implications for the durability of the AAEM and AEI). The indirect route also risks the production of HCO_3^- , which will lower the ionic conductivity of the AAEM and AEI. However, researchers have also failed to make AAEMs with the appropriate functionality to maintain the anions as CO_3^{2-} . The equilibrium balance between OH^- , CO_3^{2-} and HCO_3^- in the membrane is dictated by the effective $\text{p}K_a$ values of the cationic functional groups. All existing AEMs have effective $\text{p}K_a$ values that are either too high (leading to mostly OH^-) or too low (leading to mostly HCO_3^-). Thus, even if CO_3^{2-} were produced with 100% selectivity at the catalyst, the lack of CO_3^{2-} -specific membranes would cause the concentration of CO_3^{2-} to shift towards HCO_3^- and OH^- ($+\text{CO}_2$) anyway. This suggests that a concerted materials design effort is needed in this area.

Carbonate as an oxidizing agent at the anode. It has been shown that the HOR by CO_3^{2-} (eqn (45)) is kinetically facile,^{279a} perhaps even more so than the HOR by OH^- (eqn (8)); however, similar to the ORR, the presence of CO_3^{2-} seems to have a deleterious effect on the mass transport near the electrode surface.²⁸⁶ Carbonate has also shown the ability to oxidise CH_3OH at a higher rate than OH^- anions on NiO catalysts.¹⁸⁰ It is thought that the enhanced kinetic rate is due the inherent difference in how the two anions oxidise fuels: OH^- essentially oxidises species by accepting protons whereas CO_3^{2-} oxidises species by abstracting an oxygen and donating it to hydrogen. Taking advantage of that mechanism, there has been other work outside of the fuel cell arena, where CO_3^{2-} anions have shown the ability to electrochemically activate methane at room temperature (see later section on CO_2 reduction

electrolysers)^{283a,b} unlike OH^- ,²⁸⁷ opening new areas for research on electrochemical synthesis that was simply not possible until now. Although CO_3^{2-} has shown initial promise as the reacting/conducting anion in low temperature electrochemical devices, a considerable amount of work remains to develop a solid fundamental understanding of the reaction mechanisms that are occurring and the materials requirements.

Hybrid AAEM/PEM fuel cells

As described in the previous sections, fuel cells and other APEFCs operating at high pH using AAEM materials have attracted attention due to their favourable operating parameters with major advantages including the use non-noble metals at the cathode and a wider range of fuel options at the anode.^{2,288} However, the lower ionic conductivity of AAEMs compared to PEMs (such as Nafion®) at lower RHs is a concern because it may lower the performance.⁵² PEMFCs and APEFCs require careful water management because water is consumed at the cathode in APEFCs and water is needed for ion hydration (in both). Eqn (8) and (9) show the reactions at an APEFC anode and cathode, respectively, while eqn (6) and (7) give the acidic PEMFC analogues. In both cases, the overall reaction is given in eqn (10). The analogous anode reactions for methanol fuelled systems are given by eqn (12)/(13) and (46):



Water management is challenging in the PEMFCs because water is produced at the cathode and needed at the anode (for hydration of the proton and production of carbon dioxide in the case of methanol). APEFCs are also challenged by water management because water is consumed at the cathode (to make the OH^- anions) and needed for hydration of the ions. Water is produced at the anode for both H_2 and methanol fuelled AAEM-based fuel cells. Thus, significant resources or careful system design are required to recycle the water from one electrode to the other for both PEM-based and AAEM-based fuel cells. In both cases, more water is produced than consumed due to the net production of water (eqn (10)).

Hybrid PEM/AAEM membranes and the junction potential.

Bipolar membranes are a combination of anion and cation conducting materials where an ionic junction is formed and the type of conducting ion changes at this materials junction.²⁸⁹ Such bipolar/hybrid membranes have been used in a wide range of electrochemical devices such as those that involve CO_2 separation *via* electrodialysis.²⁹⁰ Hybrid (bipolar) fuel cells can be constructed using an AAEM anode and PEM cathode (Fig. 5a), or PEM anode and AAEM cathode (Fig. 5b). The latter configuration, where water is created at the junction (eqn (47)), is of more interest for fuel cells because it takes advantage of the high conductivity and established infrastructure of PEMs and exploits the advantages of a high pH cathode. It also can provide self-hydration within the membrane at the junction:



This contribution allows the use of non-Pt catalysts at the cathode and an opportunity to generate the water at a junction that can be located close to where the H_2O is consumed at the alkaline cathode.²⁹¹ In principle, the PEM|AAEM junction can be placed anywhere within the structure. The water created at the PEM|AAEM junction is dual use and contributes to both the self-hydration of the membrane and the ORR at the cathode. Excess water can leave the system through either side of the structure. Thus, this structure uses a PEM anode (eqn (6)) and AAEM cathode (eqn (9)). The overall full cell reaction (sum of eqn (6), (9) and (47)) is the same as for PEMFCs and APEFCs (eqn (10)). In the case of a methanol fuelled system, the acid anode is given by eqn (46) and the overall full cell reaction at steady state is the same as for AAEM- or PEM-based DMFCs.

The equilibrium cell potential (E_{cell}) for the hybrid (bipolar) configuration needs to account for the reactions at each electrode and the junction potential (E_j) developed at the PEM|AAEM interface:

$$E_{\text{cell}} = E_{\text{Nernst}} + E_j = E_C - E_A + E_j \quad (48)$$

where E_{Nernst} is the difference between the cathode (E_C) and the anode (E_A) potentials. Using the Nernst equation, the following is obtained:

$$E_{\text{cell}} = E_C^{\circ} - E_A^{\circ} + \frac{RT}{2F} \ln \left[\frac{P_{\text{O}_2}^{\frac{1}{2}} P_{\text{H}_2}}{P_{\text{H}_2\text{O}}} \right] + \frac{RT}{F} \ln [a_{\text{OH}^-}^{\text{AEM}} a_{\text{H}^+}^{\text{PEM}}] + E_j \quad (49)$$

where E_C° and E_A° are the standard potentials for the cathode and anode reactions, R is the ideal gas constant, T is the absolute temperature, F is Faraday's constant, P_x is the partial pressure of gas x , and a_z^M is the activity of ion z in membrane M . At the PEM|AAEM interface, neutralisation of the mobile H^+ in the PEM and OH^- within the AAEM occurs leaving behind the fixed charges bound to the polymer membranes.^{291c} Neutralisation of the H^+ and OH^- ions continues until the electrostatic attraction of the fixed charges (counter ions bound to the PEM or AAEM polymer backbones) holding the ions in their respective membranes balances the diffusion across the membrane. At this point, the junction is in thermal equilibrium and a junction potential is created by the separation of fixed charge across the junction. The junction potential is given by eqn (50) and rearranged to eqn (51) recognising that $K_w = a_{\text{H}^+} a_{\text{OH}^-}$:

$$E_j = \phi^{\text{AEM}} - \phi^{\text{PEM}} = \frac{RT}{F} \ln \left(\frac{a_{\text{H}^+}^{\text{PEM}}}{a_{\text{H}^+}^{\text{AEM}}} \right) \quad (50)$$

$$E_j = \phi^{\text{AEM}} - \phi^{\text{PEM}} = \frac{RT}{F} \ln (a_{\text{H}^+}^{\text{PEM}} a_{\text{OH}^-}^{\text{AEM}}) - \frac{RT}{F} \ln (K_w) \quad (51)$$

where ϕ^M is the potential within phase M . In the hybrid, bipolar fuel cell, the theoretical maximum cell potential at 25 °C is the same as in a PEMFC or APEFC (1.23 V). Even though the Nernstian contribution ($E_C - E_A$) in eqn (48) is not 1.23 V, the difference between the Nernstian potential and cell potential is exactly off-set by E_j (eqn (51)). The width of the junction region

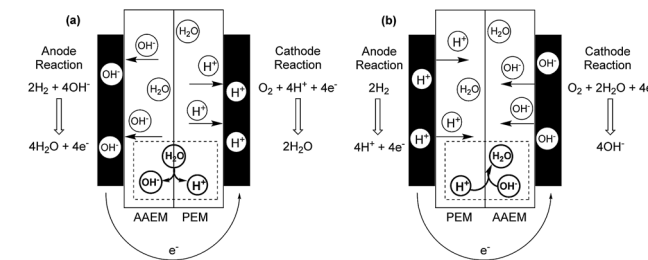


Fig. 5 Details of hybrid membrane fuel cells comprising of: (a) high pH AAEM anode + low pH PEM cathode; and (b) low pH PEM anode + high pH AAEM cathode.

(W) in the bipolar membrane is a function of the density of charge in each of the two materials is given by:^{291c}

$$W = \left[\frac{2\varepsilon E_j}{q} \left(\frac{1}{N_+} + \frac{1}{N_-} \right) \right]^{\frac{1}{2}} = \left[\frac{2\varepsilon kT}{q^2} \left(\frac{1}{N_+} + \frac{1}{N_-} \right) \ln \left(\frac{N_+ N_-}{K_w} \right) \right]^{\frac{1}{2}} \quad (52)$$

where ε is the dielectric constant, q is the elementary charge, k is the Boltzmann constant and the density of fixed charges ($N_{+/-}$) can be expressed by the IEC within the polymer electrolytes using:

$$N_{+/-} = N_A \times \text{IEC}_{+/-} \times \rho_m \quad (53)$$

where N_A is Avogadro's number and ρ_m is the density of the polymer electrolyte.

Hybrid fuel cell operation. The performance of the hybrid cells and the self-humidification was demonstrated by operation at different relative humidity levels.²⁹² The cell voltage was recorded as a function of time for a hybrid $\text{PEM}_{\text{anode}}/\text{AAEM}_{\text{cathode}}$ cell operating on H_2 and O_2 at 100 mA cm⁻² current density at 600 °C. The RH was increased from 0% to 100% in increments of 25% every 24 h. The current remained nearly constant with time and humidity. The current–voltage relationship for the cell was recorded at the end of each 24 h period and is shown in Fig. 6(top). The current–voltage curves are nearly identical at low current densities (<100 mA cm⁻²) for each RH condition. Interestingly, the performance was higher at low RHs.

In situ a.c. electrochemical impedance spectroscopy was used to help understand the change in cell performance with relative humidity. For all humidity conditions, the impedance spectra (600 mV cell voltage at 60 °C) exhibited semi-circular loops, as seen in Fig. 6(top). The high frequency x-axis intercepts (predominantly the MEA ohmic resistance derived mainly from the ionic resistance of the membrane)²⁹³ showed that the ionic resistance of the membrane was nearly constant over the gas RH range RH 0–100%. However, the radius of the semi-circular loop increased with RH. The difference between the x-intercept values of the semi-circular responses at high and low frequency is mainly governed by interfacial ORR kinetics, ionic conductivity and diffusion limitations within the depletion layer.^{293b} Since the decrease in ionic conductivity of the PEM at high humidity is not expected, diffusion limitations within the



catalyst layers is a likely reason of the increased low frequency resistances at higher RHs.

These results demonstrate that the water generated at the PEM|AAEM interface maintains adequate hydration in the hybrid membrane when the inlet gases are dry. Hydration of the gas streams results in excess water within the membrane, flooding of the electrodes, and limited O₂ diffusion in the cathode catalyst layer. This is a significant result because the performances of conventional PEMFCs (and APEFCs) often have to rely on fully humidified gas feeds. Hydration or wicking of water (from one electrode to the other) can increase complexity and lead to a loss in efficiency.

Beyond fuel cells, the hybrid (bipolar) structures could contribute to more efficient water electrolyzers, salt-splitting technologies, electrochemical separators (such as CO₂ pumps), and solar-to-fuel applications. This is because the pH of each electrode can be taken to extreme values and optimised for the highest efficiency with the materials present. In addition, the bipolar structures may improve permselectivities compared to single ion conducting membranes because the two kinds of ions migrate in opposite directions. One example of the potential optimisation of the electrolyte based on the materials present is the solar-to-fuels systems proposed by Spurgeon *et al.* (Fig. 7).²⁹⁴ Sunlight is absorbed at each of the two photoelectrodes. p-type Si in a PEM environment was proposed for the photocathode because it is cathodically stable in acidic

media.²⁹⁵ The photoanode may be a metal oxide semiconductor, which could be unstable in an acidic environment but stable at high pH.²⁹⁶ Irradiation with sunlight produces H₂ gas at the PEM cathode and O₂ at the AAEM anode. The direction of ion flow is opposite to that shown in Fig. 5b and water is split into H⁺ and OH⁻ ions at the junction (Fig. 5a). A hygroscopic junction between the PEM and AAEM materials is desired due to water consumption there.

Future needs and directions. The bipolar PEM|AAEM membrane may potentially address some of the critical issues faced by PEMFCs, especially problems of platinum utilisation and water management. There are many challenges facing hybrid (bipolar) membranes that are used at extreme pH values. The first is the formation of a tightly bonded and stable PEM|AAEM junction, the location of an abrupt conductivity change that must withstand the high internal pressure due to the formation or consumption of water at that location. Solutions to this may include the bonding of two prefabricated membranes (*i.e.* a PEM and an AAEM) with a third (deposited) layer to covalently or ionically bond the two films together. Another approach is to form a single layer and chemically convert one side into a cation conducting material and the other side into an anion conducting material (*i.e.* formation of a chemical interface without a “physical/mechanical” interface). The initial homogenous single layer may be an ionic precursor (*e.g.* contains alkyl halide functionality that can be converted to both cation- and anion-exchange groups in different regions) or may already contain ionic conducting functionality (such as sulfonic acid group) that is then subsequently converted (partially) to an anion conducting group.

The design and analysis of an efficient, low-loss, bipolar structure is important. Charge neutralisation occurs at the PEM|AAEM junction resulting in a drop in conductivity. The width of the junction region (eqn (52)), is important because the high resistance in this region will result in ohmic losses. The placement of the junction within the electrochemical device is important because water will either be generated or consumed there (depending on the type of device).²⁸⁹ The location of the junction within the membrane should consider the transport of water within the system. In the case of the fuel cell described above, this includes the consumption of water at one electrode

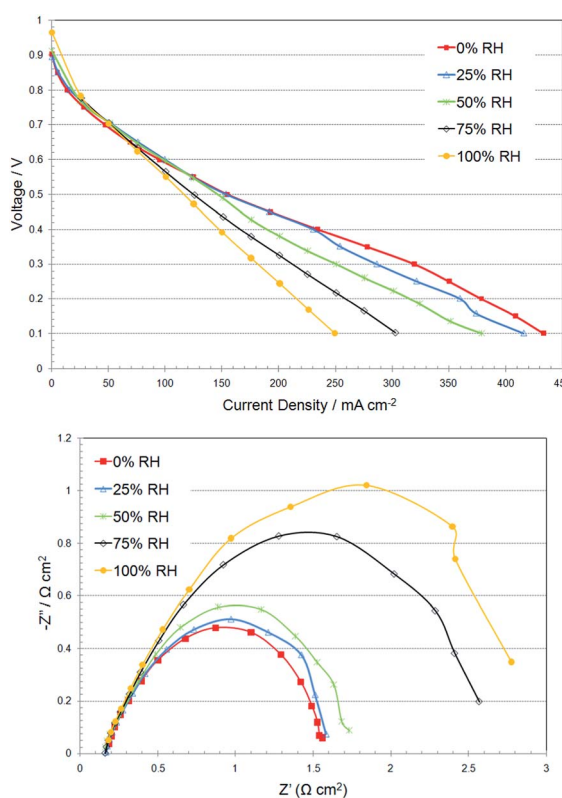


Fig. 6 Top: Cell voltage vs. current density curves at 60 °C for a hybrid PEM_{anode}/AAEM_{cathode} fuel cell with RH levels ranging from 0% to 100% (symmetrical for both H₂ and O₂ gas supplies).²⁹² Bottom: Corresponding *in situ* a.c. impedance spectra at V_{cell} = 600 mV.

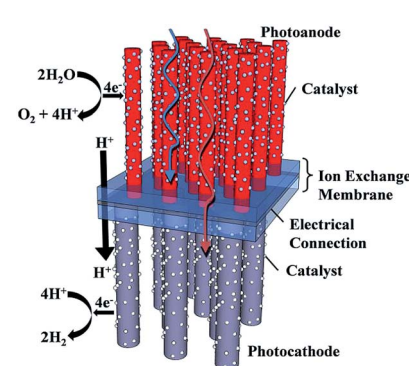


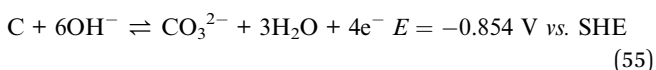
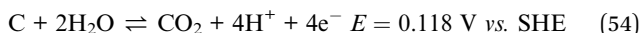
Fig. 7 A solar-to-fuel system that could incorporate bipolar membranes.²⁹⁴



and the efficient removal of excess water. The water balance is a function of the RH of the gas feed streams at the two electrodes. The analysis of the width of the junction, location of ions, and impact of conductivity across the junction is challenging. There are few analytical techniques with adequate spatial resolution, chemical specificity, and sensitivity to address the problem. High surface area, non-planar junctions may be of value to minimise the ohmic losses at the junction (*i.e.* where the real surface area is greater than the superficial surface area) and may provide additional or alternative locations for water generation/consumption (depending on changes in relative humidity of the feed streams).

The need for carbon free catalyst supports at high pHs

Carbon is the favoured material for many fuel cell components for PEMFC and APEFCs.²⁹⁷ However, carbon is thermodynamically unstable across virtually the entire potential range in which fuel cells operate. Under standard conditions (pH = 0, 298 K), carbon is thermodynamically stable only over the potential range -0.05 – 0.15 V (*vs.* SHE) as depicted in the relevant Pourbaix diagram (Fig. 8). The fact that carbon has become such an important material for catalyst supports, reactant transport layers, and bipolar plates is related to its relatively low cost, moderate electrical conductivity, and significant kinetic barrier to corrosion. The barrier to corrosion comes about because carbon, once oxidised, has a preferred oxidation state of +4 (*i.e.* carbon oxidation requires $4e^-$) and the ultimate product is an oxide, the formation of which is hindered by large activation energy barriers in acidic environments. Furthermore, there are no intermediate states of oxidised carbon that are soluble or produced in significant quantities along the reaction pathways leading to CO_2 (*e.g.* methanol, formaldehyde, and formic acid are not produced in appreciable quantities):



The corrosion properties of carbon are relatively well appreciated in PEMFCs with the issue being viewed as a concern for the longevity (durability) of these systems. The most extreme events that challenge carbon stability are faced during start-up and shutdown procedures. Fuel starvation events can lead to the cathode potentials rising up to potentials of 1.2–1.5 V (*vs.* RHE).²⁹⁸

However, carbon shows even less thermodynamic stability under alkaline conditions (as can be seen from Fig. 8); this is in addition to the fact that carbons are active towards the undesirable $n = 2e^-$ ORR at high pHs. This is not the end of the matter either as the kinetics for carbon oxidation actually accelerates in alkaline environments due to OH^- anions being excellent nucleophiles. Indeed, carbon has been suggested (as far back as 1896 by Jacques) as anode fuel in molten NaOH carbon air batteries;²⁹⁹ such systems were constructed that provided up to 1.5 kW of power.³⁰⁰ More recently, the prospect

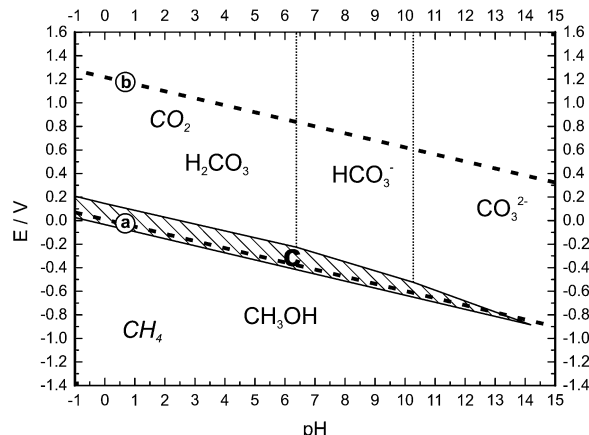


Fig. 8 Pourbaix diagram for carbon at 298 K showing the hatched domain of stability. Predominate gaseous (*italicised*) and solution phase species (non-*italicised*) are shown in the domains where the activity (or partial pressure) is 10^{-6} . (a) Corresponds to the lower stability window of water (HER) and (b) corresponds to the upper stability limit of water (oxygen evolution reaction, OER).

of using carbon as an anode fuel in a molten AFC has received further attention.³⁰¹

As might be expected from the Pourbaix diagram, the degradation of carbon is liable to be more extreme at high pHs due to the greater thermodynamic stability of CO_3^{2-} compared to CO_2 . Decomposition of fuel cell components in aqueous electrolyte AFCs was moderately well studied in the 1970s and 80s. Long-term corrosion rate studies of Black Pearls 2000 and Vulcan XC 72R in aqueous KOH (12 mol dm^{-3}) at 80 °C for >1500 h showed that the carbons are more severely attacked (*cf.* in aqueous H_3PO_4 under the same conditions): after 2300 h, the BET surface area of the Vulcan XC 72R reduced from 225 to 125 $\text{m}^2 \text{ g}^{-1}$.³⁰² In a more recent study, a carbon composite bipolar plate material (30% polymer filler, 5% XC-72R C black, 5% Toray carbon fibres, and 60% graphite powder) was tested under simulated APEFC conditions [aqueous NaOH (1 mol dm^{-3})] and compared to PEMFC conditions [aqueous H_2SO_4 (1 mol dm^{-3})]. An ~ 18 fold increase of corrosion current was observed with the alkaline conditions.³⁰³

Alternatives to carbon. Because of their relative stability in alkaline environments, two metals have been examined extensively as GDL layers and supports for use in AFCs: Ni and Ag. The original aqueous electrolyte AFC developed by Bacon for the US space programme utilised porous Ni electrodes with dual porosity, which was later modified to contain a lithium-doped nickel oxide cathode (to reduce corrosion problems).³⁰⁰ Others have noted problems with using Ni in the cathode, predominantly due to the poor conductivity of the oxide that forms; this leads to large iR losses after only a few days of operation. This can be ameliorated by either plating the Ni with Ag or by using a Ag-only cathode.³⁰²

Despite the above, the current preferred material for reactant transport layers in APEFCs is carbon as the issues with carbon corrosion in the reactant transport layers are normally minor (as the electrolyte is not mobile and hence does not tend to wet



the transport layer). As the transport layer is not exposed to overly harsh alkaline conditions, carbon is suitable for such application. However, other alternatives are possible and may be borrowed from the field of liquid (aqueous) AFCs: *e.g.* see the review by Bidault *et al.*²⁴ For example Nickel coated PTFE shows an electronic conductivity of 300 S m^{-1} ,³⁰⁴ Ni foam may also be a suitable alternative.³⁰⁵

One particularly interesting area is the production of combined catalyst/reactant transport layers utilising a porous Ag membrane.³⁰⁶ As Ag has the highest electrical and thermal conductivity of any metal, its use in the reactant transport layers may alleviate some of the issues found in high performance fuel cells caused by local heating effects. A $50 \mu\text{m}$ thick Ag reactant transport layer with a porosity of 60% yielded a sheet resistance ($0.8 \text{ m}\Omega \square^{-1}$ [where \square indicates square, a commonly used unit for sheet resistances measured using 4-point methods]) that was $400\times$ lower than that of standard carbon-based reactant transport material (Toray TGP-060, $294 \text{ m}\Omega \square^{-1}$). Hence, it is not necessary to keep the gas supply channels so narrow. Indeed, when using the Ag gas transport layer mentioned above, channels could be 20 mm wide without incurring larger ohmic losses compared to the use of a carbon based gas transport layer with 1 mm wide channels. The cost of the Ag reactant transport layer is approximately $3\times$ the cost of the Toray carbon-paper and so this is not a critical issue. A major benefit of using a Ag reactant transport medium is that it also functions as the catalyst, producing impressive electrochemical performances both in the absence and in the presence of additional catalyst.³⁰⁷ Yan *et al.* has also advocated support-less Ag nanowire ORR catalysts.³⁰⁸

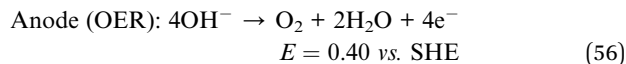
AAEMs in alkaline electrolyzers³

H₂ electrolyzers containing AAEMs and/or AEIs

H₂ production from water electrolysis. H₂ can be produced using chemical, electrochemical, catalytic, thermal or biological processes.³⁰⁹ Interest in H₂ has increased because of its potential use as a fuel produced from renewable and sustainable resources.³¹⁰ The current production of H₂ is dominated by catalytic steam reforming of methane, which produces *ca.* 95% of the H₂ used worldwide. The remaining commercial production of H₂ is mainly *via* electrolysis of water (a convenient and simple route). Electrolyzers produce very high purity H₂ for use in several applications (*e.g.* semiconductor manufacture, hydrogenation of food products, and the production and refining of high purity metals).³⁰⁹ Most commercial electrolyzers are based on alkaline electrolysis and operate at current densities in the region of $1000\text{--}3000 \text{ A m}^{-2}$ and contain aqueous electrolytes of approximately 30% mass KOH (gives the maximum ionic conductivity of 1.5 S cm^{-1} at 80°C).³¹¹ Obviously, carbon-based materials (*e.g.* in the electrodes and bipolar plates) cannot generally be used for alkali or PEM-based electrolyzers, as carbon corrosion occurs at the potentials being applied (see previous section).³¹²

For alkaline electrolyzers, the individual electrode reaction that produces H₂ (HER)³¹³ at the cathode is given in eqn (26),

while the O₂ producing reaction (oxygen evolution reaction, OER)¹²¹ at the anode is given by:



In the cell, a separator is used to keep the H₂ gas isolated from the O₂ gas (to avoid formation of a potentially explosive mixture). As with APEFCs (Fig. 9a), an alkaline electrolyte enables the use of low cost non-PGM catalysts, such as Ni, which helps to keep capital costs of the cells relatively low.

With the use of acid electrolytes, electrolyzers typically use solid polymer electrolyte (SPE, *e.g.* a PEM) and not an aqueous electrolyte (*e.g.* sulphuric acid).³¹⁴ In acid electrolysis precious metal catalysts are used to achieve efficient electrolysis, which generally means that high rates of H₂ production (per unit area of electrode) are required to minimise the capital costs of the cells. There are clear similarities between the cells used for water electrolysis and those used in PEMFCs because the central component, the polymer electrolyte membrane, is essentially the same for both. Consequently, technological developments in polymer electrolyte based fuel cells can often be transferred to SPE electrolyzers.

Why AAEMs and AEIs in electrolyzers? A traditional alkaline electrolyser uses a porous diaphragm to isolate the O₂ and H₂ gases and to prevent intermixing of the catholyte and anolyte (two-phase electrolytes) in order to obtain high gas purities and high current efficiencies.³¹⁰ The diaphragm ideally need to prevent the formation of a gas bubble “curtain” at the front side of the electrodes (when pressing the electrodes onto the elastic diaphragm) to ensure low ohmic and contact resistances. Separators for industrial alkaline water electrolyzers can be made from either inorganic or organic materials. For low temperature electrolyzers, the separator can be nickel oxide, asbestos, or a polymer. The asbestos diaphragm, widely used in alkaline water electrolysis,³¹⁵ has a high resistance, is carcinogenic (*i.e.* asbestosis), and is unsuitable for use above 100°C . Diaphragm materials have also been made from polyantimonic acid³¹⁶ and a polysulfone/zirconium oxide (Zirfon®) composite membrane³¹⁷ and both are relatively thick (1–2 mm).

Replacing the separator/diaphragms mentioned above with an IEM can offer advantages such as reduced gas crossover and

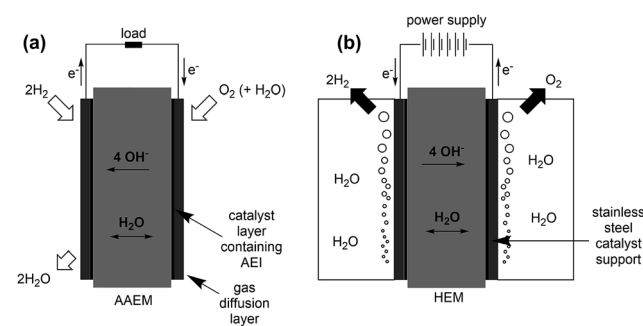


Fig. 9 Comparison of: (a) a H₂/O₂ fuel cell containing an AAEM [APEFC] with (b) an alkaline electrolyser containing an AAEM/HEM [APEE].



area resistances (especially when using thin membranes). Applying AAEMs to electrolyzers (Fig. 9b) provides the opportunity to consolidate the advantages of both types of traditional electrolyzers. The costs will be reduced with the use of the lower cost electrode materials and catalysts that are used in alkaline electrolyzers, while the AAEM electrolyser (APEE) would not be affected by the presence of cationic species (present in the feed-water). The latter is a major issue with PEM-based electrolyzers: a major reason for gradual deterioration in their performances relates to the cations binding to the proton conducting (exchange) sites of the PEM (which reduces its conductivity).³¹⁸ In operation, PEM-based electrolyzers are fed with pure water at the anode which decomposes to O₂ and H⁺ cations; the latter pass through the PEM and are subsequently converted to H₂ gas. The absence of a corrosive (aqueous/liquid) electrolyte is one of the major features of SPE-type water electrolyzers, which adds to the simplicity of operation (and reduced costs of components such as bipolar plates).

The central component of the electrolyser is an MEA (similar to PEMFCs and APEFCs). The IEM serves as the ion (but not electronically) conducting electrolyte and also as the separator for H₂ and O₂ gases. Ideal electrodes require the following attributes:

- (a) Good electronic conductors;
- (b) High structural integrity;
- (c) Corrosion resistance with the electrolyte being used and at operating potentials that are appropriate for the cathode (reducing) and the anode (oxidising);
- (d) Contain high performance electrocatalysts for both the HER and OER;
- (e) High (reaction assessable) surface areas to facilitate high current densities and/or H₂ production rates;
- (f) Stable performance over extended periods of operation (both on and off load).

SPE electrolyser cells require an intimate contact between the phases of the MEA to achieve: optimal ionic and electronic conductivities, high active surface areas of the catalysts, and rapid gas release. High electrocatalyst specific areas are required to decrease overpotentials and to avoid the appearance of hot spots (that drastically shorten the life span of the MEA).³¹⁹ For SPE water electrolyzers, both the anode and cathode electrocatalysts are deposited as thin (several μm thick) coherent layers that are bonded to either side of the IEM.

The main challenge regarding the widespread use of H₂ in small to medium size applications is cost reduction (needed to increase the commercial appeal of such H₂ generators). Low-price domestic electrolyzers can be realised through high production/sales volumes, but this will only occur after economical, efficient, and durable prototypes have been demonstrated. Adopting AAEM-based technology can open up opportunities for low cost electrolyzers systems with: low membrane, catalyst (Pt-free), and bipolar plate manufacturing costs; higher energy efficiencies (towards "zero gap");³²⁰ durable, long life operation (unlike with APEFCs [fed with gas supplies of various RHs], the AAEMs are in an environment where they remain fully hydrated in APEEs); flexibility to respond to dynamic load operation; and compact system integration and

control. The use of AAEMs may also facilitate the simultaneous production of H₂ and useful chemicals (e.g. potassium acetate) when electrolysing aqueous alcohol solutions using only $\frac{1}{3}$ of the energy required by traditional H₂/O₂ electrolyzers.³²¹

Performance of AAEM-based electrolyzers (APEE). Research into the development of AAEMs, historically for use in APEFCs, has produced materials that are of interest for use in APEEs. In comparison to proton-conducting (PEM-based) electrolyzers, the amount of research conducted to date on AAEM-based SPE-electrolyzers is, however, very small (see Fig. 11 in ref. 322). Below is a quick review of key studies.

A solid state water electrolyser has recently been reported that achieved 399 mA cm⁻² at a cell voltage of 1.8 V and nearly 1000 mA cm⁻² at 2.0 V when using Tokuyama A-201 AAEM, Tokuyama AS-4 AEI, and aqueous KOH (1 mol dm⁻³) solutions at 50 °C.³²³ This system, however, used high loadings of precious metal catalysts (RuO₂ at the anode and Pt at the cathode). An alkaline electrolyser that used nickel iron oxide coated anodes, Pt cathodes, and a developmental AAEM (ITM Power, 160 μm thick) with aqueous KOH (4 mol dm⁻³) solutions at 60 °C has been reported to achieve a cell voltage of 2.12 V at 1000 mA cm⁻².³²⁴ The use of KOH electrolyte is seen as important for achieving performances that approach those of Nafion® PEM-base systems where cell voltages between 1.6–1.7 V are possible at 1000 mA cm⁻². The use of NiMo and RuO₂ coatings on nickel or stainless steel micro-meshes have been examined as electrocatalysts for HER in conditions similar to those in "zero gap alkaline water electrolyzers".³²⁵ The NiMo and RuO₂ coatings gave performances that were comparable to Pt and also stable over 10 d of electrolysis; the performance of an electrolyser containing an AAEM (ITM Power, 160 μm thick) and a NiFe(OH)₂ coated anode (OER) with aqueous KOH (4 mol dm⁻³) was 2.1 V at a current density of 1 A cm⁻². Jang *et al.* report *ca.* 150 mA cm⁻² at 1.9 V with aqueous KOH (1 mol dm⁻³) feeds with MEAs containing a Tokuyama A201 AAEM and electrodes consisting of Ni that is electrodeposited on carbon papers with very low Ni loadings (8.5 $\mu\text{g}_{\text{Ni}} \text{ cm}^{-2}$).³²²

Recent work at Newcastle University has used a methylated melamine quaternised grafted poly(vinylbenzyl chloride) AAEM in an APEE containing a Cu_{0.7}Co_{2.3}O₄ OER catalyst (Fig. 10);³²⁶ 1 A cm⁻² was achieved at a voltage of 1.8 V in aqueous KOH (1 mol dm⁻³) at 25 °C. In order to develop APEEs, a polymethacrylate-based OH⁻ conducting AEI ionomer binder (conductivity = 59 mS cm⁻¹ at 50 °C) was synthesised.^{327,328}

A very recent study has reported the use of a dilute aqueous K₂CO₃ solution in conjunction with an AAEM (A-201, from Tokuyama Corporation).³²⁹ The MEA was based around low-cost transition-metal catalysts. The HER and OER catalysts were commercially available materials (manufactured by Acta SpA) and based on Ni/(CeO₂–La₂O₃)/C and CuCoO_x mixed oxides respectively. This system exhibited a similar performance to a PGM-catalyst benchmark. The best performance reported at 43 °C was a cell voltage of <1.95 at 500 mA cm⁻² (using 7.4 mg cm⁻² of cathode catalyst). This approach uses a CO₂ tolerant and less aggressive alkaline electrolyte (*i.e.* no OH⁻ anions). This again highlights that CO₃²⁻ electrolyte systems warrant further detailed studies.



Metal-hydroxide-free systems. An early development with a metal-hydroxide-free system (using only de-ionised water) was reported in 2012 by Zhuang *et al.* where an electrolyser with non-Pt electrodes was reported to achieve a current density of 400 mA cm^{-2} with a cell voltage of $1.8\text{--}1.85 \text{ V}$ at $70 \text{ }^\circ\text{C}$.³³⁰ The AAEM was a self-crosslinking QA polysulfone ($70 \mu\text{m}$ thickness, ionic conductivity $>0.01 \text{ S cm}^{-1}$), while the anode consisted of 40 mg cm^{-2} Ni-Mo on a Ni foam current collector and the cathode was Ni-Fe-based. A more recent study by Ramani *et al.* also reported an APEE that produced H_2 from ultrapure water;³³¹ 400 mA cm^{-2} was achieved at 1.80 V at $50 \text{ }^\circ\text{C}$ with the use of a QA polysulfone membrane, a Pt black HER catalyst, and a high performance lead ruthenate pyrochlore OER catalyst. This study is the first to report on the performance losses of an AAEM-containing APEE. Short-term degradation was due to CO_2 intrusion into the system (and was easily remedied), whilst longer-term losses were due to irreversible AAEM degradation (polysulfone backbone hydrolysis).

Reversible water electrolyzers containing AAEMs. The device that combines a water electrolyser with a fuel cell is often called a regenerative fuel cell (RFC). If a water electrolyser also works as a fuel cell (once H_2 and O_2 are supplied back to corresponding electrodes) it is often called a unitized regenerative fuel cell (URFC).³³² Such devices may also be called reversible water electrolyzers, since they exhibit both functions of storing electricity into chemical energy as electrolyzers and then release chemical energy back to electricity in the reversed electrochemical process. However, most URFC are based on acidic PFSA ionomers and expensive noble metal catalysts; corrosion resistant materials are necessary for good stability and cycle life.³³³ For example in the bifunctional oxygen electrode, the catalysts are often based on expensive Pt with IrO_2 .³³³ However in alkali, other options are available such as perovskite-doped MnO_2 for use as a bifunctional ORR/OER catalyst.³³⁴

It is of increasing interest to employ AAEMs into RFCs where non-precious-metal catalysts can be used in the electrodes. A recent study used a pore-filling AAEM made using porous PTFE filled with a QA polymethacrylate AEI.³³⁵ The composite membrane exhibited a lower swelling ratio (thickness and area

variation), stronger tensile strength, but lower ionic conductivity compared to a polymethacrylate-only AAEM. However, the composite membrane was ultra-thin and therefore exhibited a lower *in situ* MEA ionic (area) resistance and improved current densities. In fuel cell mode, the peak power densities were 0.11 and 0.16 W cm^{-2} at 20 and $45 \text{ }^\circ\text{C}$ respectively. In water electrolyser mode, cell voltages at a current density of 100 mA cm^{-2} were 1.61 V and 1.52 V at 22 and $50 \text{ }^\circ\text{C}$ respectively, while the degradation rate was only $40 \mu\text{V h}^{-1}$ at a current density of 100 mA cm^{-2} at $22 \text{ }^\circ\text{C}$.

Research challenges for AAEM-based water electrolyzers.

PEM-based SPE water electrolyzers typically have performances of cell voltages $<2.0 \text{ V}$ at current densities $>1000 \text{ mA cm}^{-2}$ (*ca.* $80 \text{ }^\circ\text{C}$) for extended operation over many thousands of hours. For AAEM-based technology to be attractive, similar performances but with lower cost materials will be required. Development of such electrolyzers will require research into several key factors (many of which have overlaps to APEFC research challenges):

- (a) Efficient OER and HER catalysts with low activation overpotentials and containing new catalyst structures or metal alloys (resulting in lower noble metal loadings);
- (b) AAEM with improved conductivities and alkali stabilities, low gas crossover, and high mechanical stabilities;
- (c) High performance AEIs for use in the catalyst layers;

These basic components are needed to fabricate the MEAs. A key challenge is to bond high surface area catalysts, using an AEI, to either the AAEM or a suitable metal supporting electrode substrate. The MEAs must enable efficient gas release to prevent gas bubble adhesion blocking the catalyst surface (and avoid undesirable increases in polarisations in the cell). Thus the surface of the MEA and AAEM should be hydrophilic. The development of AAEM-electrolyser technology can benefit from existing research and know-how in the field of electrocatalysts for electrolyzers containing liquid electrolytes.

Cathodes (HER). In alkaline water electrolysis, the cathode material is typically either steel or nickel, which may be activated. Ni shows an initial high HER electrocatalytic activity but experiences deactivation (that typically manifests itself as an increase in HER overpotential at a constant current). High surface area porous coatings of Ni, Ni-Co, Ni-Mo, and active Ni-Fe layers on mild steel substrates have been developed with various roughness factors (*e.g.* 2000 for Ni and 4000 for Ni-Co).³³⁶ The HER overpotentials for these coatings were 100 and 90 mV respectively (*ca.* 135 mA cm^{-2}) at $70 \text{ }^\circ\text{C}$. H_2 (adsorption) storage alloys have been investigated for the HER and show a pronounced improvement in HER kinetics. Ni-Mo HER catalysts have been reported to achieve 700 mA cm^{-2} at an overpotential of 150 mV in *in situ* testing at $70 \text{ }^\circ\text{C}$.³³⁷ Ti_2Ni alloy exhibited a low hydrogen evolution overpotential (*ca.* 60 mV at $70 \text{ }^\circ\text{C}$ in 30% mass aqueous KOH) and a very good stability under dynamic operating conditions.³³⁸ The HER mechanism on Ni-LaNi_5 and $\text{Ni-MnNi}_{3.4}\text{Co}_{0.8}\text{Al}_{0.8}$ materials were in accordance with the Volmer–Heyrovsky mechanism.³³⁹ State-of-the-art electrodes for HER based on RuO_2 particles co-deposited with Ni onto Ni supports have also been developed.³⁴⁰ Activity was enhanced with the use of only relatively low amounts of

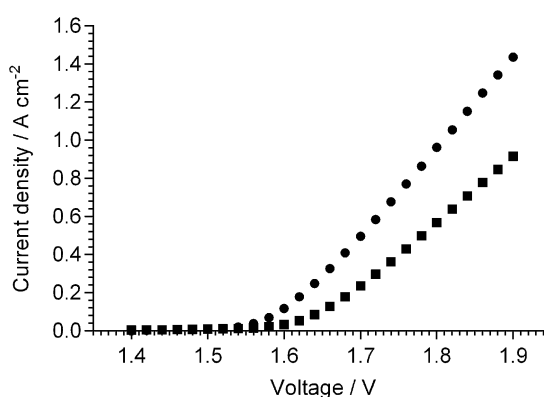


Fig. 10 Electrolyser performance with a OH^- ion conducting AAEM and a $\text{Cu}_{0.7}\text{Co}_{2.3}\text{O}_4$ cobalt oxide OER catalyst (circles) [*cf.* squares = Co_3O_4 catalyst data]. $T = 25 \text{ }^\circ\text{C}$ and aqueous KOH (1 mol dm^{-3}) electrolyte at both the anode and cathode.³²⁶



RuO_2 (in the Ni deposit) and the performance was stable under conditions of constant and intermittent electrolysis. The enhanced electrocatalytic activity of the cathodes can be mainly ascribable to increased number of active sites (and/or the RuO_2 content). Various oxides have been investigated for alkaline water electrolysis. For example, $\text{La}_{0.6}\text{Sr}_{0.4}\text{CoO}_3$ exhibited high activity and good chemical stability for both OER and HER with overpotentials for H_2 formation similar to that of Pt. The anodic OER overpotential of $\text{La}_{0.6}\text{Sr}_{0.4}\text{CoO}_3$ was found to be much smaller than those of Pt.³⁴¹

Anodes (OER). In general, the anode must be stable at OER potentials and at open-circuit. Ni has a high corrosion resistance at positive potentials in alkaline electrolytes and the efficiency of OER of Ni is among the highest for the metals. Because of the high price of nickel (>\$13 000 per tonne),³⁴² the anodes are not, as a rule, manufactured from solid Ni but are based on an electrolytically deposited non-porous nickel coatings. Increasing the electrode surface area (*i.e.* roughness factor – defined as the ratio of its real surface area to its apparent, or geometric, area) of Ni anodes have been achieved, for example, by sintering fine Ni powders prepared from $\text{Ni}(\text{CO})_4$ decomposition.³⁴³ Coated electrodes (steel and Ni) can be made by applying particulate metal coatings to the metal substrates. Applying paint-like suspensions of metal particles can yield uniform coatings of controlled thickness. Use of mild steel as an anode substrate requires the steel surface to be protected from corrosion (during OER) using fabrication methods such as alloying.³⁴⁴ Raney Ni has been used to produce high surface area anode coatings. Raney Ni is made by alloying Ni with metals such as Al or Zn, which are subsequently leached out in alkaline electrolyte yielding the desired high surface area structures with high electrochemical activities.³⁴⁵

Several material types have been studied for alkaline electrolyzers with decreased overpotentials, many of which are metal oxide electrocatalysts for the OER in alkali. Catalytically active materials such as NiCo_2O_4 have been applied.³⁴⁶ Catalysts such as NiCo_2O_4 , Li-doped Co_3O_4 ,³⁴⁷ and perovskite $\text{La}_{1-x}\text{Sr}_x\text{CoO}_3$ types (and substituted variants) have been tested extensively.³⁴⁸ Mixed Cu–Fe–Mo oxide OER catalysts have also been studied.³⁴⁹ Further research of this type may lead to important catalyst modifications or the development of entirely new catalyst systems. Excellent OER activities have been reported with oxides having the pyrochlore structure (described by the general formula $\text{A}_2[\text{B}_{2-x}\text{A}_x]\text{O}_{7-y}$, where $\text{A} = \text{Pb}$ or Bi , $\text{B} = \text{Ru}$ or Ir , $0 < x < 1$, and $0 < y < 0.5$). A typical $\text{Pb}_2[\text{Ru}_{2-x}\text{Pb}_x]\text{O}_{6.5}$ catalyst evolved oxygen at an overpotential of only 120 mV at a current density of 100 mA cm⁻² (and exhibited lower overpotentials than Pt black, RuO_2 , or NiCo_2O_4).³⁵⁰ These Pb/Ru electrocatalysts are a reasonable precious-metal-based OER catalyst option for alkaline electrolysis as ruthenium metal is relatively inexpensive (*ca.* 10% of that of Pt).

Non- H_2 electrolyzers containing AAEMs/AEIs and involving CO_2 reduction

As discussed above, low temperature CO_3^{2-} electrochemical systems are in their technological infancy but there are

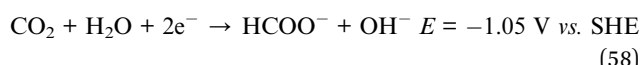
increasing reports of electrochemical cells that involve CO_3^{2-} reactions such as a CEM system for electrolysis of Na_2CO_3 and NaHCO_3 for the production of NaOH .³⁵¹ The immature state of development of room temperature AEM-based CO_3^{2-} systems makes them a potentially high impact area that is ripe for rapid growth. Perhaps the best evidence for this is preliminary work with low temperature carbonate electrochemical devices related to methane activation to various high value products including CO or methanol (Fig. 11):^{283a,352}



This synthesis process involves a CO_2 cycle when in conjunction with the CO_3^{2-} generating reaction in eqn (44) (rather than conversion of all of the CO_2 into products) and is theoretically galvanic; in reality, with the overpotentials involved, it will proceed *via* a low overpotential [driven] electrolytic process.

CO_2 emissions make the greatest contribution to greenhouse gases. Processes which convert CO_2 to useful products are thus desirable from a perspective of sustainability, and environmental protection. This type of system falls into the category of Carbon Dioxide Utilisation (CDU)³⁵³ as opposed to Carbon Capture and Storage (although OH^- containing polymer electrolytes have also been proposed for reversible CO_2 capture).³⁵⁴ Overall in the production of chemicals from CO_2 , energy is required to break the C=O bond to produce various chemicals (the conversion of CO_2 into CO_3^{2-} is a rare example where the conversion of CO_2 into something else is thermodynamically “downhill”). The electrochemical reduction of CO_2 is the conversion of CO_2 to a more reduced chemical species using electrical energy. Electrochemical reduction of CO_2 is considered a possible means to produce chemicals or fuels from CO_2 , making it a feedstock for the chemical industry.³⁵⁵ In prior studies, direct electrochemical reduction of CO_2 in low temperature electrolysis has led to production of formic acid, methanol, hydrocarbons and oxalic acid. Such transformations make the electroreduction of CO_2 of interest in a carbon energy cycle.³⁵⁶ However, such low temperature electrochemical reduction requires a relatively large amount of electrical energy.

No direct electrochemical CO_2 reduction process has been successfully commercialized, although academic and commercial efforts continue using a variety of homogenous and heterogeneous catalysts. Generally speaking, the processes developed to date either have poor thermodynamic efficiencies high overpotentials, low current efficiencies, low selectivity, slow kinetics, and/or poor stability. An exception to this is the production of formate on carbon electrodes at high pH. Det Norske Veritas and the Mantra Venture Group are both developing systems based on Sn cathodes that allow for the conversion of CO_2 to formate:³⁵⁷



The process is believed to use two phase electrochemical reactors with Sn-based cathodes. The equilibrium potentials for



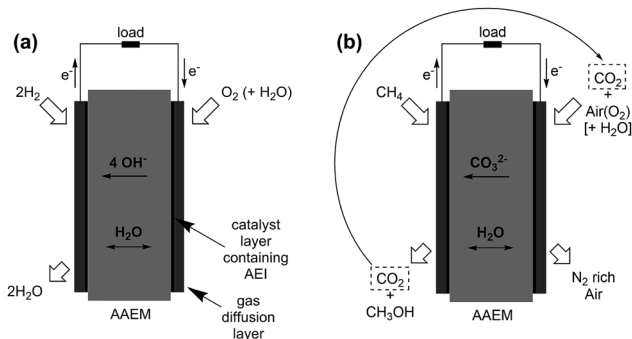


Fig. 11 Schematic comparison of (a) an APEFC and (b) a CO₃²⁻ cycle reactor for the partial oxidation of methane into methanol (refer to eqn (44) and (57) for desired cell reactions).

CO₂ reduction are not too different to that for H₂ evolution. This however hides the fact that its reduction does not occur easily and at much more negative potentials than the equilibrium values.

Previous research on electrochemical CO₂ reduction in aqueous solutions has evaluated a wide range of metals.³⁵⁸ “1st group” metals (such as In, Sn, Hg, and Pb) selectively form formic acid/formate. “2nd group” metals (such as Zn, Au, and Ag) form CO as a major product, while Ag, Au, In, Zn, and Sn can produce CO and carbonate. Ni, Pd and Pt form CO selectively. For example, a set-up involving an AEM was used to investigate the electrochemical reduction of CO₂ to C₂⁺ products on Cu surfaces.^{359,360} All of this suggests that the application of AAEMs and AEIs into low temperature electrolyser systems involving the electrochemical reduction of CO₂ (rather than the more well-known high temperature solid oxide and solid proton conductor CO₂ electrolyser systems)³⁶¹ may have a major impact.

AAEMs in alkaline batteries

Metal-air batteries (e.g. Al-, Zn-, Mg-, and Fe-air),³⁶² and other battery types such as Ni-MH (MH = metal hydride) and Ni-Zn cells, often contain alkaline electrolytes and can have higher energy densities and capacities compared to other batteries such as Li-ion batteries. Catalysts such as Ag-MnO_x/C can be used for the O₂ reactions when air electrodes are employed along with alkaline electrolytes.³⁶³ In the last decade, there have been a small number of reports of the use of AAEMs in such batteries. One of the motivations for using an alkaline solid polymer electrolyte is to prevent undesirable changes in the electrodes (such as dendritic growth at the anode [growing towards the positive electrode] in Ni-Zn cells).³⁶⁴ AEMs have even been reported in Li-O₂ batteries (to suppress direct LiOH deposition in the air electrodes).³⁶⁵ As with APEFCs/APEEs, the membranes need to have high ionic conduction and high alkali stabilities.

Early examples of the use of solid polymers electrolyte in alkaline primary and secondary batteries were reported by Fauvarque *et al.* who used KOH-doped poly(ethylene oxide) polymers and copolymers.³⁶⁶ Other examples include the work

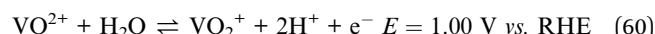
by Yang *et al.* who used a KOH-doped PVA-based copolymers in a primary solid-state Zn-air battery and a Ni-MH battery,³⁶⁷ while Arof *et al.* similarly used a KOH-doped PVA electrolyte in a Ni-Zn cell.³⁶⁴ A recent study investigated the use of KOH-doped poly(acrylic acid) polymer electrolyte for all-solid-state Al-air batteries.³⁶⁸ However, these are still metal-cation-containing (KOH-based) systems.

Yasuda *et al.* investigated a reversible air electrode concept, containing an AAEM with covalently bound cationic groups, for use in secondary air batteries;³⁶⁹ the AAEM was a hydrocarbon-based QA-type (IEC = 1.4 meq. g⁻¹, thickness = 27 μm). The rational for the use of such an AAEM-based air electrode was to reduce ORR/OER performance losses by: blocking the cations from penetrating into the air electrode (reduces carbonate precipitation), reducing the penetration of the alkaline solution into the air electrode, and preventing neutralisation of the alkaline solution *via* the CO₂ in the air electrode supply. A Pt-Ir catalyst provided reduced overpotentials in the air-electrode and the concept did exhibit a reduced (negative) influence from the presence of CO₂.

AEMs in redox flow batteries (RFB)^{2a,4}

IEMs play an important role as separators in some types of RFBs^{4c,d,370,371} where a high degree of reactant isolation is required between the anolyte and catholyte compartments. Microporous separators can be used in RFBs to provide a barrier between the two liquid streams (since the anolyte and catholyte usually contain high concentrations of acids, bases, or other electrolytes to facilitate ionic conductivity). However, while being generally inexpensive and having low ionic resistances when immersed in concentrated electrolyte solutions, microporous separators are prone to high crossover of electroactive species that result in cell performance losses and severe battery capacity fade.³⁷²

Thus, there has been a concerted effort to apply high-conductivity, low crossover IEMs in a number of different RFB systems. IEMs have been investigated for use in iron/chromium, hydrogen/bromine, vanadium/bromine, non-aqueous,³⁷³ and other types of RFB chemistries.³⁷⁰ Nafion® and other perfluorinated IEM variants have been the most heavily-studied IEM in RFBs and most new membrane research (beyond Nafion®) has centred on all-vanadium redox flow batteries (VRFB). In VRFBs, vanadium cations (in various oxidation states) are used to reversibly store and release electrical charge according to eqn (59) and (60) (Fig. 12):



Flow batteries are inherently flexible energy storage systems because the system power can be scaled by the size of the electrochemical stack, while the energy storage capacity of the battery system can be varied with the size of the electrolyte holding tanks. Hence such flow batteries have many similarities



to fuel cells. The principal degradation mechanisms for VRFBs are from the mixing of the vanadium redox couples by vanadium cation crossover between the flow compartments or the oxidative degradation of the cell components and membrane. The fact that VRFBs have vanadium based couples at each electrode [V(II)/V(III) couple at the negative electrode and V(IV)/V(V) redox couple at the positive electrode] give the ability to regenerate the electrolytes should crossover occur: the electrolyte volumes in each compartment can simply be mixed and electrochemically re-activated to regain the capacity of the battery.³⁷⁴ A primary goal in membrane research for VRFBs is to limit the vanadium cation diffusion through the membrane, while maintaining high oxidative stability in the presence of VO_2^+ (where vanadium is in the +5 oxidation state) and related species.³⁷⁵

The VRFB system is being heavily considered for grid-scale energy storage due to the fast kinetics of the redox reactions and simple mitigation of electrolyte contamination (due to the all-vanadium chemistry). However, there are hurdles to overcome such as identifying a low-cost source of vanadium (perhaps as a by-product from metal refining) and sourcing an inexpensive but high performing membrane for MW-scale installations (that will require 1000s or even 10 000s of m^2 of membrane material).

The problem with Nafion® and aromatic CEMs in RFBs

Nafion® and other PFSA IEMs have been deemed currently too expensive for large-scale grid battery systems where capital cost is a primary consideration for large-scale stationary electrical energy storage applications.^{2a,4d} To potentially lower the cost of these systems compared to PFSA benchmarks, aromatic CEMs have been explored to good effect in a range of studies.^{4c} Fig. 13 shows a VRFB performance comparison of a sulfonated aromatic CEM *versus* a Nafion® NRE-212 membrane.³⁷⁶ In this work, the aromatic backbone was selectively fluorinated to prevent oxidative degradation of the aromatic CEM structure

that has been reported for aromatic CEMs exposed to high oxidation state vanadium.^{375,377} Because of the distinctly different ionic domain morphology in the sulfonated aromatic CEM,³⁷⁸ there is much less vanadium ion crossover in aromatic IEMs compared to the Nafion® benchmark. The lower vanadium crossover mitigates the capacity loss with cycling therefore helping to maintain reasonable ionic conductivity. Similar to the membrane proton conductivity/methanol permeability selectivity parameter used in DMFCs,³⁷⁹ the proton conductivity/vanadium permeability electrochemical selectivity of the membrane is an important figure of merit for these systems.³⁸⁰ Despite their excellent *in situ* RFB performance compared to PFSA membranes, the drawback of aromatic CEMs is that their oxidative lifetime stability below that of Nafion® or that needed for long-term grid storage applications.

Optimisation of AEMs for low crossover and high conductivity

Because the electroactive vanadium species in VRFBs are positively charged, AEMs with fixed cationic groups are attractive alternatives to CEMs; they have been investigated as ultra-low vanadium crossover IEMs.³⁸¹ Additionally, if the vanadium cations cannot easily penetrate into the membrane, the degradation of aromatic AEMs (on exposure to the vanadium species) may be mitigated, resulting in a high cell cycle life.³⁸² Typically, the electroactive vanadium species are dissolved in high concentrations of aqueous H_2SO_4 or HCl as the supporting electrolyte. The charge/discharge reactions of the VRFB in eqn (59) and (60) can be balanced by H^+ diffusion between the electrode compartments, or correspondingly, the charge can be balanced by the shuttling of anions across the AEM.

AEMs can display some proton-mediated ionic conductivity because their transport numbers are not unity for anions. However, in most AEM-based VRFBs, the majority of the current will be carried by anions, such as sulphate, traversing the cell.³⁸³ Because the anions present will have lower intrinsic mobilities than protons, high conductivity AEMs and the optimisation of the conductivity/crossover selectivity ratio is critical in these systems. A series of benzyltrimethylammonium-containing

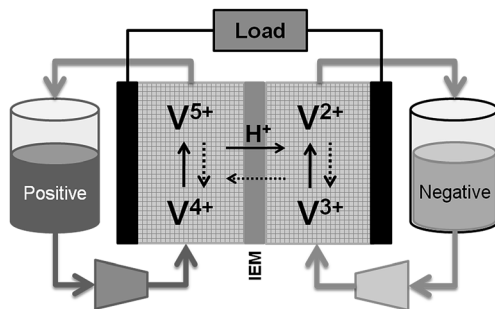


Fig. 12 Schematic of a VRFB. Typical concentrations for the vanadium electroactive species (usually sulfate salts) are 1.7 mol dm^{-3} in supporting aqueous H_2SO_4 (3.3 mol dm^{-3}) electrolyte. Dashed arrows indicate the valence change of the vanadium species during cell discharge (the positive and negative electrolytes are named after the discharge reactions), while solid lines represent cell charge processes. Undesirable vanadium cation crossover can occur, while SO_4^{2-} anions can additionally transport through the IEM when an AEM is used instead of a PEM.

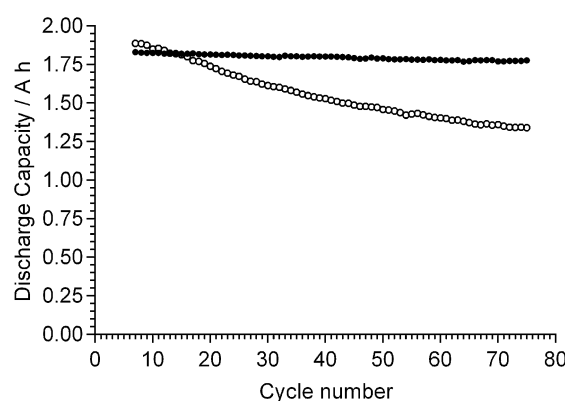


Fig. 13 Low capacity fade observed in a VRFB using a low-crossover sulfonated and selectively fluorinated aromatic CEM (filled symbols) compared to Nafion® NRE-212 (open symbols).

Table 4 Properties of select QA-polysulfone AEMs vs. Nafion®-212 in VRFBs

	IEC ^a /meq. g ⁻¹	Gravimetric water uptake ^b (%)	Ionic conductivity ^c /mS cm ⁻¹	VO ²⁺ permeability/m ² s ⁻¹
Nafion® NRE-212	0.9	28	44	3.2×10^{-12}
QA-Radel 2.0	2.0	29	41	3.7×10^{-14}
QA-Radel 1.7	1.7	16	24	nm

^a Measured using ¹H NMR. ^b Liquid water, room temperature. ^c Equilibrated in aqueous VOSO₄ (1.4 mol dm⁻³) + H₂SO₄ (2.0 mol dm⁻³) solution. nm = not measurable.

AEMs based on chloromethylated poly(sulfone) were synthesised with different IECs.³⁸⁴ Varying the IEC yielded materials with different conductivity/permeability ratios (Table 4). It is apparent that an AEM with too low conductivity (*e.g.* QA-Radel 1.7 from Table 4) will induce high ohmic losses and decrease the power density of the cell (Fig. 14). On the other hand, too high a crossover can also negatively impact the power output of the cell (as is observed with NRE-212 or AEMs with too high an IEC). The QA-Radel 2.0 AEM had intermediate crossover and conductivity compared to the other samples and produced the most power across the set of membranes examined. Similar observations can be made for thickness optimization of IEMs in VRFBs where the resistance and crossover must be balanced for a given set of VRFB conditions.³⁸⁵ Because cell designs and desired operating points vary across different RFB technologies, there is no one ideal membrane for all applications. The operating envelope of the cell must be considered in order to arrive at an optimized membrane configuration.

The study described above demonstrates that AEMs have a large role to play in VRFB technology. In fact, there are a number of other VRFB studies showing the utility of AEMs in these types of energy storage.^{9,386} In membrane development work for RFBs, to date studies have focused on basic descriptions of AEM performance in RFBs in order to codify the structure–property relationships for these materials in the unique environment of a redox flow cell. More advanced studies into the optimisation of the polymer-tethered cationic groups and membranes with engineered physical structures (to decrease thickness and increase mechanical strength) are ongoing to continue to boost the performance of the membrane in these systems.^{32a,373b,387}

In most AEM RFB studies, high current densities above 200 mA cm⁻² are still to be demonstrated.³⁸⁸ High current densities in cells with CEMs are becoming more common with close attention to the membrane thickness and cell design.³⁸⁹ In many regards the challenges of direct methanol and other liquid-fed fuel cell membranes mirror those of VRFBs. Strategies for high conductivity, low crossover membranes are needed. However, while these issues can be managed, the largest challenge for new generation VRFB membranes, lifetime, will be harder to overcome. Stationary energy storage systems will be cycled for tens of thousands of cycles over thousands of hours of operation. Because most experimental VRFB membranes are based on aromatic structures, long lifetimes have not been proven to date. For example, post-mortem spectroscopic analysis of a cardo-poly(ether ketone) AEM used in a VRFB (100 h of testing) showed a 15% decrease in the QA

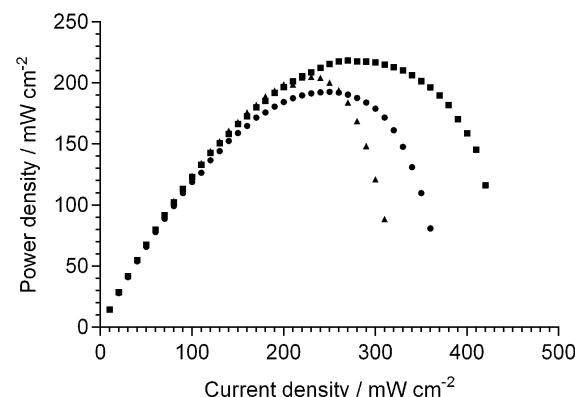


Fig. 14 Performance optimisation (trade-off between conductivity and vanadium cation crossover) in a VRFB system. IEMs: circles = QA-Radel polysulfone AEM (IEC = 1.7 meq. g⁻¹), squares = QA-Radel polysulfone AEM (IEC = 2.0 meq. g⁻¹), and triangles = Nafion® NRE-212.

content.³⁹⁰ The technical and practical challenges for developing stable membranes with proven stability over long periods of time remain and necessitate further research. As new experimental AEMs become more available for evaluation in electrochemical applications (with materials developments towards thinner membranes with higher conductivities), further systematic studies on various types of RFBs will continue to push the application of AEMs in energy storage devices forward. This will require the clarification and management of degradation issues.

AEMs in reverse electrodialysis (RED) cells

Power generation using RED⁵

Salinity gradient energy (SGE) uses the Gibbs free energy of mixing of two salt solutions with different salinity to generate energy (*i.e.* energy can be extracted where river water flows into the sea). SGE can also be extracted from industrial processes where more concentrated salt solutions are generated. SGE is a non-polluting (no emissions of CO₂, SO₂ or NO_x), sustainable technology that is available worldwide. The estimated global energy potential from estuaries only is estimated to be 2.6 TW,³⁹¹ which is approximately 20% of the worldwide energy demand.³⁹²

Two technologies are available to harvest the energy from the mixing of two solutions with different salinity:^{5b,392}



(a) Pressure Retarded Osmosis (PRO)³⁹³ uses a semi permeable membrane allowing the transport of water only, while the solute (salt) is retained;

(b) Reverse electrodialysis (RED – Fig. 15)³⁹⁴ uses IEMs (both CEMs and AEMs) that selectively transport cations and anions only. In this electrochemical technology review, the focus is on RED cell technology.

In RED cells (Fig. 15), a number of CEMs and AEMs are stacked together in an alternating pattern between an anode and a cathode with salt water and fresh water flowing between the membranes. Due to the chemical potential difference between the two solutions, anions are transported through the AEM and cations diffuse through the CEM (from the seawater to the river [fresh] water channels). In the electrode compartment, the ionic charge transport is converted into an electrical charge transport (electrons) using a reversible redox reaction (rinse solution), often based on the redox couple $\text{Fe}^{2+}/\text{Fe}^{3+}$; the use of capacitive electrodes has also been explored.³⁹⁵

Pattle³⁹⁴ was the first to demonstrate the principle of RED and Weinstein and Leitz (in the 1970s)³⁹⁶ investigated the effect of the composition of the salt solutions on the power output. They stated that large-scale application of RED could become feasible, but only after improvements in IEM manufacturing and optimization of the operating conditions. In the early 1980s, Lacey³⁹⁷ concluded that membranes for RED should be low cost and have a low electrical [ionic] resistance and a high selectivity combined with a long service lifetime, acceptable strength, and dimensional stability. Audinos³⁹⁸ compared the RED performance of two different types of electrodialysis membranes (*i.e.* homogeneous and heterogeneous membranes) for different salt solutions (NaCl vs. ZnSO_4) and obtained a maximum power output of 400 mW m^{-2} . Since the early 2000s, RED has regained attention as a technology option for sustainable energy production.^{399–405} Veerman *et al.*⁴⁰⁶ determined the power outputs and thermodynamic efficiencies for a series of six commercially available IEM pairs and used a

response parameter (the product of these two parameters) to rank the different membranes; however, this could not relate directly to the properties of the individual membranes.

Most research focuses on generating power from mixing aqueous NaCl solutions but the effect of using thermolytic solutions (*e.g.* ammonium bicarbonate) instead of NaCl has also been investigated.⁴⁰³ Additionally, the combination of RED with other technologies (*e.g.* RED with seawater desalination and solar ponds,⁴⁰⁴ RED with reverse osmosis (RO),⁴⁰⁵ closed-loop ammonium carbonate RED cells for energy efficient H_2 recovery when combined with an OER anode,⁴⁰⁷ or RED combined with microbial fuel cell technology [see later]) have also been reported. Most reports focus on the technological aspects of RED rather than the membranes. Experiments are usually performed using commercially available IEMs that have not been specifically designed for RED (usually they have a background in traditional electrodialysis). Such membranes are usually robust, mechanically strong and consequently rather thick. Moreover, membrane chemistry, structure, and properties are tailored for different applications. These can, however, play an essential role in determining the power output obtainable in a RED cell (not only in terms of ionic flux but also in relation to membrane fouling, mixing characteristics, and water composition). As such, they are key factors determining the net power output obtainable in a RED cell (discussed below).

Membrane chemistries for RED

Dlugolecki *et al.*⁴⁰⁸ were first to systematically investigate different commercially available membranes for RED applications. They experimentally determined the ionic resistance, permselectivity, and charge density of a wide range of CEMs and AEMs, and used these experimental values as input for model calculations to predict power densities obtainable in RED. Their main conclusion was that in order to obtain high power densities, the IEM resistance is critical and should be as low as possible (preferably area resistances $r < 1\text{--}2 \Omega \text{ cm}^2$), while the permselectivity is of minor importance (this parameter is already high at >95%). This was later confirmed experimentally by a study of Güler *et al.*⁴⁰⁹ who measured the power densities obtainable for a large series of different AEMs and CEMs (Fig. 16).

RED cells provide an important contrast to the use of AEMs and CEMs in chemical fuel cells (and other electrochemical systems containing high and low pH environments) where the AEMs are typically in alkaline anion form (AAEM) and the CEMs are in the acidic PEM form: the IEMs in RED cells are commonly in the Na^+ and Cl^- forms. H^+ and OH^- ions have an additional conduction mechanism available (the Grotthuss mechanism) so the conductivities of aqueous solutions containing H^+ and OH^- ions are significantly higher than those containing other ions such as Na^+ and Cl^- (recall Table 1 gives the ion mobilities, μ , at 25 °C in aqueous solutions). Hence, the IEMs will yield higher area resistances in RED cells compared to when the same IEMs are used in chemical fuel cells. This contrast also exists for microbial electrochemical cells *vs.* abiotic, chemical, fuel cells (see later). The situation is even worse for RED cells utilising

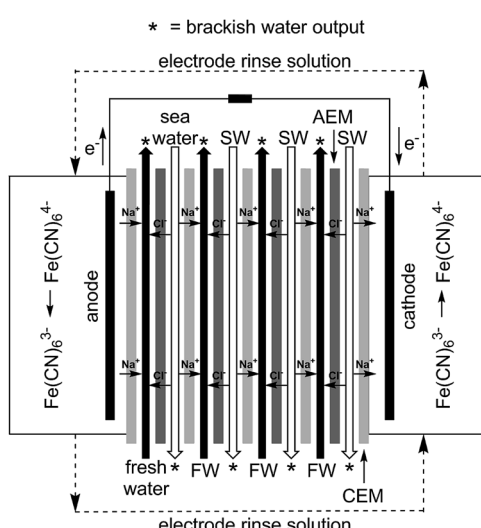


Fig. 15 Schematic of a reverse electrodialysis (RED) cell. SW = sea water and FW = fresh water.



thermolytic solutions as HCO_3^- ions are less mobile than Cl^- ions (this can be mitigated by designing polymers that swell more in ammonium bicarbonate compared to NaCl solutions).⁴⁰³

As well as using commercially available membranes, Güler *et al.* also, for the first time, tested tailor made membranes with chemistries targeted for RED.⁴¹⁰ The AEMs and CEMs synthesised for use in RED cells were systematically investigated to study the effect of charge density, resistance, and permselectivity in relation to the power output.^{409,410} Although the authors observed a reasonable statistical correlation between the thickness of all (tailor made and commercial) membranes and the area resistance, no significant correlations between both resistance and permselectivity to power output could be extracted. *The results, however, clearly showed that IEM resistance is more important than permselectivity.*

The CEMs synthesized by Güler *et al.* were based on sulfonated poly(ether ether ketone) (SPEEK), which is a common cation exchange polymer frequently used in electro-membrane processes. With a degree of sulfonation of 65%, the SPEEK membranes had an area resistance of $1.22 \Omega \text{ cm}^2$ and a permselectivity of 89%.⁴⁰⁹ For AEMs, a synthesis using a halogenated polyether [polyepichlorohydrin (PECH)] and DABCO was employed to simultaneously introduce anion exchange functionality and crosslinks into the polymer membrane (during amination);⁴¹⁰ poly(acrylonitrile) was also used (as an inert polymer matrix) to further improve the strength and stability of the materials. Area resistances of this series of AEM ranged from 0.82 to $2.05 \Omega \text{ cm}^2$ (with permselectivities of 87–90%). As shown in Fig. 16, this first attempt to use tailor made membranes resulted in the highest power output so far, for the different membranes studied, with a value of 1.27 W m^{-2} .⁴⁰⁹ Previous research showed that the thickness of the membranes is a critical parameter as well (as it directly influences the area resistance). In a non-optimized RED stack (inflow limitations

dominate the power output), a decrease in membrane thickness from 130 to 33 μm resulted in an increase in power output of about 20%; with an optimized stack design, a more pronounced effect is predicted.⁴¹⁰

Geise *et al.*⁴¹¹ investigated the ionic resistance and permselectivity of a series of synthesized quaternary ammonium PPO- and poly(phenylsulfone)-based AEMs. They aimed to develop structure–property relationships between transport properties and water content and fixed charge concentration that can be used to assess the membranes with respect to their applicability in a wide range of electro-membrane processes. It was reported that the water content of the membranes turned out to be essential and that the polymers with higher water content tended to have lower ionic resistances and lower permselectivities. This relationship was not, however, straightforward as it was highly dependent on the membrane chemistry.

Kwon *et al.*⁴¹² used a nanoporous polycarbonate track-etch membrane in a parallel structure with nanofluidic channels and a membrane diameter of 10 mm. These membranes are characterized by their low thickness, straight pores, high flexibility, and mechanical stability. The pore sizes investigated were 15, 50, and 100 nm. The authors report that the mechanism for selective ion transport is based on the formation of a charged electrical double layer (EDL) on the inner surface of the negatively charged pores. When the EDLs of both pore surfaces overlap, counter-ions (anions in the case of a positively charged surface) are preferentially transported while co-ions (cations) are mostly retained due to electrostatic repulsion. The authors showed this principle for CEMs, but indicate it should also work with AEMs. Although the exact type of membrane, material and concept is not very well addressed in the paper, the mechanism seems to work best for the smallest pore size (15 nm) and the power output significantly decreased on application of membranes with larger pore sizes. Although not measured in a real RED stack, the concept was evaluated in a simple two compartment cell (where only a CEM was used with salt solutions with different salinity on either side); the authors reported a maximum power of *ca.* 5 μW ($5.8 \mu\text{W cm}^{-2}$).

Microstructured (profiled) membranes

Usually, the IEMs in a RED stack are separated by non-ionically-conductive “spacers”, which block part of the membrane area available for ion transport (the so-called spacer shadow effect).^{399,413} To overcome this approach, Długołęcki *et al.*⁴¹³ proposed the use of profiled IEMs (that contain intrinsic “spacer” functionality) and recently Vermaas *et al.*⁴¹⁴ (Fig. 17) and Güler *et al.*⁴¹⁵ demonstrated this concept in practice. These microstructured IEMs (with integrated spacer functionality) were developed either by the hot pressing of commercially available membranes or by solution casting of the previously described PECH-based AEMs on a structured mould. Although the boundary layer resistances were higher and the mixing was poorer inside a stack containing profiled IEMs with non-optimised microstructures (compared to a stack using conventional spacers), higher stack power densities were nonetheless observed.⁴¹⁴ Despite the small improvements observed, profiled

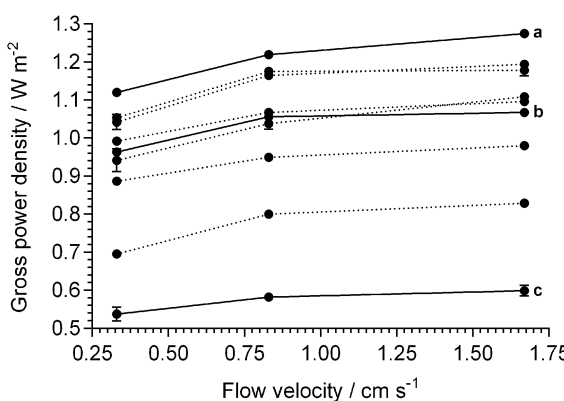


Fig. 16 Experimental power densities obtainable in RED cells for different membrane couples as a function of the flow rate (number of cells = 5; spacer thickness = 200 μm).⁴⁰⁹ Highlighted examples: (a) University of Twente in-house developed CEM = sulfonated PEEK and AEM = quaternary ammonium poly(epichlorohydrin); (b) commercially available Tokuyama CEM = CMX and AEM = AMX; (c) commercially available Ralex CEM = CMH and AEM = AMH.



IEMs have a strong future development potential as they lead to lower pressure drops (loss of power) in the stack and more optimised structure designs (in terms of mixing and improved boundary layer resistances) can be envisaged. A very recent study that has looked into optimising the microstructure design is the start of efforts to address this.⁴¹⁶

Multivalent ions and fouling in RED cells

Although most experiments in laboratory conditions are performed using artificial sea and river water (e.g. containing only NaCl), real world application is different and natural waters contain significant amounts (*ca.* 10%) of multivalent ions (predominantly MgSO₄) and potential foulants such as humic acids, clay, colloids, and scale inducing minerals. Post *et al.*⁴¹⁷ performed laboratory experiments with feeds containing not just NaCl but also MgSO₄ or MgCl₂. A major effect was observed when the multivalent ions were present where the resistance increased and the stack voltage decreased. This was attributed to the transport of these multivalent ions from the dilute solution side to the concentrated solution side (against the concentration gradient). In a follow-up study, Vermaas *et al.*⁴¹⁸ characterized this transport as “uphill transport”, in accordance with other membrane processes. They experimentally and theoretically investigated the effect of increasing the fraction of MgSO₄ (0, 5, 10, 25, 50, and 100%), alongside the NaCl, on the open circuit voltage and power density with three different membrane pairs. The presence of MgSO₄ in the river water compartment was shown to have an especially significant negative (performance deteriorating) effect. For example, the presence of only 10% MgSO₄ yielded a decrease in stationary state power output by 29–50% compared to the benchmark (NaCl only) case. In addition, switching from a NaCl only solution to a mixture of NaCl and MgSO₄, led to voltage response times in the range of tens of minutes and several hours (due to ion exchange processes between the membranes and the feed water). Both researchers concluded that the

presence of MgSO₄ in natural feed waters is a serious factor that needs to be taken into account and that the development of monovalent selective membranes (that preferentially allow the transport of monovalent ions over multivalent ions) are required to minimise this undesirable characteristic.

Vermaas *et al.*⁴¹⁹ also performed long term (25 days) experiments with realistic natural feed waters. Before entering the RED stack, these were filtered through a 20 µm filter (to remove particulates only). Both a system with IEMs and spacers and a system with profiled IEMs were investigated. The power output showed a major (40–60%) decrease in only the first few hours (Fig. 18). In all cases involving realistic water feeds, deposition of remnants of diatoms (algae) and clay minerals, organic fouling, and scaling were observed, depending on the type of IEM being used. The AEMs were mainly covered with diatoms and clay minerals, whereas scaling dominated with the CEM. Although fouling was observed for both profiled IEM and spacer-containing systems, it was less severe with the use of profiled membranes. In addition, recent work has shown that anti-fouling strategies (e.g. periodic feed water switching or air sparging) can be very effective in maintaining higher RED cell power outputs.⁴²⁰

Future perspective

The importance of IEMs that are specifically designed for use in RED cells is evident. Specifically tailored IEMs are mandatory if power outputs (for an economically and commercially viable process) are to be achieved at the target values of 2–3 W m⁻² (normalised to membrane geometric area). Modification of membrane chemistry is a strong tool to allow this goal to be reached. Focus should be on decreasing the membrane resistance rather than increasing permselectivity. New chemistries would not only allow the design of membranes with improved ionic conduction properties, but would also make it possible to combine this with the additionally desirable development of monovalent selective (to mitigate against the negative effect of multivalent species such as MgSO₄) and “anti-fouling” (chemical and biological) IEMs.⁴²¹ Efforts on IEM, including AEM, development should be focused at these research directions.

AEMs in biological energy systems

All of the above are chemical, abiotic systems. However, in the last decade there has been resurgence in the development of biological fuel cells and related systems. Such systems normally operate at more neutral pHs compared to most of the abiotic electrochemical energy systems discussed above, apart from RED. As with RED, high pH and low pH degradation processes are less of a concern. Most of the biotic systems that report the use of AEMs contain a microbial component (Fig. 19).^{422,423} There are, however, non-microbial biotic systems that have used AEMs. For example, there has been a notable report of the use of a polysulfone-AEM in a methanol-fuelled enzymatic fuel cell.⁷ This system contained a fuel tolerant enzyme-based cathode (laccase from *Rhus vernicifera* with an enzyme loading of 0.22 mg cm⁻²) along with Pt/Ru-based anodes. This enzymatic fuel

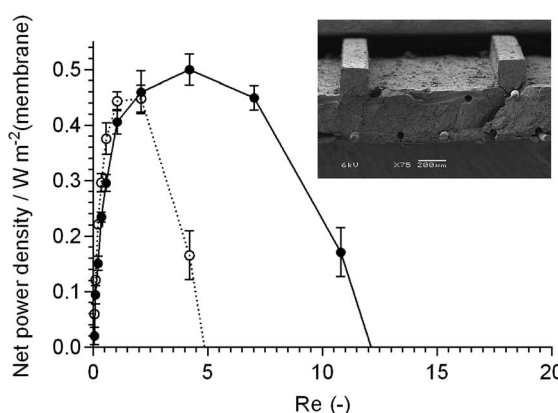


Fig. 17 The improved net power output in a RED cell system using profiled IEMs (solid circles, *i.e.* an IEM with integrated spacer functionality [see inset SEM micrograph]) in comparison to a standard system containing non-conductive spacers (open circles).⁴¹⁴ SEM: scale bar = 200 µm, 75× magnification.



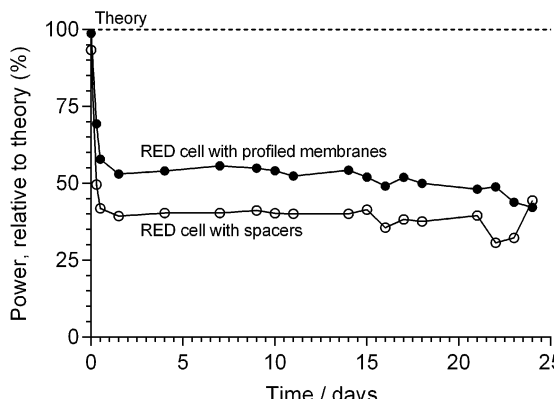


Fig. 18 Peak power densities as function of the number of days after the start of the experiment for a stack with spacers (open circles) and a stack with profiled membranes (filled circles).⁴¹⁹

cell demonstrated a very promising power performance (for a biological fuel cell): 8.5 mW cm^{-2} with a 290 h lifetime.

Microbial fuel cells

Microbial fuel cells⁴²⁴ (MFCs, see Fig. 19a), are generally being developed for energy efficient treatment of various wastewaters (containing a variety of substrates [fuels], such as acetate or sucrose) rather than energy generation *per se*. They can also be operated with additional added value functions (e.g. water softening, NH_3 remediation^{422a,g} or electrosynthesis – see later). MFCs typically contain carbon-based anodes that have been inoculated with either: (a) a microbial consortia that contain electroactive microbial species (commonly designated as exoelectrogens and more historically as electricigens) for real world applications involving a supply of target wastewater (include human wastewater) that requires treatment; or (b) single species [monoculture] exoelectrogens (such as *Escherichia coli* [*E. coli*], *Shewanella oneidensis*, or *Geobacter Sulfurreducens*) for more fundamental studies. The exoelectrogens oxidise the substrates and use the anode as the terminal electron acceptor when they are located in the target anaerobic (or anoxic) environment of the anode chamber. This avoids the microbes using dissolved O_2 as the terminal electron acceptor (as with normal microbial respiration), which would be the case if the anode chamber contains an aerobic environment.

The electrons then pass through an external circuit to the cathode, which is most commonly an ORR type. The cathode can be either “air breathing” (supplied directly with air [passively or actively]) or solution-based (uses O_2 [or other electron accepting species] that is dissolved in a catholyte). MFCs, therefore operate because the O_2 is separated away from the microbes. The cathodes can contain a variety of catalysts.⁴²⁵ They can be abiotic: *e.g.* contain Pt -, Mn_xO_y ,^{422b,426} or CoTMPP^{422p} based catalysts or they can even be “non-catalysed” (*i.e.* metal-free and carbon-based).⁴²⁷ They can also be biotic: *i.e.* either microbial (*e.g.* containing autotrophic bacteria)^{422c} or enzymatic (*e.g.* containing laccase including that excreted from

the white-rot fungus *Coriolus versicolor*).⁴²⁸ Cathodes can also be photocatalytic (*e.g.* contain algae or cyanobacteria).⁴²⁹

MFCs can be constructed with a variety configurations including packed-bed,^{422d} single chamber, or 2 chamber; 3 or more chambers are often found with related systems that involve added-value functions (see later). A large proportion of these configurations contain an IEM (or other non-ionic and/or porous separator). One of the earliest reports of a comparison of 2-chambered MFCs containing AEMs *vs.* CEMs *vs.* non-ionic ultrafiltration membranes was by Logan *et al.* in 2007.^{422q} This study discusses the transfer of protons through the AEM *via* negatively charged species (phosphate anions) and compared the use of CMI-7000 CEM and AMI-7001 AEM (both from Membrane International, USA). A number of key themes, apparent on review of the literature regarding MFCs containing AEMs [a small proportion of the total MFC literature], will now be discussed.

Many studies indicate that MFCs containing (dense) IEMs have superior performances (*e.g.* power density outputs[‡] and coulombic efficiencies [CE]) and more stable performances with time⁴²²ⁿ when they contain AEMs (as opposed to CEMs). Major reasons that are put forward for this include:

- The lower O_2 permeability of the AEMs, especially compared to Nafion® perfluorinated CEMs, where reduced O_2 crossover from the cathode to the anode is beneficial in maintaining an anaerobic environment at the anode (for sustaining high CEs *etc.*);
- Reduced “pH splitting” effects leading to smaller pH gradients across the membrane with AEM-based systems: “pH splitting” is the undesirable lowering of the anode chamber pH and a raising of the pH at the cathode (common with CEM-based systems);
- “Reduced” [or different] membrane fouling characteristics;
- Reduced cathode resistances;
- Reduced cation-derived precipitates on the cathode catalyst;
- The higher ionic conductivities (lower internal ohmic resistances[§]) of the AEMs (*vs.* CEMs) in MFCs.

The latter point (f) above is an important contrast to the scenario of AAEM *vs.* PEMs in (abiotic) chemical fuel cells where H^+ and OH^- ions are the main conducting ions and where the OH^- anions have the lower intrinsic mobilities (Table 1).

[‡] Currents and power densities can be normalised to various areas (such as geometric or “projected” anode, cathode, or membrane areas) and volumes (such as anode chamber volume or total MFC volume). These are not always well defined in reported W m^{-2} or W m^{-3} values in the MFC-related literature. A recommendation is to either unambiguously define the normalisation being used or report the absolute currents and powers alongside detailed listing of relevant areas and volume of the system (and its most relevant components). The latter will facilitate easier comparisons between the wide diversity of different systems (configurations) reported in the literature, which currently use a wide variety of normalisations.

[§] Care should be taken when referring to internal resistances, which should be unambiguously defined. MFC studies often refer to internal resistances as meaning the total internal resistances (sum of ohmic + anodic charge transfer + cathodic charge transfer + contact + interfacial resistances + mass transport resistances *etc.*). However, chemical fuel cell (and related devices) studies often refer to internal resistances as meaning the internal ohmic resistances.

However, IEMs in MFCs are predominantly in ionic forms that are not OH^- and H^+ ; the ions present depend on the nature of the anolyte and catholyte media and buffers (if present). If you compare Na^+ to Cl^- , the anion now has the higher mobility. Early generation (non-phase segregated) AAEMs generally have higher IECs compared to PEMs to offset the lower mobility OH^- ions in APEFCs compared to H^+ ions in PEMFCs. The combination of these factors (anion having higher mobility and AEMs having higher IECs) is why the conductivities of AEMs are now higher than CEMs when they are compared in MFCs (*cf.* the same IEMs used in abiotic fuel cells).

However, a major drawback in the use of AEMs is enhanced substrate (*e.g.* acetate) crossover from the anode to the cathode, which can lead to mixed potentials at the cathode and parasitic internal currents. If the system in question involves a catholyte solution (*i.e.* the O_2 is dissolved as part of an aerated electrolyte), then changing this frequently can mitigate against this substrate crossover effect (if this is realistic in a real world application?). The loss of metabolites when using an AEM (especially at low external resistances) can lead to voltage losses over longer operational periods.⁴²²ⁱ Membrane deformation (often in the opposite direction to that seen with the use of CEMs) has also been witnessed, which led to an inferior performance with the use of an AEM;⁴²²ⁱ this was due to the trapping of water and gas between the AEM and cathode. This latter problem can be rectified by using a stainless steel mesh on the anode side to push the membrane onto the cathode.

The internal resistances[§] of MFCs containing dense ion-exchange membranes (AEMs and CEMs) can also be higher compared to MFCs containing porous membranes or with membrane-less (*e.g.* single chamber) MFCs, though the lack of IEM can lead to higher O_2 and substrate crossover. For example, a membrane-free MFC containing a cloth-cathode assembly (containing a GoreTex® cloth which enhances proton transport and O_2 diffusion to the cathode) had a superior performance compared to MFCs containing a membrane-cathode assembly involving either an AEM or a CEM.^{422m} The preparation of MFCs using the cloth-cathode assembly method was also less time consuming and is also claimed to be more optimal for scale-up.

Various types of AEMs have been evaluated in MFCs and these include AMI-7001 (the most commonly encountered),^{422c,d,f,g,p,q} AEMs by Ralex,^{422b,i,j} Tokuyama Neosepta types (this study compares Neosepta AFN, AM-1, and ACS AEMs and probes the interface resistances between the AEM and low buffer [low ionic strength] electrolyte),^{422k} pore-filled type AEMs,^{422e} and Chinese AEM types by Tianwei⁴²²ⁿ and Qianqiu Group (Zhejiang).^{422a,m}

A selected case study is the recent comparison of an in-house synthesised QA poly(ether ether ketones) [QA-PEEK] AEM to AMI-7001 in a single chamber MFC.^{422h} The “hydroxide conducting” QA-PEEK AEM ([allegedly] 0.2 μm thick, IEC = 1.39 meq. g^{-1}) outperformed the AMI-7001 (450 μm thickness, IEC = 1.6 meq. g^{-1} , gel polystyrene-divinylbenzene chemistry) with lower O_2 crossover, despite higher substrate crossover; peak power densities of 60 W m^{-3} and 45 W m^{-3} and CE = 66 and 51%, respectively, were obtained at 30 °C. The MFCs contained PTFE wet-proofed Vulcan XC-72 covered carbon cloth anodes

and carbon-cloth-based air-breathing cathodes that additionally contained a Pt catalyst (loading = 0.5 mg_{Pt} cm^{-2} geometric) and the anodes were inoculated with Anna University domestic wastewater in a phosphate buffer medium (pH = 7.3–7.6 and chemical oxygen demand = 400–600 mg dm^{-3}). The AMI-7001 visibly degraded after 250 d of testing, unlike the QA-PEEK AEM.

A second case study⁴²²ⁱ is where a Ralex AM(H)-PES AEM (QA polyethylene/polyester based, unspecified thickness and IEC in the report but normally supplied with < 450 μm dry thickness and < 750 μm fully hydrated thickness) similarly outperformed a Nafion® CEM in comparable flat-plate dual-chamber *Shewanella putrefaciens* (single species) inoculated MFCs at 27 °C; “non-catalysed” graphite plates were used for both the anode and cathode (maximum voltage and power density of 0.729 V and 57.8 mW m^{-2} for the AEM *vs.* 0.676 V and 39.2 mW m^{-2} for Nafion® [power densities normalised to anode geometric areas]).

A number of the above studies^{422m,n,q} compared the performances of MFCs containing AEMs *vs.* CEMs. ¶ This includes the original study by Logan *et al.*,^{422q} which compared the performances of 2-chambered MFCs containing either AMI-7001 as an AEM or CMI-7000 as a CEM (450 μm thickness, IEC = 1.4 meq. g^{-1} , gel polystyrene-divinylbenzene type). A research priority should be more in-depth comparisons between identical MFC set-ups containing thinner CEMs and AEMs of identical thicknesses, identical IECs and similar chemistries: *i.e.* the same backbone chemistries and just where the cationic (anion-exchange) and anionic (cation-exchange) head-groups are the variable. Aspects that should be studied, including for fundamental investigations, include:

(a) *In situ* beginning-of-life and longer term performances (including data on internal resistances [specifically including internal ohmic resistances][§] and current and power outputs [with clearly defined normalisation][¶]);

(b) *In situ* and *ex situ* durabilities (*i.e.* changes in the IEM chemistry, IEC, conductivity, mechanical stability, and membrane (bio)fouling with time);

(c) Effects of the different membranes on the nature of the biofilms and microbial consortia in the various zones of the biotic chambers during *in situ* MFC testing;

(d) *In situ* and *ex situ* studies into the stability and longer-term performances of the electrodes (catalysts) including those at the cathode (*e.g.* cathode fouling).

There should also be concerted efforts into the development of cheap and thin (*i.e.* low area resistance especially in MFC-relevant anion forms) AEMs that are specifically tailored for MFC-related applications. The AEMs should maintain low O_2 permeabilities, exhibit reduced substrate crossovers (to the cathode), and yield optimised biological outcomes including reduced performance losses due to biofouling (positively charged [polycationic] AEMs would selectively inhibit adhesion or fouling with positively charged bacteria [the opposite to when

¶ The properties of the membranes being used are not always unambiguously reported. As a minimum, we recommend that the following is reported: thickness (in a well-defined hydration state), IEC, and the chemical nature of the membrane.



CEMs are used]]. More research aimed at unambiguously confirming the nature of the *in situ* ion movement through the AEM (including exactly what ions are involved [OH^- , PO_4^{3-} , CO_3^{2-} etc.]) is also justified.

Variant systems related to MFCs

Microbial electrolysis cells (MEC).⁴³⁰ MECs are similar to MFCs but are operated in electrolytic mode (power supplied to the cell), rather than galvanostatic mode (power generated by the cell), and are being developed for the energy efficient (low overpotential) generation of H_2 (*i.e.* that can then be used in chemical fuel cells *etc.*). There have been a number of reports on the use of AEMs in MECs. *e.g.*⁴³¹ It has been shown that AEM-MECs can outperform CEM-MECs (*i.e.* improved H_2 generation at a fixed applied voltage), often due to the lower resistances to ion transport through the AEM. The advantages, disadvantages, and future challenges regarding the use of AEMs in MECs are similar to the use of AEMs in MFCs.

Microbial Desalination Cells (MDC).^{432,433} MDCs are an MFC variant first reported in 2009 [Fig. 19b]⁴³³ⁿ that typically involve a middle desalination chamber that is separated from the bio-anode chamber by an AEM and from the cathode chamber by a CEM. Some designs also involve a series of desalination chambers involving AEM and CEM pairs.^{432,433k} A review of the different types of MDC related systems can be found in ref. 432. MDCs can use the energy content of the wastewater to help power the desalination process: *i.e.* the microbial electricity generation capacity (or part of it) goes towards desalination. Total desalination is, however, not possible as the ionic resistance of the desalination chambers would be very high if they contain totally desalinated water. MDCs are therefore likely to be applied to water softening applications including softening prior to a further non-[bio]electrochemical desalination process.^{433f,m} As the AEM tends to be located between the bioanode chamber and a salt water containing chamber, the AEM-related advantages, disadvantages, and future challenges are again not dissimilar to those discussed above for MFCs and RED cells.

MDC investigations are varied and include studies that have looked into: spatially decoupling the anode and cathode,^{433c} hydraulically connecting multiple MDCs,^{433b} hydraulically connecting an MDC to an osmotic MFC (MOFCs⁴³⁴ contain a Forward Osmosis [FO] membrane that can, on their own, allow desalinated water recovery along with power generation with superior energy recoveries compared to MFCs containing AEMs or CEMs),^{433e} scaling up MDCs to litre scale capacities,^{433h} developing MDC stacks (for faster desalination),^{432,433k} developing hybrid desalination and electrolysis systems for water desalination and H_2 generation,^{433l} developing hybrid microbial electrolysis desalination and chemical production cells for desalination as well as acid and alkali production (this type of system also contains a bipolar membrane between the anode and chemical production chamber [the AEM separates the chemical production chamber and the desalination chamber]),^{432,433i} packing MDCs with ion-exchange resins,^{433a} pH control by using electrolyte circulation,^{433j} and AEM biofouling.^{433d}

Microbial reverse electrodialysis cells (MRC).⁴³⁵ Another closely related variant is the MRC that was first reported by Logan's group in 2011 [Fig. 19c].^{435e,f} An MRC is a combination of an MFC anode chamber and a RED cell stack that allows for

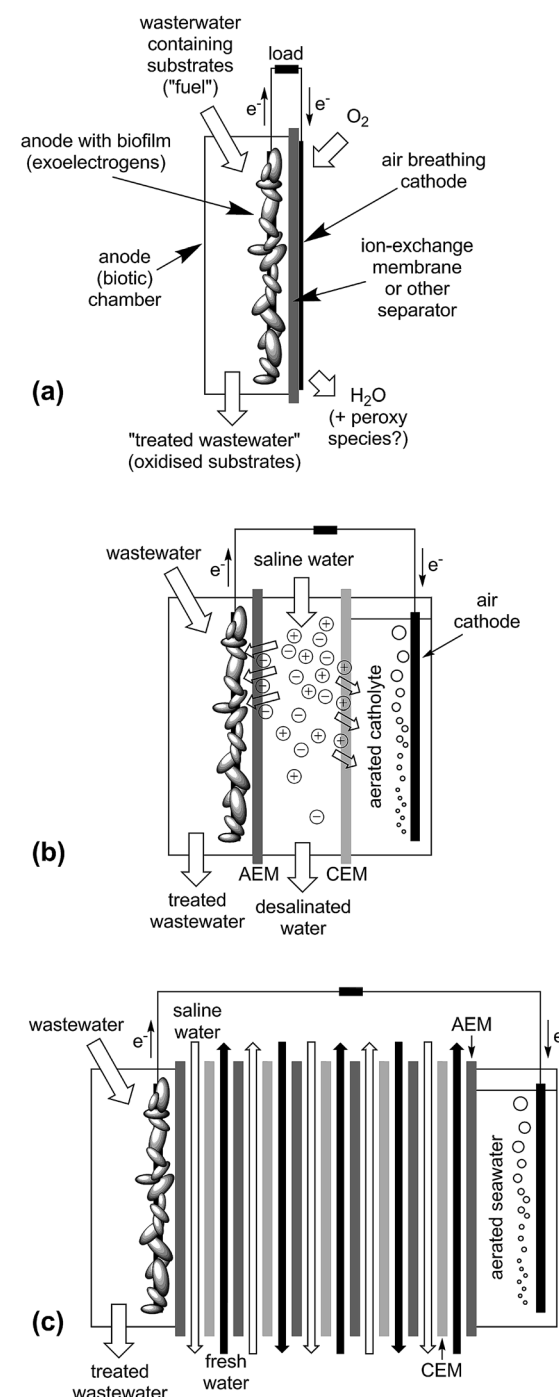


Fig. 19 Simple schematics of: (a) a Microbial Fuel Cells [MFC] in air-breathing single-chamber mode [alternative configuration (not shown): a 2-chamber MFC would contain a cathode chamber containing an aerated catholyte and a submerged cathode]; (b) the simplest configuration of a 3-chamber Microbial Desalination Cell [MDC]; (c) the simplest configuration of a microbial reverse electrodialysis cell [MRC]. Engineering components, such as gaskets and end plates, are not shown.



the synergistic enhancement of power production or the energy efficient production of H₂ (the latter when operated as a microbial reverse electrodialysis electrolysis cell^{435b,f}). An AEM is located next to the bioanode chamber (à la MFC) and AEMs are also located as part of the multiple AEM/CEM pairs (as found in traditional abiotic RED cells where the AEMs separate chambers with different salinities). As the AEMs are both in contact with and spatially separated from the biology, the AEM-related advantages, disadvantages, and future challenges are again not dissimilar to those discussed above for MFCs and RED cells. MRC investigations are also varied and have studied topics such as MRC-based chemical (again acid and alkali) production cells (the bipolar membrane is located next to the anode chamber)^{435c} and also systems that involve thermolytic (ammonium bicarbonate) solutions.^{435d} Recently, a “MRC” with only a single cell “pair” (a single AEM, no CEM and an [NH₄][HCO₃] catholyte) has been reported to lead to improved performances compared to a MRC containing a AEM|CEM|AEM configuration.^{435a}

Microbial electrosynthesis in microbial carbon capture cells (MCCC).⁴³⁶ Biological conversion of CO₂ to fuels and electrofuels is a potentially important clean technology.⁴³⁷ Hence, a final bioelectrochemical variant that is worth a quick mention, and where the application of AEMs may have a future impact, is for microbial electrosynthesis in MCCCs.⁴³⁶ The example where an AEM (AMI-7001) has already been applied in an MCCC is where CO₂ is supplied to the cathode (containing a photosynthetic cyanobacteria *Anabaena* sp.) and is sequestered by biological conversion to organic matter.^{436c} Microbial reverse-electrodialysis and electrolysis functions can also be combined to give a system that produces H₂ and sequesters CO₂ (conversion into inorganic carbonates).⁴³⁸

Summary and concluding remarks

Alkaline anion-exchange membranes (AAEMs) are being developed for application in electrochemical devices such as alkaline polymer electrolyte fuel cells (APEFC). As with the more well-known proton-exchange membrane fuel cells (PEMFCs), APEFCs can be operated with Pt-based catalysts. However, it should be noted that even though the oxygen reduction reaction is slightly less of a problem at high pHs, the hydrogen oxidation reaction kinetics is poorer with Pt catalysts in alkali than in acid. In contrast to PEMFCs, the anode of APEFCs tends to produce larger performance limitations than the cathode. The main rationale for the development of devices such as APEFCs is the promise of the ability to use a broad range of non-precious metal (non-Pt-group-metals) catalysts.

The conductivities of AAEMs in the OH⁻ form can be as high as H⁺ conduction in proton-exchange membranes (PEMs such as Nafion®) when the AAEMs are well hydrated, which is the situation in electrolyzers containing polymer electrolytes. However, the conductivities of AAEMs are much more sensitive to hydration levels and drop rapidly when exposed to lower humidity environments (e.g. as found in APEFCs). The development of AAEMs that retain conductivity at lower hydration levels is a research priority. If OH⁻ conductivities are being measured, it is essential to totally exclude CO₂ from each stage

of the experiment otherwise conductivities will be underestimated (as a mixture of anions [OH⁻/CO₃²⁻/HCO₃⁻] will be present). To aid in inter-laboratory comparisons, HCO₃⁻ conductivities should also be reported.

The biggest research challenge for devices with high pH environments is to develop chemically stable AAEMs and anion-exchange ionomers (AEIs), especially when less than fully hydrated. Most studies have focussed only on the alkali stabilities (especially of the cationic [anion-exchange] head-groups), as this is seen as the biggest problem. However, the stability to *in situ* generated peroxy species (and resulting radicals) needs to be explored in much more detail as not much is known to date regarding AAEMs in APEFCs *etc.* (in contrast to PEMs in PEMFCs). Even though a polymer backbone is stable in alkali, it may not be alkali stable once it is functionalised with cationic side-groups. Studies of the alkali stabilities of AAEMs and AEIs must consider the synergistic effects of the cation head-groups and the backbone. Stability studies should always use spectroscopic evidence alongside secondary evidence such as changes in ion-exchange capacities with ageing time; the relative changes in quaternary and non-quaternary exchange capacities should also be studied.

Despite all of this, AAEMs containing simple (low molecular weight) quaternary ammonium cationic head-groups (such as R-N⁺Me₃) may well be stable enough in the OH⁻ forms for some applications if they are kept fully hydrated. This will be especially true for AAEMs that possess phase segregated morphologies, where location of the cationic head-groups in the hydrophilic channels/clusters will maximise the chances that they remain suitably hydrated. It is vital that AAEMs/AEIs are developed with long term stabilities in the OH⁻ form at temperatures >80 °C (especially when less than fully hydrated) for application in APEFCs. Operation at such elevated temperatures (and/or at high current densities) is suspected to lead to an enhanced or intrinsic tolerance to CO₂ in the cathode air supplies. An alternative approach may be to deliberately direct the system to utilise CO₃²⁻ (but not HCO₃⁻) conduction as AAEMs are generally much more stable in the CO₃²⁻ forms.

The use of alternative fuels in APEFCs is a mixed bag. The use of alcohols appears not to be viable without the addition of Na/KOH into the aqueous fuel supplies, which then begs the question: why use polymer electrolytes in such fuel cells? On the other hand, the use of non-carbon fuel options may have more application, especially sodium borohydride for niche (military) applications and hydrazine hydrate (not anhydrous hydrazine) for more main-stream markets.

Stability to OH⁻ (or CO₃²⁻) anions is also required if the AAEMs are to be used in alkaline water electrolyzers. However, such electrolyzers have the advantage over APEFCs in that the AAEMs and AEIs can be kept well hydrated to maximise stability and conductivity. An aspiration is to develop alkaline polymer electrolyte electrolyzers that generate H₂ from pure water (no added alkali or acid). Electrolysis devices that are aimed at CO₂ utilisation are also of increasing interest.

For application in redox flow batteries (RFBs), the anion-exchange membranes (AEMs) need to instead be stable to the redox species present (e.g. vanadium species in all-vanadium



RFBs [VRFBs]) as well as to low pHs if acidic electrolytes are present. The hope is that AEMs selectively reject vanadium cations in VRFBs to reduce vanadium species crossover. A reduction in water crossover is also considered to be important with various RFBs and the use of AEMs should be investigated with regards to this technological requirement.

When applied to electrochemical devices such as reverse electrodialysis (RED) cells and microbial fuel cells (MFCs), the alkali stabilities of AEMs are almost irrelevant (as the membranes are not exposed to high pH environments). However, the conductivities are lower with ions that are typically present in these devices (e.g. Cl^- and not OH^-). The research challenge here is to develop thinner membranes (to counteract the lower conductivities with non- OH^- anions) but where there is no reduction in other properties (e.g. no increase in O_2 permeability in microbial systems or no lowering of permselectivity or mechanical properties in RED cells). As the AEMs are in environments with less extreme pHs, then chemistries that are not stable in alkali (such as imidazolium, phosphonium, and pyridinium cationic head-groups) may be applicable. This selection of a wider range of AEM chemistries may well be advantageous when applied to devices where fouling (including bio-fouling) may be an issue and needs to be minimised.

It is clear that a single AEM will not be optimal for all applications and AEMs will need to be specifically tailored for the job at hand. However, there is a significant chemical and materials space that can be probed and utilised for the development of tailored AEMs/AEIs.

Statement of author contributions

John Varcoe is lead author who wrote the bulk of the sections on membrane chemistries and the sections on biological systems and batteries. He also coordinated all efforts and integrated all contributions into the manuscript in a consistent manner. Plamen Atanassov provided the information on fuels that are alternative to hydrogen for use in fuel cells (such as hydrazine). Dario Dekel led the discussion (and provided an industrial perspective) on the application on AAEMs in hydrogen-based fuel cells. Andrew Herring, Tongwen Xu and Lin Zhuang all provided significant contributions on membrane chemistry, especially the critically important phase segregated systems. Lin Zhuang also provided input on alternative fuels and electrolyzers. Michael Hickner wrote the section on redox flow batteries. Paul Kohl wrote the section on hybrid anion- and cation-exchange membrane systems. Anthony Kucernak wrote the key sections on issues with carbon and carbon-free supports. He gave some input into various catalyst chemistries. William Mustain wrote the sections on carbonate cycle fuel cells and electrolyzers. Kitty Nijmeijer wrote the section on Reverse Electrodialysis Cells. Keith Scott led on the sections on hydrogen-based electrolyzers.

Abbreviations

This lists the subject-specific acronyms used in the main text for quick reference. This table does not list commonly used

chemical symbols and nomenclature (e.g. NMR, TEM etc.) that are well known to the general chemistry audience. *Acronyms in italics* are carefully defined in the preamble at the start of the article.

<i>AAEM</i>	<i>Alkaline anion-exchange membrane</i>
AB	Ammonia borane
ABCO	1-Azabicyclo[2.2.2]octane (quinuclidine)
ADFFC	Alkaline direct formate fuel cell
<i>AEI</i>	<i>Anion-exchange ionomer</i>
<i>AEM</i>	<i>Anion-exchange membrane</i>
AEMFC	Anion-exchange membrane fuel cell [= APEFC]
AFC	Alkaline fuel cell (taken here as the fuel cell type containing aqueous K/NaOH electrolytes and not a AAEM)
AMFC	Alkaline membrane fuel cell [= APEFC]
<i>APEE</i>	<i>Alkaline polymer electrolyte electrolyser</i>
<i>APEFC</i>	<i>Alkaline polymer electrolyte fuel cell</i>
APM	Alkali-doped poly(benzimidazole)
CCM	Catalysed coated membrane
CDU	Carbon dioxide utilisation
CE	Coulombic efficiency
<i>CEM</i>	<i>Cation-exchange membrane</i>
CNT	Carbon nanotube
DABCO	1,4-Diazabicyclo[2.2.2]octane
DAFC	Direct alcohol fuel cell
DBHFC	Direct borohydride fuel cell
DEFC	Direct ethanol fuel cell
DEGFC	Direct ethylene glycol fuel cell
DHFC	Direct hydrazine fuel cell
DMFC	Direct methanol fuel cell
EDL	Electrical double layer
EG	Ethylene glycol
EOR	Ethanol oxidation reaction
FO	Forward osmosis
<i>HEM</i>	<i>Hydroxide-exchange membrane</i>
HER	Hydrogen evolution reaction
HOR	Hydrogen oxidation reaction
IEC	Ion-exchange capacity
<i>IEM</i>	<i>Ion-exchange membrane</i>
MCCC	Microbial carbon capture cells
MDC	Microbial desalination cell
MEA	Membrane electrode assembly
MEC	Microbial electrolysis cell
MFC	Microbial fuel cell
MOFC	Microbial osmotic fuel cell
MOH	Metal (normally alkali metal) hydroxide
MOR	Methanol oxidation reaction
MRC	Microbial reverse electrodialysis cell
ORR	Oxygen reduction reaction
OER	Oxygen evolution reaction
PBI	Poly(benzimidazole)
PECH	Poly(epichlorohydrin)
PEEK	Poly(ether ether ketone)
<i>PEM</i>	<i>Proton-exchange membrane</i>
PEMFC	<i>Proton-exchange membrane fuel cell</i>
PFSA	Perfluoro sulfonic acid
PGM	Platinum-group metal
PPO	Poly(phenylene oxide)



PRO	Pressure retarded osmosis
PTFE	Poly(tetrafluoroethylene)
PVA	Poly(vinyl alcohol)
QA	Quaternary ammonium
QAPS	Quaternary ammonium poly(sulfone)
RED	Reverse electrodialysis
RFB	Redox flow battery
RFC	Regenerative fuel cell
RH	Relative humidity
RO	Reverse osmosis
ROMP	Ring opening metathesis polymerisation
RTCFC	Room temperature carbonate fuel cell
SAFC	Solid alkaline fuel cell [\equiv APEFC]
SGE	Salinity gradient energy
SPE	Solid polymer electrolyte
SPEEK	Sulfonated poly(ether ether ketone)
URFC	Unitized regenerative fuel cell
VRFB	Vanadium redox flow battery

Acknowledgements

We wish to thank the following funders and sponsors of the workshop on “Anion-exchange membranes for energy generation technologies” held at the University of Surrey on 25th – 26th July 2013:¹ The UK’s Engineering and Physical Sciences Research Council (EPSRC grants EP/I004882/1, EP/H019480/1 and EP/H025340/1), the University of Surrey’s Institute of Advanced Studies (especially Mirela Dumic for her extensive assistance),¹ the Research Council UK’s Energy Programme’s Supergen Hydrogen and Fuel Cell Research Hub (EPSRC grant EP/J016454/1), Royal Society of Chemistry publishing, Caltest Instruments Ltd. (UK), Alvatek Ltd. (UK), and Solartron Analytical UK (Ametek). We also thank the US Army Research Office for funding from a Multidisciplinary University Research Initiative (MURI contract W911NF-10-1-0520). The following members of the local organising committee are also thanked: Dr Simon Poynton, Dr Cathryn Hancock, Dr Ai Lien Ong, Sam Murphy, Sarah Mallinson, Jessica Whitehead and Lucy Howes.

References

- 1 <http://www.ias.surrey.ac.uk/workshops/membranes/>.
- 2 (a) K.-D. Kreuer, *Chem. Mater.*, 2014, **26**, 361; (b) M. A. Hickner, A. M. Herring and E. B. Coughlin, *J. Polym. Sci., Part B: Polym. Phys.*, 2013, **51**, 1727; (c) Y.-J. Wang, J. Qiao, R. Baker and J. Zhang, *Chem. Soc. Rev.*, 2013, **42**, 5768; (d) A. Brouzgou, A. Podias and P. Tsiakaras, *J. Appl. Electrochem.*, 2013, **43**, 119; (e) J. Pan, C. Chen, L. Zhuang and J. Lu, *Acc. Chem. Res.*, 2012, **45**, 473; (f) H. Zhang and P. K. Shen, *Chem. Soc. Rev.*, 2012, **41**, 2382; (g) H. Zhang and P. K. Shen, *Chem. Rev.*, 2012, **112**, 2780; (h) G. Couture, A. Alaaeddine, F. Boschet and B. Ameduri, *Prog. Polym. Sci.*, 2011, 1521; (i) G. Merle, M. Wessling and K. Nijmeijer, *J. Membr. Sci.*, 2011, **377**, 1; (j) Y. A. Elabd and M. A. Hickner, *Macromolecules*, 2011, **44**, 1; (k) R. Zeng and J. R. Varcoe, *Recent Pat. Chem. Eng.*, 2011, **4**, 93; (l) E. H. Yu, U. Krewer and K. Scott, *Energies*, 2010, **3**, 1499; (m) V. V. Shevchenko and M. A. Gumennaya, *Theor. Exp. Chem.*, 2010, **46**, 139; (n) D. Tang, J. Pan, S. Lu, L. Zhuang and J. Lu, *Sci. China: Chem.*, 2010, **53**, 357; (o) E. Antolini and E. R. Gonzalez, *J. Power Sources*, 2010, **195**, 3431; (p) A. Serov and C. Kwak, *Appl. Catal., B*, 2010, **98**, 1; (q) F. Bidault, D. J. L. Brett, P. H. Middleton and N. P. Brandon, *J. Power Sources*, 2009, **187**, 39; (r) J. R. Varcoe, J. P. Kizewski, D. M. Halepoto, S. D. Poynton, R. C. T. Slade and F. Zhao, in *Encyclopedia of Electrochemical Power Sources*, ed. C. Garche, P. Dyer, Z. Moseley, D. R. Ogumi and B. Scrosati, Elsevier, Amsterdam, 2009, vol. 2, pp. 329–343; (s) J. R. Varcoe, S. D. Poynton and R. C. T. Slade, in *Handbook of Fuel Cells - Fundamentals, Technology and Applications*, ed. W. Vielstich, H. Yokokawa and H. A. Gasteiger, John Wiley and Sons, Ltd., 2009, vol. 5, ch. 21, pp. 322–333; (t) R. C. T. Slade and J. R. Varcoe, *Fuel Cells*, 2005, **5**, 187; (u) T. Xu, *J. Membr. Sci.*, 2005, **263**, 1.
- 3 S. Marini, P. Salvi, P. Nelli, R. Pesenti, M. Villa, M. Berrettoni, G. Zangari and Y. Kiros, *Electrochim. Acta*, 2012, **82**, 384.
- 4 (a) W. Wang, Q. Luo, B. Li, X. Wei, L. Li and Z. Yang, *Adv. Funct. Mater.*, 2013, **23**, 970; (b) B. Schwenzer, J. Zhang, S. Kim, L. Li and Z. Yang, *ChemSusChem*, 2011, **4**, 1388; (c) X. Li, H. Zhang, Z. Mai, H. Zhang and I. Vankelecom, *Energy Environ. Sci.*, 2011, **4**, 1147; (d) M. Skyllas-Kazacos, M. H. Chakrabarti, S. A. Hajimolana, F. S. Mjalli and M. Saleem, *J. Electrochem. Soc.*, 2011, **158**, R55; also ref. 2a above.
- 5 (a) B. E. Logan and M. Elimelech, *Nature*, 2012, **488**, 313; (b) G. Z. Ramon, B. J. Feinberg and E. M. V. Hoek, *Energy Environ. Sci.*, 2011, **4**, 4423.
- 6 (a) J. X. Leong, W. R. W. Daud, M. Ghasemi, K. B. Liew and M. Ismail, *Renewable Sustainable Energy Rev.*, 2013, 575; (b) V. B. Oliveria, M. Simões, L. F. Melo and A. M. F. R. Pinto, *Biochem. Eng. J.*, 2013, **73**, 53; (c) Y. Yang, G. Sun and M. Xu, *J. Chem. Technol. Biotechnol.*, 2011, **86**, 625; also ref. 5a above.
- 7 W. Gallet, J. Schumacher, M. Kesmez, D. Le and S. D. Minteer, *J. Electrochem. Soc.*, 2010, **157**, B557.
- 8 (a) X. Li, Q. Liu, Y. Yu and Y. Meng, *J. Mater. Chem. A*, 2013, **1**, 4324; (b) A. Jasti and V. K. Shahi, *J. Mater. Chem. A*, 2013, **1**, 6134; (c) D. Chen, M. A. Hickner, S. Wang, J. Pan, M. Xiao and Y. Meng, *Int. J. Hydrogen Energy*, 2012, **37**, 16168; (d) M. Tanaka, M. Koike, K. Miyatake and M. Watanabe, *Polym. Chem.*, 2011, **2**, 99; (e) J. Fang and P. K. Shen, *J. Membr. Sci.*, 2006, **285**, 317.
- 9 (a) X. Li, Y. Yu and Y. Meng, *ACS Appl. Mater. Interfaces*, 2013, **5**, 1414; (b) D. W. Seo, Y. D. Lim, M. A. Hossain, S. H. Lee, H. C. Lee, H. H. Jang, S. Y. Choi and W. G. Kim, *Int. J. Hydrogen Energy*, 2013, **38**, 579; (c) D. W. Seo, M. A. Hossain, D. H. Lee, Y. D. Lim, S. H. Lee, H. C. Lee, T. W. Hong and W. G. Kim, *Electrochim. Acta*, 2012, **86**, 360; (d) Q. Zhang, Q. Zhang, J. Wang, S. Zhang and S. Li, *Polymer*, 2010, 5407; (e) J. Zhou, M. Ünlü, J. A. Vega and





P. A. Kohl, *J. Power Sources*, 2009, **190**, 285; (f) D. Xing, S. Zhang, C. Yin, C. Yan and X. Jian, *Mater. Sci. Eng., B*, 2009, **157**, 1; (g) L. Li and Y. Wang, *J. Membr. Sci.*, 2005, **262**, 1; (h) J. Kerres, A. Ullrich and M. Hein, *J. Polym. Sci., Part A: Polym. Chem.*, 2001, **39**, 2874.

10 (a) X. Yan, S. Gu, G. He, X. Wu and J. Benziger, *J. Power Sources*, 2014, **250**, 90; (b) J. Han, H. Peng, J. Pan, L. Wei, G. Li, C. Chen, L. Xiao, J. Lu and L. Zhuang, *ACS Appl. Mater. Interfaces*, 2013, **5**, 13405; (c) Z. Liu, X. Li, K. Shen, P. Feng, Y. Zhang, X. Xu, W. Hu, Z. Jiang, B. Liu and M. D. Guiver, *J. Mater. Chem. A*, 2013, **1**, 6481; (d) X. Lin, Y. Liu, S. D. Poynton, A. Ong, J. R. Varcoe, L. Wu, Y. Li, X. Liang, Q. Li and T. Xu, *J. Power Sources*, 2013, **233**, 259; (e) Z. Liu, X. Zhu, G. Wang, X. Hou and D. Liu, *J. Polym. Sci., Part B: Polym. Phys.*, 2013, **51**, 1632; (f) K. Shen, J. Pang, S. Feng, Y. Wang and Z. Jiang, *J. Membr. Sci.*, 2013, **440**, 20; (g) X. Yan, G. He, X. Wu and J. Benziger, *J. Membr. Sci.*, 2013, **429**, 13; (h) A. Jasti, S. Prakash and V. K. Shahi, *J. Membr. Sci.*, 2013, **428**, 470; (i) J. Wang, J. Wang and S. Zhang, *J. Membr. Sci.*, 2012, **415–416**, 205; (j) H. Zhang and Z. Zhou, *Solid State Ionics*, 2008, **179**, 1296.

11 X. Yan, S. Gu, G. He, X. Wu, W. Zheng and X. Ruan, *J. Membr. Sci.*, 2014, **466**, 220.

12 (a) G. Wang, Y. Weng, J. Zhao, D. Chu, D. Xie and R. Chen, *Polym. Adv. Technol.*, 2010, **21**, 554; (b) G. Wang, Y. Weng, D. Chu, D. Xie and R. Chen, *J. Membr. Sci.*, 2009, **326**, 4.

13 (a) W. Wang, S. Wang, W. Li, X. Xie and Y. Lv, *Int. J. Hydrogen Energy*, 2013, **38**, 11045; (b) C. Li, S. Wang, W. Wang, X. Xie, Y. Lv and C. Deng, *Int. J. Hydrogen Energy*, 2013, **38**, 11038; (c) Q. Hu, Y. Shang, Y. Wang, M. Xu, S. Wang, X. Xie, Y. Liu, H. Zhang, J. Wang and Z. Mao, *Int. J. Hydrogen Energy*, 2012, **37**, 12659.

14 (a) N. T. Rebek, Y. Li and D. M. Knauss, *J. Polym. Sci., Part B: Polym. Phys.*, 2013, **51**, 1770; (b) A. Katzfus, V. Gogel, L. Jörissen and J. Kerres, *J. Membr. Sci.*, 2013, **425–426**, 131; (c) X. Lin, C. Wu, Y. Wu and T. Xu, *J. Appl. Polym. Sci.*, 2012, **123**, 3644; (d) S. Gu, J. Skovgard and Y. Yan, *ChemSusChem*, 2012, **5**, 843; (e) A. Ong, S. Saad, R. Lan, R. J. Goodfellow and S. Tao, *J. Power Sources*, 2011, **196**, 8272; (f) Y. Wu, C. Wu, J. R. Varcoe, S. D. Poynton, T. Xu and Y. Fu, *J. Power Sources*, 2010, **195**, 3069; (g) L. Wu, T. Xu, D. Wu and X. Zheng, *J. Membr. Sci.*, 2008, **310**, 577; (h) L. Wu, T. Xu and W. Yang, *J. Membr. Sci.*, 2006, **286**, 185; (i) T. Xu and F. F. Zha, *J. Membr. Sci.*, 2002, **199**, 203.

15 (a) R. Janarthanan, J. L. Horan, B. R. Caire, Z. C. Zieger, Y. Yang, X. Zuo, M. W. Liberatore, M. R. Hibbs and A. M. Herring, *J. Polym. Sci., Part B: Polym. Phys.*, 2013, **51**, 1743; (b) C. Fujimoto, D.-S. Kim, M. Hibbs, D. Wroblewski and Y. S. Kim, *J. Membr. Sci.*, 2012, **423–424**, 438; (c) E. E. Switzer, T. S. Olson, A. K. Datye, P. Atanassov, M. R. Hibbs, C. Fujimoto and C. J. Cornelius, *Electrochim. Acta*, 2010, **55**, 3404.

16 (a) M. A. Vandiver, J. L. Horan, Y. Yang, E. T. Tansey, S. Seifert, M. W. Liberatore and A. M. Herring, *J. Polym. Sci., Part B: Polym. Phys.*, 2013, **51**, 1761; (b) D. S. Kim, C. H. Fujimoto, M. R. Hibbs, A. Labouriau, Y.-K. Choe and Y. S. Kim, *J. Polym. Sci., Part B: Polym. Phys.*, 2013, **46**, 7826; (c) D. S. Kim, C. H. Fujimoto, M. R. Hibbs, A. Labouriau, Y.-K. Choe and Y. S. Kim, *Macromolecules*, 2013, **46**, 7826; (d) X. Kong, K. Wadhwa, J. G. Verkade and K. Schmidt-Rohr, *Macromolecules*, 2009, **42**, 1659.

17 A. Bosnjakovic, M. Danilczuk, S. Schlick, P. N. Xiong, G. M. Haugen and S. J. Hamrock, *J. Membr. Sci.*, 2014, **467**, 136.

18 (a) D. Henkensmeier, H. Cho, M. Brela, A. Michalak, A. Dyck, W. Germer, N. M. H. Duong, J. H. Jang, H.-J. Kim, N.-S. Woo and T.-H. Lim, *Int. J. Hydrogen Energy*, 2014, **39**, 2842; (b) H.-J. Lee, J. Choi, J. Y. Han, H.-J. Kim, Y.-E. Sung, H. Kim, D. Henkensmeier, E. A. Cho, J. H. Jang and S. J. Yoo, *Polym. Bull.*, 2013, **70**, 2619; (c) L. An, L. Zeng and T. S. Zhao, *Int. J. Hydrogen Energy*, 2013, **38**, 10602; (d) O. D. Thomas, K. J. W. Y. Soo, T. J. Peckham, M. P. Kulkarni and S. Holdcroft, *J. Am. Chem. Soc.*, 2012, **134**, 10753; (e) Z. Xia, S. Yuan, G. Jiang, X. Guo, J. Fang, L. Liu, J. Qiao and J. Yin, *J. Membr. Sci.*, 2012, **390–391**, 152; (f) D. Henkensmeier, H.-R. Cho, H.-J. Kim, C. N. Kirchner, J. Leppin, A. Dyke, J. H. Jang, E. A. Cho, S.-W. Nam and T.-H. Lim, *Polym. Degrad. Stab.*, 2012, **97**, 264; (g) H. Luo, G. Vaivars, B. Agboola, S. Mu and M. Mathe, *Solid State Ionics*, 2012, **208**, 52; (h) O. D. Thomas, K. J. W. Y. Soo, T. J. Peckham, M. P. Kulkarni and S. Holdcroft, *Polym. Chem.*, 2011, **2**, 1641; (i) H. Hou, G. Sun, R. He, B. Sun, W. Jin, H. Liu and Q. Xin, *Int. J. Hydrogen Energy*, 2008, **33**, 7172; (j) B. Xing and O. Savadogo, *Electrochim. Commun.*, 2000, **2**, 697.

19 (a) C. C. Yang, *J. Appl. Electrochem.*, 2012, **42**, 305; (b) T. Y. Guo, Q. H. Zeng, C. H. Zhao, Q. L. Liu, A. M. Zhu and I. Broadwell, *J. Membr. Sci.*, 2011, **371**, 268; (c) C. Sollogoub, A. Guinault, C. Bonnebat, M. Bennjima, L. Akrou, J. F. Fauvarque and L. Ogier, *J. Membr. Sci.*, 2009, **335**, 37; (d) D. Stoica, F. Alloin, S. Marais, D. Langevin, C. Chappé and P. Judeinstein, *J. Phys. Chem. B*, 2008, **112**, 12338; (e) D. Stoica, L. Ogier, L. Akrou, F. Alloin and J. F. Fauvarque, *Electrochim. Acta*, 2007, **53**, 1596; (f) E. Agel, J. Bouet and J. F. Fauvarque, *J. Power Sources*, 2001, **101**, 267.

20 A. M. Maes, T. P. Pandey, M. A. Vandiver, L. K. Lundquist, Y. Yang, J. L. Horan, A. Krosovsky, M. W. Liberatore, S. Seifert and A. M. Herring, *Electrochim. Acta*, 2013, **110**, 260.

21 (a) M. Zhang, H. K. Kim, E. Chalkova, F. Mark, S. L. Lvov and T. C. M. Chung, *Macromolecules*, 2011, **44**, 5937; (b) H. A. Kostalik IV, T. J. Clark, N. J. Robertson, P. F. Mutolo, J. M. Longo, H. D. Abruña and G. W. Coates, *Macromolecules*, 2010, **43**, 7147; (c) N. J. Robertson, H. A. Kostalik IV, T. J. Clark, P. F. Mutolo, H. D. Abruña and G. W. Coates, *J. Am. Chem. Soc.*, 2010, **132**, 3400.

22 T. J. Clarke, N. J. Robertson, H. A. Kostalik IV, E. B. Lobkovsky, P. F. Mutolo, H. D. Abruña and G. W. Coates, *J. Am. Chem. Soc.*, 2009, **131**, 12888.

23 (a) W. Lu, Z.-G. Shao, G. Zhang, Y. Zhao and B. Yi, *J. Power Sources*, 2014, **248**, 905; (b) T.-H. Tsai, A. M. Maes, M. A. Vandiver, C. Versek, S. Seifert, M. Tuominen,

M. W. Liberatore, A. M. Herring and E. B. Coughlin, *J. Polym. Sci., Part B: Polym. Phys.*, 2013, **51**, 1751; (c) J. Zhou, J. Guo, D. Chu and R. Chen, *J. Power Sources*, 2012, **219**, 272.

24 C. Chen, A. R. Hess, A. R. Jones, X. Liu, G. D. Barber, T. E. Mallouk and H. R. Allcock, *Macromolecules*, 2012, **45**, 1182.

25 (a) L. Gubler, *Adv. Energy Mater.*, 2014, **4**, 1300827; (b) H. Koshikawa, K. Yoshimura, W. Sinnananchi, T. Yamaki, M. Asano, K. Yamamoto, S. Yamaguchi, H. Tanaka and Y. Maekawa, *Macromol. Chem. Phys.*, 2013, **214**, 1756; (c) T. A. Sharazi, J. Y. Sohn, Y. M. Lee and M. D. Guiver, *J. Membr. Sci.*, 2013, **441**, 148; (d) J. P. Kizewski, N. H. Mudri and J. R. Varcoe, *Radiat. Phys. Chem.*, 2013, **89**, 64; (e) M. Mamlouk, J. A. Horsfall, C. Williams and K. Scott, *Int. J. Hydrogen Energy*, 2012, **37**, 11912; (f) B.-S. Ko, J.-Y. Sohn and J. Shin, *Polymer*, 2012, **53**, 4652; (g) L. Ajis, A. A. Nazli, M. A. Abd Malik, M. D. Khairul Zaman and Y. Muhd Zu Azhan, *Adv. Mater. Res.*, 2012, **476–478**, 636; (h) J. Fang, Y. Yang, X. Lu, M. Ye, W. Li and Y. Zhang, *Int. J. Hydrogen Energy*, 2012, **37**, 594; (i) J. R. Varcoe, R. C. T. Slade, E. Lam How Yee, S. D. Poynton, D. J. Driscoll and D. C. Apperley, *Chem. Mater.*, 2007, **19**, 2686; (j) T. N. Danks, R. C. T. Slade and J. R. Varcoe, *J. Mater. Chem.*, 2003, **13**, 712; (k) B. L. Svarvar, K. B. Ekman, M. J. Sundell and J. H. Nasman, *Polym. Adv. Technol.*, 1996, **7**, 839.

26 (a) Z. Jiang and Z.-J. Jiang, *J. Membr. Sci.*, 2014, **456**, 84; (b) J. Hu, C. Zhang, L. Jiang, S. Fang, X. Zhang, X. Wang and Y. Meng, *J. Power Sources*, 2014, **248**, 831; (c) N. Follain, S. Roualdès, S. Marais, J. Frugier, M. Reinholdt and J. Durand, *J. Phys. Chem. C*, 2012, **116**, 8510; (d) C. Zhang, J. Hu, X. Wang, H. Toyoda, M. Nagatsu, X. Zhang and Y. Meng, *J. Power Sources*, 2012, **198**, 112; (e) C. Zhang, J. Hu, Y. Meng, M. Nagatsu and H. Toyoda, *Chem. Commun.*, 2011, **47**, 10230; (f) C. Zhang, J. Hu, J. Cong, Y. Zhao, W. Shen, H. Toyoda, M. Nagatsu and Y. Meng, *J. Power Sources*, 2011, **196**, 5386; (g) J. Hu, Y. Meng, C. Zhang and S. Fang, *Thin Solid Films*, 2011, **519**, 2155; (h) M. Sudoh, S. Niimi, N. Takaota and M. Watanabe, *ECS Trans.*, 2010, **25**, 61; (i) K. Matsuoka, S. Chiba, Y. Iriyama, T. Abe, M. Matsuoka, K. Kikuchi and Z. Ogumi, *Thin Solid Films*, 2008, **516**, 3309; (j) M. Schieda, S. Roualdès, J. Durand, A. Martinent and D. Marsacq, *Desalination*, 2006, **199**, 286.

27 (a) D.-H. Kim, J.-H. Park, S.-J. Seo, J.-S. Park, S. Jung, Y. S. Kang, J.-H. Choi and M.-S. Kang, *J. Membr. Sci.*, 2013, **447**, 80; (b) S.-H. Park, Y.-W. Choi, C.-S. Kim and S. B. Park, *J. Solid State Chem.*, 2013, **17**, 1247; (c) H. Jung, H. Ohashi, T. Tamaki and T. Yamaguchi, *Chem. Lett.*, 2013, **42**, 14; (d) H. Zhang, H. Ohashi, T. Tamaki and T. Yamaguchi, *J. Phys. Chem. C*, 2012, **116**, 7650; (e) H. Jung, K. Fujii, T. Tamaki, H. Ohashi, T. Ito and T. Yamaguchi, *J. Membr. Sci.*, 2011, **373**, 107; (f) X. Zhang, S. W. Tay, Z. Liu and L. Hong, *J. Power Sources*, 2011, **196**, 5494; (g) A. K. Pandey, R. F. Childs, M. West, J. N. A. Lott, B. E. McCarry and J. M. Dickson, *J. Polym. Sci., Part A: Polym. Chem.*, 2001, **39**, 807.

28 (a) A. M. Park, F. E. Turley, R. J. Wycisk and P. N. Pintauro, *Macromolecules*, 2014, **47**, 227; (b) S. Roddecha, Z. Dong, Y. Wu and M. Anthamatten, *J. Membr. Sci.*, 2012, **389**, 478.

29 (a) G. Li, J. Pan, J. Han, C. Chen, J. Lu and L. Zhuang, *J. Mater. Chem. A*, 2013, **1**, 12497; (b) Y. Zhao, J. Pan, H. Yu, D. Yang, J. Li, L. Zhuang, Z. Shao and B. Yi, *Int. J. Hydrogen Energy*, 2013, **38**, 1983; (c) Y. Zhao, H. Yu, D. Yang, J. Li, Z. Shao and B. Yi, *J. Power Sources*, 2013, **221**, 247; (d) Y.-C. Cao, K. Scott and X. Wang, *Int. J. Hydrogen Energy*, 2012, **37**, 12688; (e) F. Zhang, H. Zhang, J. Ren and C. Qu, *J. Mater. Chem.*, 2010, **20**, 8139.

30 (a) T. Zhou, J. Zhang, J. Jingfu, G. Jiang, J. Zhang and J. Qiao, *Synth. Met.*, 2013, **167**, 43; (b) L. Zeng, T. S. Zhao and Y. S. Li, *Int. J. Hydrogen Energy*, 2012, **37**, 18425; (c) G. Merle, S. S. Hosseiny, M. Wessling and K. Nijmeijer, *J. Membr. Sci.*, 2012, **409–410**, 191; (d) Y. Wu, J. Luo, L. Yao, C. Wu, F. Mao and T. Xu, *J. Membr. Sci.*, 2012, **399–400**, 16; (e) C.-C. Yang, S.-S. Chiu, S.-C. Kuo and T. H. Liou, *J. Power Sources*, 2012, **199**, 37; (f) J. Fu, J. Qiao, X. Wang, J. Ma and T. Okada, *Synth. Met.*, 2010, **160**, 193; (g) Y. Xiao, J. Fang, Q. H. Zeng and Q. L. Liu, *J. Membr. Sci.*, 2008, **311**, 319; (h) C.-C. Yang, S.-J. Chiu and W.-C. Chien, *J. Power Sources*, 2006, **162**, 21; (i) T. Sata, K. Kawamura and K. Matsusaki, *J. Membr. Sci.*, 2001, **181**, 167.

31 O. I. Deavin, S. Murphy, A. Ong, S. D. Poynton, R. Zeng, H. Herman and J. R. Varcoe, *Energy Environ. Sci.*, 2012, **5**, 8584.

32 (a) S. Maurya, S.-H. Shin, M.-K. Kim, S.-H. Yun and S.-H. Moon, *J. Membr. Sci.*, 2013, **443**, 28; (b) X. Wang, M. Li, B. T. Golding, M. Sadeghi, Y. Cao, E. H. Yu and K. Scott, *Int. J. Hydrogen Energy*, 2011, **36**, 10022; (c) M. Faraj, E. Elia, M. Boccia, A. Filpi, A. Pucci and F. Ciardelli, *J. Polym. Sci., Part A: Polym. Chem.*, 2011, **49**, 3437; (d) A. K. Pandey, A. Goswami, D. Sen, S. Mazumder and R. F. Childs, *J. Membr. Sci.*, 2003, **217**, 117; (e) B. Bauer, H. Strathmann and F. Effenberger, *Desalination*, 1990, **79**, 125.

33 (a) J. Zhou, K. Joseph, J. M. Ahlfield, D.-Y. Park and P. A. Kohl, *J. Electrochem. Soc.*, 2013, **160**, F573; (b) C. G. Arges, L. Wang, J. Parrondo and V. Ramani, *J. Electrochem. Soc.*, 2013, **160**, F1258.

34 (a) M. A. Hossain, Y. Lim, S. Lee, H. Jang, S. Choi, Y. Jeon, S. Lee, H. Ju and W. G. Kim, *Solid State Ionics*, 2014, **262**, 754; (b) J. Wang, S. Gu, R. B. Kaspar, B. Zhang and Y. Yan, *ChemSusChem*, 2013, **6**, 2079; (c) O. M. M. Page, S. D. Poynton, S. Murphy, A. Ong, D. M. Hillman, C. A. Hancock, M. G. Hale, D. C. Apperley and J. R. Varcoe, *RSC Adv.*, 2013, **3**, 579; (d) B. Lin, H. Dong, Y. Li, Z. Si, F. Gu and F. Yan, *Chem. Mater.*, 2013, **25**, 1858; (e) X. Lin, J. R. Varcoe, S. D. Poynton, X. Liang, A. Ong, J. Ran, Y. Li and T. Xu, *J. Mater. Chem. A*, 2013, **1**, 7262; (f) D. Chen and M. A. Hickner, *ACS Appl. Mater. Interfaces*, 2012, **4**, 5775; (g) J. Ran, L. Wu, J. R. Varcoe, A. Ong, S. D. Poynton and T. Xu, *J. Membr. Sci.*, 2012, **415–416**, 242; (h) B. Qiu, B. Lin, Z. Si, L. Qiu, F. Chu, J. Zhao and F. Yan, *J. Power Sources*, 2012, **217**, 329; (i) B. S. Aitken, C. F. Buitrago, J. D. Heffley, M. Lee,



H. W. Gibson, K. I. Winey and K. B. Wagener, *Macromolecules*, 2012, **45**, 681; (j) B. Qiu, B. Lin, L. Qiu and F. Yan, *J. Mater. Chem.*, 2012, **22**, 1040; (k) B. Lin, L. Qiu, B. Qiu, Y. Peng and F. Yan, *Macromolecules*, 2011, **44**, 9642; (l) Y. Ye and Y. A. Elabd, *Macromolecules*, 2011, **44**, 8494; (m) F. Zhang, H. Zhang and C. Qu, *J. Mater. Chem.*, 2011, **21**, 12744; (n) W. Li, J. Fang, M. Lv, C. Chen, X. Chi, Y. Yang and Y. Zhang, *J. Mater. Chem.*, 2011, **21**, 11340; (o) B. Lin, L. Qiu, J. Lu and F. Yan, *Chem. Mater.*, 2010, **22**, 6718; (p) M. Guo, J. Fang, H. Xu, W. Li, X. Lu, C. Lan and K. Li, *J. Membr. Sci.*, 2010, **362**, 97.

35 X. Lin, X. Liang, S. D. Poynton, J. R. Varcoe, A. Ong, J. Ran, Y. Li, Q. Li and T. Xu, *J. Membr. Sci.*, 2013, **443**, 193.

36 L.-C. Jheng, S. L.-C. Hsu, B.-Y. Lin and Y.-L. Hsu, *J. Membr. Sci.*, 2014, **460**, 160.

37 (a) J. Miyake, K. Fukasawa, M. Watanabe and K. Miyatake, *J. Polym. Sci., Part A: Polym. Chem.*, 2014, **52**, 383; (b) X. Li, Y. Yu, Q. Luiu and Y. Meng, *Int. J. Hydrogen Energy*, 2013, **38**, 11067; (c) L. I. Şanlı and S. A. Gürsel, *J. Appl. Polym. Sci.*, 2011, **120**, 2313; (d) Y. Li and T. Xu, *Sep. Purif. Tech.*, 2008, **61**, 430; (e) A. Huang, C. Xia, C. Xiao and L. Zhuang, *J. Appl. Polym. Sci.*, 2006, **100**, 2248; (f) A. Huang, C. Xiao and L. Zhuang, *J. Appl. Polym. Sci.*, 2005, **96**, 2146.

38 (a) S. D. Sajjad, Y. Hong and F. Liu, *Polym. Adv. Technol.*, 2014, **25**, 108; (b) C. H. Zhao, Y. Gong, Q. L. Liu, Q. G. Zhang and A. M. Zhu, *Int. J. Hydrogen Energy*, 2012, **37**, 11383; (c) X. Lin, L. Wu, Y. Liu, A. Ong, S. D. Poynton, J. R. Varcoe and T. Xu, *J. Power Sources*, 2012, **217**, 373; (d) C. Qu, H. Zhuang, F. Zhang and B. Liu, *J. Mater. Chem.*, 2012, **22**, 8203; (e) D. S. Kim, A. Labouriau, M. D. Guiver and Y. S. Kim, *Chem. Mater.*, 2011, **23**, 3795; (f) M. Li, L. Yang, S. Fang and S. Dong, *J. Membr. Sci.*, 2011, **366**, 245; (g) J. Wang, S. Li and S. Zhang, *Macromolecules*, 2010, **43**, 3890; (h) Q. Zhang, S. Li and S. Zhang, *Chem. Commun.*, 2010, **46**, 7495.

39 (a) L. Jiang, X. Lin, J. Ran, C. Li, L. Wu and T. Xu, *Chin. J. Chem.*, 2012, **30**, 2241; (b) S. Gu, R. Cai and Y. Yan, *Chem. Commun.*, 2011, **47**, 2856; (c) K. K. Stokes, J. A. Orlicki and F. L. Beyer, *Polym. Chem.*, 2011, **2**, 80; (d) C. G. Arges, S. Kulkarni, A. Baranek, K.-J. Pan, M.-S. Jung, D. Patton, K. A. Mauritz and V. Ramani, *ECS Trans.*, 2010, **33**, 1903; (e) S. Gu, R. Cai, T. Luo, K. Jensen, C. Contreras and Y. Yan, *ChemSusChem*, 2010, **3**, 555; (f) S. Gu, R. Cai, T. Luo, Z. Chen, M. Sun, Y. Liu, G. He and Y. Yan, *Angew. Chem., Int. Ed.*, 2009, **48**, 6499; (g) M. Wada and S. Higashizaki, *J. Chem. Soc., Chem. Commun.*, 1984, 482.

40 K. J. T. Noonan, K. M. Hugar, H. A. Kostalik IV, E. B. Lobkovsky, H. A. Abruña and G. W. Coates, *J. Am. Chem. Soc.*, 2012, **134**, 18161.

41 B. Zhang, S. Gu, J. Wang, Y. Liu, A. M. Herring and Y. Yan, *RSC Adv.*, 2012, **2**, 12683.

42 (a) Y. Wang, A. Rapakousiou and D. Astruc, *Macromolecules*, 2014, **47**, 3767; (b) M. L. Disabb-Miller, Y. Zha, A. J. DeCarlo, M. Pawar, G. N. Tew and M. A. Hickner, *Macromolecules*, 2013, **46**, 9279; (c) P. Y. Xu, C. H. Zhao and Q. L. Liu, *J. Appl. Polym. Sci.*, 2013, **130**, 1172; (d) Y. Zha, M. L. Disabb-Miller, Z. D. Johnson, M. A. Hickner and G. N. Tew, *J. Am. Chem. Soc.*, 2012, **134**, 4493.

43 (a) Z. Siroma, S. Watanabe, K. Yasuda, K. Fukuta and H. Yanagi, *J. Electrochem. Soc.*, 2011, **158**, B682; (b) H. Yanagi and K. Fukuta, *ECS Trans.*, 2008, **16**, 257.

44 Y.-L. S. Tse, H. N. Sarode, G. E. Lindberg, T. A. Witten, A. M. Herring and G. A. Voth, *J. Phys. Chem. C*, 2014, **118**, 845.

45 V. Heagu, I. Bunia and I. Plesca, *Polym. Degrad. Stab.*, 2000, **70**, 463.

46 (a) M. R. Hibbs, M. A. Hickner, T. M. Alam, S. K. McIntyre, C. H. Fujimoto and C. J. Cornelius, *Chem. Mater.*, 2008, **20**, 2566; (b) C. Zhang, J. Hu, M. Nagatsu, Y. Meng, W. Shen, H. Toyoda and X. Shu, *Plasma Processes Polym.*, 2011, **8**, 1024; (c) R. C. T. Slade and J. R. Varcoe, *Solid State Ionics*, 2005, **176**, 585.

47 (a) E. N. Komkova, D. F. Stamatialis, H. Strathmann and M. Wessling, *J. Membr. Sci.*, 2004, **244**, 25; (b) A. A. Zagorodni, D. L. Kotova and V. F. Selemenev, *React. Funct. Polym.*, 2002, **53**, 157.

48 F. Karas, J. Hnát, M. Paidar, J. Schauer and K. Bouzek, *Int. J. Hydrogen Energy*, 2014, **39**, 5054.

49 D. Y. Park, P. A. Kohl and H. W. Beckham, *J. Phys. Chem. C*, 2013, **117**, 15468.

50 N. Li, Y. Leng, M. A. Hickner and C.-Y. Wang, *J. Am. Chem. Soc.*, 2013, **135**, 10124.

51 (a) H. Long, K. Kim and B. S. Pivovar, *J. Phys. Chem. C*, 2012, **116**, 9419; (b) J. B. Edson, C. S. Macomber, B. S. Pivovar and J. M. Boncella, *J. Membr. Sci.*, 2012, **399–400**, 49–59; (c) S. Chempath, J. M. Boncella, L. R. Pratt, N. Henson and B. S. Pivovar, *J. Phys. Chem. C*, 2010, **114**, 11977; (d) S. Chempath, B. R. Einsla, L. R. Pratt, C. S. Macomber, J. M. Boncella, J. A. Rau and B. S. Pivovar, *J. Phys. Chem. C*, 2008, **112**, 3179; (e) C. S. Macomber, J. M. Boncella, B. S. Pivovar and J. A. Rau, *J. Therm. Anal. Calorim.*, 2008, **93**, 225.

52 J. R. Varcoe, *Phys. Chem. Chem. Phys.*, 2007, **9**, 1479.

53 J. Yan and M. A. Hickner, *Macromolecules*, 2010, **43**, 2349.

54 (a) W. Lu, Z.-G. Shao, G. Zhang, Y. Zhao, J. Li and B. Yi, *Int. J. Hydrogen Energy*, 2013, **38**, 9285; (b) P. Y. Xu, T. Y. Guo, C. H. Zhao, I. Broadwell, Q. G. Zhang and Q. L. Liu, *J. Appl. Polym. Sci.*, 2013, **128**, 3853; (c) F. Schönberger, J. Kerres, H. Dilger and E. Roduner, *Phys. Chem. Chem. Phys.*, 2009, **11**, 5782; (d) G. Hübner and E. Roduner, *J. Mater. Chem.*, 1999, **9**, 409.

55 (a) M. P. Rodgers, L. J. Bonville, H. R. Kunz, D. K. Slattery and J. F. Fenton, *Chem. Rev.*, 2012, **112**, 6075; (b) R. Borup, J. Meyers, B. Pivovar, Y. S. Kim, R. Mukundan, N. Garland, D. Myers, M. Wilson, F. Garzon, D. Wood, P. Zelenay, K. More, K. Stroh, T. Zawodzinski, J. Boncella, J. E. McGrath, M. Inaba, K. Miyatake, M. Hori, K. Ota, Z. Ogumi, S. Miyata, A. Nishikata, Z. Siroma, Y. Uchimoto, K. Yasuda, K.-I. Kimijima and N. Iwashita, *Chem. Rev.*, 2007, **107**, 3904.

56 T. Sata, M. Tsujimoto, T. Yamaguchi and K. Matsusaki, *J. Membr. Sci.*, 1996, **112**, 161.

57 (a) M. R. Hibbs, *J. Polym. Sci., Part B: Polym. Phys.*, 2013, **51**, 1736; (b) Z. Zhang, L. Wu, J. R. Varcoe, C. Li, A. Ong, S. D. Poynton and T. Xu, *J. Mater. Chem. A*, 2013, **1**, 2595; (c) L. Zeng and T. S. Zhao, *Electrochem. Commun.*, 2013, **34**, 278; (d) W. Lu, Z.-S. Shao, G. Zhang, J. Li, Y. Zhao and B. Yi, *Solid State Ionics*, 2013, **245–246**, 8; (e) J.-S. Park, S.-H. Park, S.-D. Yim, Y.-G. Yoon, W.-Y. Lee and C.-S. Kim, *J. Power Sources*, 2008, **178**, 620; (f) J.-S. Park, G.-G. Park, S.-H. Park, Y.-G. Yoon, C. S. Kim and W. Y. Lee, *Macromol. Symp.*, 2007, **249–250**, 174; (g) M. Tomoi, K. Yamaguchi, R. Ando, Y. Kantake, Y. Aosaki and H. Kubota, *J. Appl. Polym. Sci.*, 1997, **64**, 1161.

58 R. Janarthanan, S. K. Pilli, J. L. Horan, D. A. Gamarra, M. R. Hibbs and A. M. Herring, *J. Electrochem. Soc.*, 2014, **161**, F944.

59 C. Iojoui, F. Chabert, M. Maréchal, N. El Kissi, J. Guindet and J.-Y. Sanchez, *J. Power Sources*, 2006, **153**, 198.

60 U.-S. Hwang and J.-H. Choi, *Sep. Purif. Technol.*, 2006, **48**, 16.

61 <http://www.sigmadlrich.com/>, USA website accessed 12 January 2014.

62 <http://www.sigmadlrich.com/catalog/product/aldrich/197602>, Safety Data Sheet.

63 L. Liu, Q. Li, J. Dai, H. Wang, B. Jin and R. Bai, *J. Membr. Sci.*, 2014, **453**, 52.

64 Y. Yang and P. Knauss, *Proceedings of the 242nd American Chemical Society Meeting*, Denver, USA, 2011, Abstract 241.

65 (a) J. Hu, D. Wan, W. Zhu, L. Huang, S. Tan, X. Cai and X. Zhang, *ACS Appl. Mater. Interfaces*, 2014, **6**, 4720; (b) A. H. N. Rao, S. Nam and T.-H. Kim, *Int. J. Hydrogen Energy*, 2014, **39**, 5919.

66 C. G. Arges and V. Ramani, *J. Electrochem. Soc.*, 2013, **160**, F1006.

67 (a) W. Wang, S. Wang, X. Xie, Y. Lv and V. Ramani, *Int. J. Hydrogen Energy*, 2014, DOI: 10.1016/j.ijhydene.2014.03.053; (b) W. Wang, S. Wang, X. Xie, Y. Lv and V. K. Ramani, *J. Membr. Sci.*, 2014, **462**, 112.

68 (a) Z. Si, L. Qiu, H. Dong, F. Gu, Y. Li and F. Yan, *ACS Appl. Mater. Interfaces*, 2014, **6**, 4346; (b) Z. Si, Z. Sun, F. Gu, L. Qiu and F. Yan, *J. Mater. Chem. A*, 2014, **2**, 4413; (c) Y. Yang, J. Wang, J. Zheng, S. Li and S. Zhang, *J. Membr. Sci.*, 2014, **467**, 48.

69 F. Gu, H. Dong, Y. Li, Z. Si and F. Yan, *Macromolecules*, 2014, **47**, 208.

70 H. Long and B. S. Pivovar, *J. Phys. Chem. C*, 2014, **118**, 9880.

71 S. C. Price, K. S. Williams and F. L. Beyer, *ACS Macro Lett.*, 2014, **3**, 160.

72 Y. Liu, J. Wang, Y. Yang, T. M. Brenner, S. Seifert, Y. Yan, M. W. Liberatore and A. M. Herring, *J. Phys. Chem. C*, 2014, **118**, 15136.

73 K. C. Lethesh, W. Dehaen and K. Binnemans, *RSC Adv.*, 2014, **4**, 4472.

74 A. G. Wright and S. Holdcroft, *ACS Macro Lett.*, 2014, **3**, 444.

75 Y. Ye, K. K. Stokes, F. L. Beyer and Y. A. Elabd, *J. Membr. Sci.*, 2013, **443**, 93.

76 R. Schwesinger, R. Link, P. Wenzl, S. Kossek and M. Keller, *Chem.-Eur. J.*, 2006, **12**, 429.

77 S. A. Nuñez and M. A. Hickner, *ACS Macro Lett.*, 2013, **2**, 49.

78 A. Amel, L. Zhu, M. Hickner and Y. Ein-Eli, *J. Electrochem. Soc.*, 2014, **161**, F615.

79 (a) A. D. Mohanty, Y.-B. Lee, L. Zhu, M. A. Hickner and C. Bae, *Macromolecules*, 2014, **47**, 1973; (b) X. Li, G. Nie, J. Tao, W. Wu, L. Wang and S. Liao, *ACS Appl. Mater. Interfaces*, 2014, **6**, 7585.

80 (a) Q. Li, L. Liu, Q. Miao, B. Jin and R. Bai, *Chem. Commun.*, 2014, **50**, 2791; (b) J. Pan, Y. Li, J. Han, G. Li, L. Tan, C. Chen, J. Lu and L. Zhuang, *Energy Environ. Sci.*, 2013, **6**, 2912.

81 (a) C. G. Arges and V. Ramani, *Proc. Natl. Acad. Sci. U. S. A.*, 2013, **110**, 2490; (b) Z. Zhao, F. Gong, S. Zhang and S. Li, *J. Power Sources*, 2012, **218**, 368.

82 D. M. Hillman, S. H. Stephens, S. D. Poynton, S. Murphy, A. Ong and J. R. Varcoe, *J. Mater. Chem. A*, 2013, **1**, 1018.

83 J. P. Kizewski, N. H. Mudri, R. Zeng, S. D. Poynton, R. C. T. Slade and J. R. Varcoe, *ECS Trans.*, 2010, **33**, 27.

84 D. Marx, A. Chandra and M. E. Tukerman, *Chem. Rev.*, 2010, **110**, 2174.

85 R. F. Silva, M. De Francesco and A. Pozio, *J. Power Sources*, 2004, **134**, 18.

86 M. A. Vandiver, B. R. Caire, J. R. Carver, K. Waldrop, M. R. Hibbs, J. R. Varcoe, A. M. Herring and M. W. Liberatore, *J. Electrochem. Soc.*, 2014, **161**, H677.

87 T. Kimura and Y. Yamazaki, *Electrochemistry*, 2011, **79**, 94.

88 Atkins' *Physical Chemistry*, ed. P. Atkins and J. de Paula, Oxford University Press, Oxford, 8th edn, Table 21.6, p. 019.

89 http://web.med.unsw.edu.au/phbsoft/mobility_listings.htm, accessed 27 September 2013.

90 I. T. Lucas, S. Durand-Vidal, E. Dubois, J. Chevalet and P. Turq, *J. Phys. Chem. C*, 2007, **111**, 18568.

91 D. Chaturvedi and S. Ray, *Monatshefte für Chemie*, 2006, **137**, 459.

92 M. G. Marino, J. P. Melchior, A. Wohlfarth and K. D. Kreuer, *J. Membr. Sci.*, 2014, **464**, 61.

93 H. N. Sarode, G. E. Lindberg, Y. Yang, L. Felberg, G. A. Voth and A. M. Herring, *J. Phys. Chem. B*, 2014, **118**, 1363.

94 (a) M. Mamlouk, K. Scott, J. A. Horsfall and C. Williams, *Int. J. Hydrogen Energy*, 2011, **36**, 7191; (b) T. Soboleva, Z. Xie, Z. Shi, E. Tsang, T. Navessin and S. Holdcroft, *J. Electroanal. Chem.*, 2008, **622**, 145; (c) S. Ma, Z. Siroma and H. Tanaka, *J. Electrochem. Soc.*, 2006, **153**, A2274.

95 (a) K. W. Han, K. K. Ko, K. Abu-Hakmeh, C. Bae, Y. J. Sohn and S. S. Jang, *J. Phys. Chem. C*, 2014, **118**, 12577; (b) A. M. Kiss, T. D. Myles, K. N. Grew, A. A. Peracchino, G. J. Nelson and W. K. S. Chiu, *J. Electrochem. Soc.*, 2013, **160**, F994; (c) B. V. Merinov and W. A. Goddard III, *J. Membr. Sci.*, 2013, **431**, 79; (d) G. A. Giffin, S. Lavina, G. Pace and V. Di Noto, *J. Phys. Chem. C*, 2012, **116**, 23965; (e) T. D. Myles, A. M. Kiss, K. N. Grew, A. A. Peracchino, G. J. Nelson and W. K. S. Chiu, *J. Electrochem. Soc.*, 2011, **158**, B790; (f) K. N. Grew, X. Ren and D. Chu, *Electrochem. Solid-State Lett.*, 2011, **14**, B127; (g) K. N. Grew, D. Chu and W. K. S. Chiu, *J. Electrochem. Soc.*, 2010, **57**, B1024; (h) K. N. Grew and W. K. S. Chiu, *J. Electrochem. Soc.*, 2010, **157**, B327; (i) Y. S. Li, T. S. Zhao and W. W. Yang, *Int. J. Hydrogen Energy*, 2010, **35**, 5656.





96 (a) S. Zhang, C. Li, X. Xie and F. Zhang, *Int. J. Hydrogen Energy*, 2014, **39**, 13718; (b) J. Wang, G. He, X. Wu, X. Yan, Y. Zhang, Y. Wang and L. Du, *J. Membr. Sci.*, 2014, **459**, 86; (c) L. Wang and M. A. Hickner, *Polym. Chem.*, 2014, **5**, 2928.

97 N. Li, M. D. Guiver and W. H. Binder, *ChemSusChem*, 2013, **6**, 1376.

98 N. Li and M. D. Guiver, *Macromolecules*, 2014, **47**, 2175.

99 K. A. Mauritz and R. B. Moore, *Chem. Rev.*, 2004, **104**, 4535.

100 M. E. Tuckerman, D. Marx and M. Parrinello, *Nature*, 2002, **417**, 925.

101 J. Pan, S. Lu, Y. Li, A. Huang, L. Zhuang and J. Lu, *Adv. Funct. Mater.*, 2010, **20**, 312.

102 (a) G. L. Han, P. Y. Xu, K. Zhou, Q. G. Zhang, A. M. Zhu and Q. L. Liu, *J. Membr. Sci.*, 2014, **464**, 72; (b) H.-C. Lee, K.-L. Liu, L.-D. Tsai, J.-Y. Lai and C.-Y. Chao, *RSC Adv.*, 2014, **4**, 10944; (c) J. Ran, L. Wu, X. Lin, L. Jiang and T. Xu, *RSC Adv.*, 2012, **2**, 4250.

103 T. J. Peckham and S. Holdcroft, *Adv. Mater.*, 2010, **22**, 4667.

104 (a) M. A. Hossain, Y. Lim, S. Lee, H. Jang, S. Choi, Y. Jeon, J. Lim and W. G. Kim, *Int. J. Hydrogen Energy*, 2014, **39**, 2731; (b) Y. Ye, S. Sharick, E. M. Davis, K. I. Winey and Y. A. Elabd, *ACS Macro Lett.*, 2013, **2**, 575; (c) X. Wang, M. Goswami, R. Kumar, B. G. Sumpter and J. Mays, *Soft Matter*, 2012, **8**, 3036; (d) Z. Zhao, J. Wang, S. Li and S. Zhang, *J. Power Sources*, 2011, **196**, 4445; (e) M. Tanaka, K. Fukasawa, E. Nishino, S. Yamaguchi, K. Yamada, H. Tanaka, B. Bae, K. Miyatake and M. Watanabe, *J. Am. Chem. Soc.*, 2011, **133**, 10646.

105 M. L. Disabb-Miller, Z. D. Johnson and M. A. Hickner, *Macromolecules*, 2013, **46**, 949.

106 S. C. Price, X. Ren, A. C. Jackson, Y. Ye, Y. A. Elabd and F. B. Beyer, *Macromolecules*, 2013, **46**, 7332.

107 Q. Li, L. Liu, Q. Mao, B. Jin and R. Bai, *Polym. Chem.*, 2014, **5**, 2208.

108 N. Li, Q. Zhang, C. Wang, Y. M. Lee and M. D. Guiver, *Macromolecules*, 2012, **45**, 2411.

109 N. Li, T. Yan, Z. Li, T. Thurn-Albrecht and W. H. Binder, *Energy Environ. Sci.*, 2012, **5**, 7888.

110 N. Li, L. Wang and M. A. Hickner, *Chem. Commun.*, 2014, **50**, 4092.

111 J. Ran, L. Wu and T. Xu, *Polym. Chem.*, 2013, **4**, 4612.

112 J. Pan, C. Chen, Y. Li, L. Wang, L. Tan, G. Li, X. Tang, L. Xiao, J. Lu and L. Zhuang, *Energy Environ. Sci.*, 2014, **7**, 354.

113 S. Karaborni, K. Esselink, P. A. J. Hilbers, B. Smit, J. Karthäuser, N. M. Van Os and R. Zana, *Science*, 1994, **266**, 254.

114 http://www2.dupont.com/FuelCells/en_US/products/nafion.html, accessed February 2014.

115 K. Scott, E. H. Yu, G. Vlachogiannopoulos, M. Shivare and N. Duteanu, *J. Power Sources*, 2008, **175**, 452.

116 (a) G. K. S. Prakash, F. C. Krause, F. A. Viva, S. R. Narayanan and G. A. Olah, *J. Power Sources*, 2011, **196**, 7967; (b) K. Fukuta, H. Inoue, Y. Chikashige and H. Yanagi, *ECS Trans.*, 2010, **28**, 221; (c) Y. S. Li, T. S. Zhao and Z. X. Liang, *J. Power Sources*, 2009, **190**, 223; (d) H. Bunazawa and Y. Yamazaki, *J. Power Sources*, 2008, **182**, 48.

117 (a) M. S. Naughton, G. H. Gu, A. A. Moradia and P. J. A. Kenis, *J. Power Sources*, 2013, **242**, 581; (b) C. V. Rao and Y. Ishikawa, *J. Phys. Chem. C*, 2012, **116**, 4340; (c) A. Santasalo-Aarnio, S. Hietala, T. Rauhala and T. Kallio, *J. Power Sources*, 2011, **196**, 6153; (d) C. Delacourt, P. L. Ridgway, J. B. Kerr and J. Newman, *J. Electrochem. Soc.*, 2008, **155**, B42.

118 (a) L. Sun, J. Guo, J. Zhou, Q. Xu, D. Chu and R. Chen, *J. Power Sources*, 2012, **202**, 70; (b) M. Ünlü, J. Zhou, I. Anestis-Richard and P. A. Kohl, *ChemSusChem*, 2011, **3**, 1398; (c) F. Zhang, H. Zhang, C. Qu and J. Ren, *J. Power Sources*, 2011, **196**, 3099; (d) K. Miyazaki, N. Sugimura, K.-I. Kawakita, T. Abe, K. Nishio, H. Nakanishi, M. Matsuoka and Z. Ogumi, *J. Electrochem. Soc.*, 2010, **157**, A1153; (e) M. Piana, M. Boccia, A. Filipi, E. Flammia, H. A. Miller, M. Orsini, F. Salusti, S. Santiccioli, F. Ciardelli and A. Pucci, *J. Power Sources*, 2010, **195**, 5875; (f) J. R. Varcoe, R. C. T. Slade and E. Lam How Yee, *Chem. Commun.*, 2006, 1428.

119 R. Zeng, J. Handsel, S. D. Poynton, A. J. Roberts, R. C. T. Slade, H. Herman, D. C. Apperley and J. R. Varcoe, *Energy Environ. Sci.*, 2011, **4**, 4925.

120 D. Dekel, Alkaline membrane fuel cells, in *Encyclopedia of Applied Electrochemistry*, ed. R. Savinell, K.-I. Ota and G. Kreysa, Springer, Berlin/Heidelberg, SpringerReference number 303632.

121 I. Katsounaros, S. Cherevko, A. R. Zeradjanin and K. J. J. Mayrhofer, *Angew. Chem., Int. Ed.*, 2014, **53**, 102.

122 M. Weissmann, C. Coutanceau, P. Brault and J.-M. Léger, *Electrochem. Commun.*, 2007, **9**, 1097.

123 (a) T. Lee, E. K. Jeon and B.-S. Kim, *J. Mater. Chem. A*, 2014, **2**, 6167; (b) J. Ohyama, Y. Okata, N. Watabe, M. Katagiri, A. Nakamura, H. Arikawa, K.-I. Shimizu, T. Takeguchi, W. Ueda and A. Satsuma, *J. Power Sources*, 2014, **245**, 998; (c) Q. Wu, L. Jiang, Q. Tang, J. Liu, S. Wang and G. Sun, *Electrochim. Acta*, 2013, **91**, 314; (d) S. Gu, W. Sheng, R. Cai, S. M. Alia, S. Song, K. O. Jensen and Y. Yan, *Chem. Commun.*, 2013, **49**, 131; (e) N. Ramaswamy, U. Tylus, Q. Jia and S. Mukerjee, *J. Am. Chem. Soc.*, 2013, **135**, 15443; (f) Y. Fang, X. Yang, L. Wang and Y. Li, *Electrochim. Acta*, 2013, **90**, 421; (g) J. Xu, P. Gao and T. S. Zhao, *Energy Environ. Sci.*, 2012, **5**, 5333; (h) J. Sunarso, A. A. J. Torriero, W. Zhou, P. C. Howlett and M. Forsyth, *J. Phys. Chem. C*, 2012, **116**, 5827; (i) N. Ramaswamy and S. Mukerjee, *J. Phys. Chem. C*, 2011, **115**, 18015; (j) J. Guo, A. Hsu, D. Chu and R. Chen, *J. Phys. Chem. C*, 2010, **114**, 4324; (k) T. S. Olson, S. Pylypenko, P. Atanassov, K. Asazawa, K. Yamada and H. Tanaka, *J. Phys. Chem. C*, 2010, **114**, 5049; (l) R. Chen, H. Li, D. Chu and G. Wang, *J. Phys. Chem. C*, 2009, **113**, 20689.

124 B. S. Pivovar, AMFC Workshop Final Report, 2006, located at, http://www1.eere.energy.gov/hydrogenandfuelcells/pdfs/amfc_dec2006_workshop_report.pdf.

125 H. A. Gasteiger, S. S. Kocha, B. Sompalli and F. T. Wagner, *Appl. Catal., B*, 2005, **56**, 9.

126 D. S. Su and G. Sun, *Angew. Chem., Int. Ed.*, 2011, **50**, 11570.

127 (a) Q. Hu, G. Li, J. Pan, L. Tan, J. Lu and L. Zhuang, *Int. J. Hydrogen Energy*, 2013, **38**, 16264; (b) D. Dekel, *ECS Trans.*, 2012, **50**, 2051; (c) S. Lu, J. Pan, A. Huang, L. Zhuang and J. Li, *Proc. Natl. Acad. Sci. U. S. A.*, 2008, **105**, 20611; (d) J. R. Varcoe, R. C. T. Slade, G. L. Wright and Y. Chen, *J. Phys. Chem. B*, 2006, **110**, 21041.

128 C. A. Hancock, A. Ong, P. R. Slater and J. R. Varcoe, *J. Mater. Chem. A*, 2014, **2**, 3047.

129 J. S. Spendelow and A. Wieckowski, *Phys. Chem. Chem. Phys.*, 2007, **9**, 2654.

130 W. Sheng, H. A. Gasteiger and Y. Shao-Horn, *J. Electrochem. Soc.*, 2010, **157**, B1529.

131 L. Jiang, A. Hsu, D. Chu and R. Chen, *Electrochim. Acta*, 2010, **55**, 4506.

132 M. Piana, S. Catanorchi and H. A. Gasteiger, *ECS Trans.*, 2008, **16**, 2045.

133 H. Meng, F. Jaouen, E. Proietti, M. Lefèvre and J. P. Dodelet, *Electrochem. Commun.*, 2009, **11**, 1986.

134 Q. He, X. Yang, R. He, A. Bueno-López, H. Miller, X. Ren, W. Yang and B. E. Koel, *J. Power Sources*, 2012, **213**, 169.

135 K. C. Neyerlin, W. Gu, J. Jorne and H. A. Gasteiger, *J. Electrochem. Soc.*, 2007, **154**, B631.

136 (a) R. Zeng, R. C. T. Slade and J. R. Varcoe, *Electrochim. Acta*, 2010, **56**, 607; (b) R. Zeng, S. D. Poynton, J. P. Kizewski, R. C. T. Slade and J. R. Varcoe, *Electrochim. Commun.*, 2010, **12**, 823.

137 P. Rheinländer, S. Henning, J. Herranz and H. A. Gasteiger, *ECS Trans.*, 2012, **50**, 2163.

138 R. Jervis, N. Mansor, C. Gibbs, C. A. Murray, C. C. Tang, P. R. Shearing and D. J. L. Brett, *J. Electrochim. Soc.*, 2014, **161**, F458.

139 W. Sheng, A. P. Bivens, M. Myint, Z. Zhuang, R. V. Forest, Q. Fang, J. G. Cheng and Y. Yan, *Energy Environ. Sci.*, 2014, **7**, 1719.

140 (a) I. Gunasekara, M. Lee, D. Abbott and S. Mukerjee, *ECS Electrochim. Lett.*, 2012, **1**, F16; (b) A. E. S. Sleightholme and A. R. Kucernak, *Electrochim. Acta*, 2011, **56**, 4396; (c) A. E. S. Sleightholme, J. R. Varcoe and A. R. Kucernak, *Electrochim. Commun.*, 2008, **10**, 151; (d) A. R. Kucernak and E. Toyoda, *Electrochim. Commun.*, 2008, **10**, 1728; (e) J. Jiang and A. R. Kucernak, *J. Electroanal. Chem.*, 2004, **567**, 123.

141 A. Ong, D. K. Whelligan, M. L. Fox and J. R. Varcoe, *Phys. Chem. Chem. Phys.*, 2013, **15**, 18992.

142 A. Ong, D. K. Whelligan, S. Murphy and J. R. Varcoe, manuscript in preparation.

143 T. J. Schmidt, U. A. Paulus, H. A. Gasteiger and R. J. Behm, *J. Electroanal. Chem.*, 2001, **508**, 41.

144 A. Anastasopoulos, J. C. Davis, L. Hannah, B. E. Hayden, C. E. Lee, C. Milhano, C. Mormiche and L. Offin, *ChemSusChem*, 2013, **6**, 1973.

145 W. Lu, Z.-G. Shao, G. Zhang, Y. Zhao, J. Li and B. Yi, *Int. J. Hydrogen Energy*, 2013, **38**, 9285.

146 D. Konopka, M. A. Johnson, M. Errico, P. Bahrami and C. A. Hays, *Electrochim. Solid-State Lett.*, 2012, **15**, B17.

147 A. J. Lemke, A. W. O'Toole, R. S. Phillips and E. T. Eisenbraun, *J. Power Sources*, 2014, **256**, 319.

148 M. H. Robson, K. Artyushkova, W. Patterson, P. Atanassov and M. R. Hibbs, *Electrocatalysis*, 2014, **5**, 148.

149 S. D. Poynton, R. C. T. Slade, W. E. Mustain, T. J. Omasta, R. Escudero-Cid, P. Ocón and J. R. Varcoe, *J. Mater. Chem. A*, 2014, **2**, 5124.

150 (a) G. F. McLean, T. Niet, S. Prince-Richard and N. Djilali, *Int. J. Hydrogen Energy*, 2002, **27**, 507; (b) A. J. Appleby and F. R. Foulkes, *Fuel Cell Handbook*, Van Nostrand Reinhold, New York, 1989.

151 Y. Wang, L. Li, L. Hu, L. Zhuang, J. Lu and B. Xu, *Electrochim. Commun.*, 2003, **5**, 662.

152 L. A. Adams, S. D. Poynton, C. Tamain, R. C. T. Slade and J. R. Varcoe, *ChemSusChem*, 2008, **1**, 79.

153 M. Ünlü, J. Zhou and P. A. Kohl, *Electrochim. Solid-State Lett.*, 2009, **12**, B27.

154 (a) M. Carmo, G. Doubek, R. C. Sekol, M. Linardi and A. D. Taylor, *J. Power Sources*, 2013, **230**, 169; (b) Q. He and X. Ren, *J. Power Sources*, 2012, **220**, 373; (c) X. Wang, J. P. McClure and P. S. Fedkiw, *Electrochim. Acta*, 2012, **79**, 126.

155 Y. S. Kim, US DOE Hydrogen and fuel cells program and vehicle technologies program annual merit review, 2011, http://www.hydrogen.energy.gov/pdfs/review11/fc043_kim_2011_o.pdf.

156 M. J. Jung, C. G. Arges and V. Ramani, *J. Mater. Chem.*, 2011, **21**, 6158.

157 Y. Luo, J. Guo, C. Wang and D. Chu, *Macromol. Chem. Phys.*, 2011, **212**, 2094.

158 S. D. Poynton, J. P. Kizewski, R. C. T. Slade and J. R. Varcoe, *Solid State Ionics*, 2010, **181**, 219.

159 K. Fukuta, "Electrolyte Materials for AMFCs and AMFC Performance" at the AMFC Workshop held on 8th May 2011 in Washington (USA).

160 H. Zhang, H. Ohashi, T. Tamaki and T. Yamaguchi, *J. Phys. Chem. C*, 2013, **117**, 16791.

161 K. Jiao, P. He, Q. Du and Y. Yin, *Int. J. Hydrogen Energy*, 2014, **39**, 5981.

162 E. M. Sommer, L. S. Martins, J. V. C. Vargas, J. E. F. C. Gardolinski, J. C. Ordonez and C. E. B. Marino, *J. Power Sources*, 2012, **213**, 16.

163 (a) E. H. Yu, X. Wang, U. Krewer, L. Li and K. Scott, *Energy Environ. Sci.*, 2012, **5**, 5668; (b) L. An, T. S. Zhao, Y. Li and Q. Wu, *Energy Environ. Sci.*, 2012, **5**, 7536.

164 (a) C. Jin, Y. Song and Z. Chen, *Electrochim. Acta*, 2009, **54**, 4136; (b) Y. Chen, L. Zhuang and J. Lu, *Chin. J. Catal.*, 2007, **28**, 870; (c) A. V. Tripković, K. D. Popović and J. D. Lović, *Electrochim. Acta*, 2001, **46**, 3163.

165 R. R. Adzic, M. L. Avramovic and A. V. Tripković, *Electrochim. Acta*, 1984, **29**, 1353.

166 (a) J. Zhang, C. Guo, L. Zhang and C. M. Li, *Chem. Commun.*, 2013, **49**, 6334; (b) S. Maheswari, P. Sridhar and S. Pitchmani, *Fuel Cells*, 2012, **12**, 963; (c) G. Dong, M. Huang and L. Guan, *Phys. Chem. Chem. Phys.*, 2012, **14**, 2557; (d) M. Zhiani, H. A. Gasteiger, M. Piana and S. Catanorchi, *Int. J. Hydrogen Energy*, 2011, **36**, 5110; (e) S. Song, Y. Wang, P. Tsakaras and P. K. Shen, *Appl. Catal., B*, 2008, **78**, 381; (f) N. Park, T. Shiraishi,



K. Kamisugi, Y. Hara, K. Iizuka, T. Kado and S. Hayase, *J. Appl. Electrochem.*, 2008, **38**, 371; (g) H. Meng, M. Wu, X. X. Hu, M. Nie, Z. D. Wei and P. K. Shen, *Fuel Cells*, 2006, **6**, 447; (h) E. H. Yu, K. Scott and R. W. Reeve, *Fuel Cells*, 2003, **3**, 169.

167 (a) M. Saito, S. Tsuzuki, K. Hayamizu and T. Okada, *J. Phys. Chem. B*, 2006, **110**, 24410; (b) J. Ling and O. Savadogo, *J. Electrochem. Soc.*, 2004, **151**, A1604; (c) X. Ren, T. E. Springer and S. Gottesfeld, *J. Electrochem. Soc.*, 2000, **147**, 92.

168 C. Xu and T. S. Zhao, *J. Power Sources*, 2007, **168**, 143.

169 C. Weinzierl and U. Krewer, *J. Power Sources*, 2014, **268**, 911.

170 J. Divisek, *US Pat.* 20030049509, 2003; M. Stefener and J. Müller, *US Pat.* 20050069757, 2005.

171 K. Matsuoka, Y. Iriyama, T. Abe, M. Matsuoka and Z. Ogumi, *J. Power Sources*, 2005, **150**, 27.

172 T. F. Fuller and D. J. Wheeler, *US Pat.* 6068941 A, 2000.

173 (a) J. Liu, J. Ye, C. Xu, S. P. Jiang and Y. Tong, *J. Power Sources*, 2008, **177**, 67; (b) J. Ye, J. Liu, C. Xu, S. P. Jiang and Y. Tong, *Electrochem. Commun.*, 2007, **9**, 2760; (c) M. E. P. Markiewicz, D. M. Hebert and S. H. Bergens, *J. Power Sources*, 2006, **161**, 761.

174 J. R. Varcoe, R. C. T. Slade, E. Lam How Yee, S. D. Poynton and R. C. T. Slade, *J. Power Sources*, 2007, **173**, 194.

175 G. A. Koscher and K. Kordesch, *J. Solid State Electrochem.*, 2003, **7**, 632.

176 (a) Y. Zhang, J. Fang, Y. Wu, H. Xu, X. Chi, W. Li, Y. Yang, G. Yan and Y. Zhuang, *J. Colloid Interface Sci.*, 2012, **381**, 59; (b) C.-C. Yang, *J. Appl. Electrochem.*, 2012, **42**, 305; (c) H. Kim, J. Zhou, M. Ünlü, I. Anestis-Richard, K. Joseph and P. A. Kohl, *Electrochim. Acta*, 2011, **56**, 3085; (d) J.-H. Kim, H.-K. Kim, K.-T. Hwang and J.-Y. Lee, *Int. J. Hydrogen Energy*, 2010, **35**, 768; (e) J. Kim, T. Momma and T. Osaka, *J. Power Sources*, 2009, **189**, 999; (f) E. H. Yu and K. Scott, *J. Appl. Electrochem.*, 2005, **35**, 91; (g) E. H. Yu and K. Scott, *Electrochim. Commun.*, 2004, **6**, 361.

177 R. W. Verjulio, J. Santander, N. Sabaté, J. P. Esquivel, N. Torres-Herrero, A. Habrioux and N. Alonso-Vante, *Int. J. Hydrogen Energy*, 2014, **39**, 5406.

178 A. V. Tripković, K. D. Popović, B. N. Grgur, B. Blizanac, P. N. Ross and N. M. Marković, *Electrochim. Acta*, 2002, **47**, 3707.

179 K. L. Nagashree and M. F. Ahmed, *Synth. Met.*, 2008, **158**, 610.

180 N. Spinner and W. E. Mustain, *Electrochim. Acta*, 2011, **56**, 5656.

181 M. Ünlü, D. Abbott, N. Ramaswamy, X. Ren, S. Mukerjee and P. A. Kohl, *J. Electrochem. Soc.*, 2011, **158**, B1423.

182 (a) P. Joghee, S. Pylypenko, K. Wood, G. Bender and R. O'Hayre, *ChemSusChem*, 2014, **7**, 1854; (b) J. Wang, R. Shi, X. Guo, J. Xin, J. Zhao, C. Song, L. Wang and J. Zhang, *Int. J. Hydrogen Energy*, 2014, **123**, 309; (c) E. E. Switzer, T. S. Olson, A. K. Datye, P. Atanassov, M. R. Hibbs and C. J. Cornelius, *Electrochim. Acta*, 2009, **54**, 989; (d) C. Nishihara and T. Okada, *J. Electroanal. Chem.*, 2005, **577**, 355; (e) P. V. Samant, C. M. Rangel, M. H. Romero, J. B. Fernandes and J. L. Figueiredo, *J. Power Sources*, 2005, **151**, 79; (f) X. Zhang, K.-Y. Tsang and K.-Y. Chan, *J. Electroanal. Chem.*, 2004, **573**, 1.

183 C. Bianchini and P. K. Shen, *Chem. Rev.*, 2009, **109**, 4183.

184 V. Bambagioni, C. Bianchini, A. Marchionni, J. Filippi, F. Vizza, J. Teddy, P. Serp and M. Zhiani, *J. Power Sources*, 2009, **190**, 241.

185 (a) D. H. Nagaraju and V. Lakshminarayanan, *J. Phys. Chem. C*, 2009, **113**, 14922; (b) K. A. Assiongbon and D. Roy, *Surf. Sci.*, 2005, **594**, 99; (c) Z. Borkowska, A. Tymosiak-Zielinska and R. Nowakowski, *Electrochim. Acta*, 2004, **49**, 2613.

186 M. G. Hosseini, M. Abdolmaleki and S. Ashrafpoor, *J. Appl. Electrochem.*, 2012, **42**, 153; M. A. Abdel Rahim, R. M. Abdel Hameed and M. W. Khalil, *J. Power Sources*, 2004, **134**, 160; J. Taraszewska and G. Rosłonek, *J. Electroanal. Chem.*, 1994, **364**, 209.

187 G. G. W. Lee, J. Leddy and S. D. Minteer, *Chem. Commun.*, 2012, **48**, 11972.

188 (a) E. Antolini and J. Perez, *Int. J. Hydrogen Energy*, 2011, **36**, 15752; (b) R. N. Singh, T. Sharma, A. Singh, D. Anindita, D. Mishra and S. K. Tiwari, *Electrochim. Acta*, 2008, **53**, 2322.

189 (a) J. Zhou, M. Ünlü, I. Anestis-Richard and P. A. Kohl, *J. Membr. Sci.*, 2010, **350**, 286; (b) H. Hou, G. Sun, R. He, B. Sun, W. Jin, H. Liu and Q. Xin, *Int. J. Hydrogen Energy*, 2008, **33**, 7172; (c) E. H. Yu and K. Scott, *J. Power Sources*, 2004, **137**, 248.

190 T. M. Alam and M. R. Hibbs, *Macromolecules*, 2014, **47**, 1073.

191 (a) A. Jasti and V. K. Shahi, *RSC Adv.*, 2014, **4**, 19238; (b) C. Zhao, W. Ma, W. Sun and H. Na, *J. Appl. Polym. Sci.*, 2014, **131**, 40256; (c) A. H. N. Rao, H.-J. Kim, S. Nam and T.-H. Kim, *Polymer*, 2013, **54**, 6918; (d) M. M. Nasef, N. A. Zubirm, A. F. Ismail, M. Khayet, K. Z. M. Dahlan, H. Saidi, R. Rohani, T. I. S. Ngah and N. A. Sulaiman, *J. Membr. Sci.*, 2006, **268**, 96.

192 (a) G. K. Goswami, R. Nandan, B. K. Barman and K. K. Nanda, *J. Mater. Chem. A*, 2013, **1**, 3133; (b) A. Santasalo-Aarnio, S. Tuomi, K. Jalkanen, K. Kontturi and T. Kallio, *Electrochim. Acta*, 2013, **87**, 730; (c) H. Bunazawa and Y. Yamazaki, *J. Power Sources*, 2009, **190**, 210.

193 H. Deng, J. Chen, K. Jiao and X. Huang, *Int. J. Heat Mass Transfer*, 2014, **7**, 376.

194 A. Katzfuss, S. Poynton, J. Varcoe, V. Gogel, U. Storr and J. Kerres, *J. Membr. Sci.*, 2014, **465**, 129.

195 T. S. Zhao, Y. S. Li and S. Y. Shen, *Front. Energy Power Eng. Chin.*, 2010, **4**, 443.

196 (a) S. Zinoviev, F. Müller-Langer, P. Das, N. Bertero, P. Fornasiero, M. Kaltschmitt, G. Centi and S. Miertus, *ChemSusChem*, 2010, **3**, 1106; (b) K. David and A. J. Ragauskas, *Energy Environ. Sci.*, 2010, **3**, 1182.

197 S. Y. Shen, T. S. Zhao and Q. X. Wu, *Int. J. Hydrogen Energy*, 2012, **37**, 575.

198 V. Rao, Hariyanto, C. Cremers and U. Stimming, *Fuel Cells*, 2007, **7**, 417.

199 (a) S. Sun, Z. Jusys and R. J. Behm, *J. Power Sources*, 2013, **231**, 122; (b) E. Antolini, *J. Power Sources*, 2007, **170**, 1.

200 (a) P. A. Christensen, S. W. M. Jones and A. Hamnett, *J. Phys. Chem. C*, 2012, **116**, 24681; (b) Y. Bai, J. Wu, J. Xi,

J. Wang, W. Zhu, L. Chen and X. Qiu, *Electrochim. Commun.*, 2005, **7**, 1087; (c) C. Su and P. K. Shen, *J. Power Sources*, 2005, **142**, 27.

201 (a) E. Antolini, *Energy Environ. Sci.*, 2009, **2**, 915; (b) G. Cui, S. Song, P. K. Shen, A. Kowal and C. Bianchini, *J. Phys. Chem. C*, 2009, **113**, 15639; (c) Z. X. Liang, T. S. Zhao, J. B. Xu and L. D. Zhu, *Electrochim. Acta*, 2009, **54**, 2203; (d) Q. He, W. Chen, S. Mukerjee, S. Chen and F. Laufek, *J. Power Sources*, 2009, **187**, 298; (e) F. P. Hu, Z. Wang, Y. Li, C. Li, X. Zhang and P. K. Shen, *J. Power Sources*, 2008, **177**, 61; (f) C. Xu, H. Wang, P. K. Shen and S. P. Jiang, *Adv. Mater.*, 2007, **19**, 4256; (g) H. Wang, C. Xu, F. Cheng and S. Jiang, *Electrochim. Commun.*, 2007, **9**, 1212; (h) J. Bagchi and S. K. Bhattacharya, *Transition Met. Chem.*, 2007, **32**, 47.

202 T. Sheng, W.-F. Lin, C. Hardacre and P. Hu, *J. Phys. Chem. C*, 2014, **118**, 5762.

203 Y. S. Li and T. S. Zhao, *Int. J. Hydrogen Energy*, 2012, **37**, 4413.

204 C. Xu, Z. Tian, P. K. Shen and S. P. Jiang, *Electrochim. Acta*, 2008, **53**, 2610.

205 F. Hu, C. Chen, Z. Wang, G. Wei and P. K. Shen, *Electrochim. Acta*, 2006, **52**, 1087.

206 P. K. Shen and C. Xu, *Electrochim. Commun.*, 2006, **8**, 184.

207 A. N. Geraldes, D. F. da Silva, E. S. Pino, J. C. M. da Silva, R. F. B. de Souza, P. Hammer, E. V. Spinancé, A. O. Neto, M. Linardi and M. C. dos Santos, *Electrochim. Acta*, 2013, **111**, 455.

208 A. Dutta and J. Datta, *J. Phys. Chem. C*, 2012, **116**, 25677.

209 S. Shen, T. S. Zhao, J. Xu and Y. Li, *Energy Environ. Sci.*, 2011, **4**, 1428.

210 L. Ma, H. He, A. Hsu and R. Chen, *J. Power Sources*, 2013, **241**, 696.

211 Y. Li and Y. He, *RSC Adv.*, 2014, **4**, 16879.

212 (a) R. B. de Lima and H. Varela, *Gold Bull.*, 2008, **41**, 15; (b) C. Xu, H. Yu, J. Rong, S. P. Jiang and Y. Liu, *Electrochim. Commun.*, 2007, **9**, 2009; (c) S. S. Gupta and J. Datta, *J. Power Sources*, 2005, **145**, 124.

213 M. R. Tarasevich, Z. R. Karichev, V. A. Bogdanovskaya, E. N. Lubnin and A. V. Kapustin, *Electrochim. Commun.*, 2005, **7**, 141.

214 H. Hou, G. Sun, R. He, Z. Wu and B. Sun, *J. Power Sources*, 2008, **182**, 95.

215 L. An, T. S. Zhao, Q. X. Wu and L. Zeng, *Int. J. Hydrogen Energy*, 2012, **37**, 14536.

216 C. Bianchini, V. Bambagioni, J. Filippi, A. Marchionni, F. Vizza, P. Bert and A. Tampucci, *Electrochim. Commun.*, 2009, **11**, 1077.

217 J. B. Xu, T. S. Zhao, Y. S. Li and W. W. Yang, *Int. J. Hydrogen Energy*, 2010, **35**, 9693.

218 L. An and T. S. Zhao, *Int. J. Hydrogen Energy*, 2011, **36**, 9994.

219 (a) L. An, T. S. Zhao, S. Y. Shen, Q. X. Wu and R. Chen, *Int. J. Hydrogen Energy*, 2010, **35**, 4329; (b) K. Miyazaki, N. Sugimura, K. Matsuoka, Y. Iriyama, T. Abe, M. Matsuoka and Z. Ogumi, *J. Power Sources*, 2008, **178**, 683; (c) L. Demarconnay, S. Brimaud, C. Coutanceau and J.-M. Léger, *J. Electroanal. Chem.*, 2007, **601**, 169; (d) C. Coutanceau, L. Demarconnay, C. Lamy and J.-M. Léger, *J. Power Sources*, 2006, **156**, 14.

220 (a) K. Matsuoka, Y. Iriyama, T. Abe, M. Matsuoka and Z. Ogumi, *J. Electrochim. Soc.*, 2005, **182**, A729; (b) K. Matsuoka, M. Inaba, Y. Iriyama, T. Abe, Z. Ogumi and M. Matsuoka, *Fuel Cells*, 2002, **2**, 35.

221 K. Matsuoka, Y. Iriyama, T. Abe, M. Matsuoka and Z. Ogumi, *Electrochim. Acta*, 2005, **51**, 1085.

222 C. Cremers, D. Bayer, J. Meier, S. Berenger, B. Kintzel, M. Joos and J. Tübke, *ECS Trans.*, 2010, **25**, 27.

223 A. Serov, U. Martinez and P. Atanassov, *Electrochim. Commun.*, 2013, **34**, 185.

224 (a) J. Qi, L. Xin, D. J. Chadderton, Y. Qiu, Y. Jiang, N. Benipal, C. Liang and W. Li, *Appl. Catal., B*, 2014, **154–155**, 360; (b) Z. Wang, L. Xin, X. Zhao, Y. Qiu, Z. Zhang, O. A. Baturina and W. Li, *Renewable Energy*, 2014, **62**, 556; (c) Z. Zhang, L. Xin, J. Qi, D. J. Chadderton and W. Li, *Appl. Catal., B*, 2013, **136–137**, 29; (d) Z. Zhang, L. Xin and W. Li, *Int. J. Hydrogen Energy*, 2012, **37**, 9393; (e) Z. Zhang, L. Xin and W. Li, *Appl. Catal., B*, 2012, **119–120**, 40; (f) A. Ilie, M. Simões, S. Baranton, C. Coutanceau and S. Martemianov, *J. Power Sources*, 2011, **196**, 4965.

225 R. Luque, L. Herrero-Davila, J. M. Campelo, J. H. Clark, J. M. Hidalgo, D. Luna, J. M. Marinas and A. A. Romero, *Energy Environ. Sci.*, 2008, **1**, 542.

226 R. L. Arechederra and S. D. Minteer, *Fuel Cells*, 2009, **9**, 63.

227 (a) V. L. Oliveira, C. Morais, K. Servat, T. W. Napporn, G. Tremiliosa-Filho and K. B. Kokoh, *Electrochim. Acta*, 2014, **117**, 255; (b) L. Roquet, E. M. Belgsir, J.-M. Léger and C. Lamy, *Electrochim. Acta*, 1994, **39**, 2387.

228 M. Simões, S. Baranton and C. Coutanceau, *Appl. Catal., B*, 2010, **93**, 354.

229 J.-H. Zhang, Y.-J. Liang, N. Li, Z.-Y. Li, C.-W. Xu and S. P. Jiang, *Electrochim. Acta*, 2012, **59**, 156.

230 D. J. Jeffrey and G. A. Camara, *Electrochim. Commun.*, 2010, **12**, 1129.

231 A. Zalineeva, A. Serov, M. Padilla, U. Martinez, K. Artyushkova, S. Baranton, C. Coutanceau and P. B. Atanassov, *J. Am. Chem. Soc.*, 2014, **136**, 3937.

232 <http://www.superiorideas.org/projects/fuel-cells>.

233 (a) L. Zeng, Z. K. Tang and T. S. Zhao, *Appl. Energy*, 2014, **115**, 405; (b) A. M. Bartrom, J. Ta, T. Q. Nguyen, J. Her, A. Donovan and J. L. Haan, *J. Power Sources*, 2013, **229**, 234; (c) A. M. Bartrom and J. L. Haan, *J. Power Sources*, 2012, **214**, 68.

234 (a) R. Pathak and S. Basu, *Electrochim. Acta*, 2013, **113**, 42; (b) J. Chen, C. X. Zhao, M. M. Zhi, K. Wang, L. Deng and G. Xu, *Electrochim. Acta*, 2012, **66**, 133; (c) L. An, T. S. Zhao, S. Y. Shen, Q. X. Wu and R. Chen, *J. Power Sources*, 2011, **196**, 186; (d) N. Fujiwara, S.-I. Yamazaki, Z. Siroma, T. Ioroi, H. Senoh and K. Yasuda, *Electrochim. Commun.*, 2009, **11**, 390.

235 (a) R. Lan and S. W. Tao, *J. Power Sources*, 2011, **196**, 5021; (b) A. N. Rollinson, J. Jones, V. Dupont and M. V. Twigg, *Energy Environ. Sci.*, 2011, **4**, 1216; (c) R. Lan, S. W. Tao and J. T. S. Irvine, *Energy Environ. Sci.*, 2010, **3**, 438.



236 K. Xu, S. J. Lao, H. Y. Qin, B. H. Liu and Z. P. Li, *J. Power Sources*, 2010, **195**, 5606.

237 N. V. Rees and R. G. Compton, *Energy Environ. Sci.*, 2011, **4**, 1255.

238 (a) G. E. Evans and K. V. Kordesch, *Science*, 1967, **158**, 1148; (b) A. Kunugi, Z. Takehara and S. Yoshizawa, *Denki Kagaku*, 1965, **33**, 211; (c) S. Karp and L. Meites, *J. Am. Chem. Soc.*, 1962, **84**, 906.

239 S. Takahashi, S. Higuchi, R. Fujii and Y. Miyake, *Report of Governmental Industrial Research Institute*, Osaka (Japan), 1974, vol. 346.

240 K. Yamada, K. Yasuda, N. Fujiwara, Z. Siroma, H. Tanaka, Y. Miyazaki and T. Kobayashi, *Electrochem. Commun.*, 2003, **5**, 892.

241 K. Asazawa, K. Yamada, H. Tanaka, A. Oka, M. Taniguchi and T. Kobayashi, *Angew. Chem., Int. Ed.*, 2007, **46**, 8024.

242 (a) T. Sakamoto, K. Asazawa, J. Sanabria-Chinchilla, U. Martinez, B. Halevi, P. Antanassov, P. Strasser and H. Tanaka, *J. Power Sources*, 2014, **247**, 605; (b) T. Sakamoto, K. Asazawa, U. Martinez, B. Halevi, T. Susuki, S. Arai, D. Matsumura, Y. Nishihata, P. Atanassov and H. Tanaka, *J. Power Sources*, 2013, **234**, 252.

243 H. Tanaka, K. Asazawa, T. Sakamoto, T. Kato, M. Kai, S. Yamaguchi, K. Yamada and H. Fujikawa, *ECS Trans.*, 2008, **16**, 459.

244 W. X. Yin, Z. P. Li, J. K. Zhu and H. Y. Qin, *J. Power Sources*, 2008, **182**, 520.

245 K. Asazawa, K. Yamada, H. Tanaka, M. Taniguchi and K. Oguro, *J. Power Sources*, 2009, **191**, 362.

246 (a) U. Martinez, K. Asazawa, B. Halevi, A. Falase, B. Kiefer, A. Serov, M. Padilla, T. Olson, A. Datye, H. Tanaka and P. Atanassov, *Phys. Chem. Chem. Phys.*, 2012, **14**, 5512; (b) T. Sakamoto, K. Asazawa, K. Yamada and H. Tanaka, *Catal. Today*, 2011, **164**, 181.

247 G. Karim-Nezhad, R. Jafarloo and P. S. Dorraji, *Electrochim. Acta*, 2009, **54**, 5721.

248 H. Gao, Y. Wang, F. Xiao, C. B. Chung and H. Duan, *J. Phys. Chem. C*, 2012, **116**, 7719.

249 S. J. Lao, H. Y. Qin, L. Q. Ye, B. H. Liu and Z. P. Li, *J. Power Sources*, 2010, **195**, 4135.

250 (a) M. H. M. T. Assumpção, S. G. da Silva, R. F. B. de Souza, G. S. Buzzo, E. V. Spinacé, A. O. Neto and J. C. M. Silva, *Int. J. Hydrogen Energy*, 2014, **39**, 5148; (b) R. Lan, J. T. S. Irvine and S. W. Tao, *Int. J. Hydrogen Energy*, 2012, **37**, 1482; (c) S. Suzuki, H. Muroyama, T. Matsui and K. Eguchi, *J. Power Sources*, 2012, **208**, 257; (d) R. Lan and S. W. Tao, *Electrochim. Solid-State Lett.*, 2010, **13**, B83.

251 K. R. Lee, D. Song, S. B. Park and J.-I. Han, *RSC Adv.*, 2014, **4**, 5638.

252 (a) E. Bertin, C. Roy, S. Garbarino, D. Guay, J. Solla-Gullón, F. J. Vidal-Iglesias and J. M. Feliu, *Electrochem. Commun.*, 2012, **22**, 197; (b) B. K. Boggs and G. G. Botte, *Electrochim. Acta*, 2010, **55**, 5287; (c) K. Yao and Y. F. Cheng, *Int. J. Hydrogen Energy*, 2008, **33**, 6681; (d) L. Zhou, Y. F. Cheng and M. Amrein, *J. Power Sources*, 2008, **177**, 50; (e) F. J. Vidal-Iglesias, J. Solla-Gullón, V. Montiel, J. M. Feliu and A. Aldaz, *J. Power Sources*, 2007, **171**, 448; (f) V. Rosca and M. T. M. Koper, *Phys. Chem. Chem. Phys.*, 2006, **8**, 2513; (g) F. J. Vidal-Iglesias, J. Solla-Gullón, J. M. Feliu, H. Baltruschat and A. Aldaz, *J. Electroanal. Chem.*, 2006, **588**, 331; (h) F. J. Vidal-Iglesias, J. Solla-Gullón, J. M. Pérez and A. Aldaz, *Electrochim. Commun.*, 2006, **8**, 102; (i) K. Endo, Y. Katayama and T. Miura, *Electrochim. Acta*, 2005, **50**, 2181; (j) A. C. A. de Vooys, M. T. M. Koper, R. A. Van Santen and J. A. R. Van Veen, *J. Electroanal. Chem.*, 2001, **506**, 127.

253 W. Peng, L. Xiao, B. Huang, L. Zhuang and J. Lu, *J. Phys. Chem. C*, 2011, **115**, 23050.

254 T. Hejze, J. O. Besenhard, K. Kordesch, M. Cifrain and R. R. Aronsson, *J. Power Sources*, 2008, **176**, 490.

255 R. Halseid, P. J. S. Vie and R. Tunold, *J. Power Sources*, 2006, **154**, 343.

256 T. Lopes, D. S. Kim, Y. S. Kim and F. H. Garzon, *J. Electrochem. Soc.*, 2012, **159**, B265.

257 I. Merino-Jiménez, C. Ponce de León, A. A. Shah and F. C. Walsh, *J. Power Sources*, 2012, **219**, 339.

258 A. Serov, A. Aziznia, P. H. Benhangi, K. Artyushkova, P. Atanassov and E. Gyenge, *J. Mater. Chem. A*, 2013, **1**, 14384.

259 C. Ponce de León, F. C. Walsh, C. J. Patrissi, M. G. Medeiros, R. R. Bessette, R. W. Reeve, J. B. Lakeman, A. Rose and D. Browning, *Electrochim. Commun.*, 2008, **10**, 1610.

260 H. Cheng, K. Scott, K. V. Lovell, J. A. Horsfall and S. C. Waring, *J. Membr. Sci.*, 2007, **288**, 168.

261 (a) B. Šljukić, D. M. F. Santos and C. A. C. Sequeira, *J. Electroanal. Chem.*, 2013, **694**, 77; (b) M. Chatenet, F. Micoud, I. Roche, E. Chainet and J. Vondrák, *Electrochim. Acta*, 2006, **51**, 5452; (c) R. X. Feng, H. Dong, Y. D. Wang, X. P. Ai, Y. L. Cao and H. X. Yang, *Electrochim. Commun.*, 2005, **7**, 449.

262 (a) C. Celik, F. G. Boyaci San and H. I. Sarac, *Int. J. Hydrogen Energy*, 2010, **35**, 8678; (b) R. Jamard, A. Latour, J. Salomon, P. Capron and A. Martinent-Beaumont, *J. Power Sources*, 2008, **176**, 287; (c) U. B. Demirci, *Electrochim. Acta*, 2007, **52**, 5119.

263 B. H. Liu, Z. P. Li, J. K. Zhu and S. Suda, *J. Power Sources*, 2008, **183**, 151.

264 J.-H. Wee, *J. Power Sources*, 2006, **155**, 329.

265 (a) F. H. B. Lima, A. M. Pasqualeti, M. B. M. Concha, M. Chatenet and E. A. Ticianelli, *Electrochim. Acta*, 2012, **84**, 202; (b) M. Chatenet, F. H. B. Lima and E. A. Ticianelli, *J. Electrochim. Soc.*, 2010, **157**, B697; (c) D. A. Finkelstein, N. Da Mota, J. L. Cohen and H. D. Abuña, *J. Phys. Chem. C*, 2009, **13**, 19700.

266 D. A. Finkelstein, C. D. Letcher, D. J. Jones, L. M. Sandberg, D. J. Watts and H. D. Abuña, *J. Phys. Chem. C*, 2013, **117**, 1571.

267 (a) M. H. Atwan, D. O. Northwood and E. L. Gyenge, *Int. J. Hydrogen Energy*, 2007, **32**, 3116; (b) E. Sanli, H. Çelikkan, B. Z. Uysal and M. L. Aksu, *Int. J. Hydrogen Energy*, 2006, **31**, 1920.

268 (a) G. Behmenyar and A. N. Akin, *J. Power Sources*, 2014, **249**, 239; (b) M. Simões, S. Baranton and C. Coutanceau, *J. Phys. Chem. C*, 2009, **113**, 13369.



269 G. Rostamikia and M. J. Janik, *Energy Environ. Sci.*, 2010, **3**, 1262.

270 (a) C.-C. Huang, Y.-L. Liu, W.-H. Pan, C.-M. Chang, C.-M. Shih, H.-Y. Chu, C.-H. Chien, C.-H. Juan and S. J. Lue, *J. Polym. Sci., Part B: Polym. Phys.*, 2013, **51**, 1779; (b) N. Duteanu, G. Vlachogiannopoulos, M. R. Shihhare, E. H. Yu and K. Scott, *J. Appl. Electrochem.*, 2007, **37**, 1085.

271 C. Qu, H. Zhang, F. Zhang and B. Liu, *J. Mater. Chem.*, 2012, **22**, 8203.

272 L. Gu, N. Luo and G. H. Miley, *J. Power Sources*, 2007, **173**, 77.

273 Y. Wang, P. He and H. Zhou, *Energy Environ. Sci.*, 2010, **3**, 1515.

274 X. Yang, Y. Liu, S. Li, X. Wei, L. Wang and Y. Chen, *Sci. Report.*, 2012, **2**, 567.

275 H. Qin, Z. Liu, Y. Guo and Z. Li, *Int. J. Hydrogen Energy*, 2010, **35**, 2868.

276 (a) L. C. Nagle and J. F. Rohan, *J. Electrochem. Soc.*, 2011, **158**, B772; (b) U. B. Demirci and P. Miele, *Energy Environ. Sci.*, 2009, **2**, 627; (c) X.-B. Zhang, J.-M. Yan, S. Han, H. Shioyama, K. Yasuda, N. Kuriyama and Q. Xu, *J. Power Sources*, 2008, **182**, 515; (d) X.-B. Zhang, S. Han, J.-M. Yan, M. Chandra, H. Shioyama, K. Yasuda, N. Kuriyama, T. Kobayashi and Q. Xu, *J. Power Sources*, 2007, **168**, 167; (e) C. Yao, H. Yang, L. Zhuang, X. Ai, Y. Cao and J. Lu, *J. Power Sources*, 2007, **165**, 125.

277 T. B. Marder, *Angew. Chem., Int. Ed.*, 2007, **46**, 8116.

278 X.-B. Zhang, S. Han, J.-M. Yan, H. Shioyama, N. Kuriyama, T. Kobayashi and Q. Xu, *Int. J. Hydrogen Energy*, 2009, **34**, 174.

279 (a) J. A. Vega, S. Smith and W. E. Mustain, *J. Electrochem. Soc.*, 2011, **158**, B349; (b) J. A. Vega, C. Chartier and W. E. Mustain, *J. Power Sources*, 2010, **195**, 7176; (c) J. A. Vega and W. E. Mustain, *Electrochim. Acta*, 2010, **55**, 1638.

280 I. Gunasekara, M. Lee, D. Abbott and S. Mukerjee, *ECS Electrochem. Lett.*, 2012, **1**, F16.

281 (a) B. Connors and B. Ramson, *J. Physiol.*, 1984, **355**, 619; (b) E. Nightingale, *J. Phys. Chem.*, 1959, **63**, 1381.

282 C. M. Lang, K. Kim and P. A. Kohl, *Electrochem. Solid-State Lett.*, 2006, **9**, A545.

283 (a) N. Spinner and W. E. Mustain, *J. Electrochem. Soc.*, 2013, **160**, F1275; (b) N. Spinner and W. E. Mustain, *J. Electrochem. Soc.*, 2012, **159**, E187; (c) J. A. Vega, N. Spinner, M. Catanese and W. E. Mustain, *J. Electrochem. Soc.*, 2012, **159**, B19; (d) J. A. Vega, S. Shrestha, M. Ignatowich and W. E. Mustain, *J. Electrochem. Soc.*, 2012, **159**, B12; (e) H. W. Pennline, E. J. Granite, D. R. Luebke, J. R. Kitchin, J. Landon and L. M. Weiland, *Fuel*, 2010, **89**, 1307.

284 I. Gunasekara, M. Lee, D. Abbott and S. Mukerjee, *ECS Electrochem. Lett.*, 2012, **1**, F16.

285 C. A. Hancock, A. Ong and J. R. Varcoe, *RSC Adv.*, 2014, **4**, 30035.

286 (a) I. Gunasekara, D. Abbott and S. Mukerjee, *Proceedings of the 221st Electrochemical Society Meeting*, Seattle USA, 2012, Abstract 228; (b) M. S. Naughton, F. R. Brushett and P. A. Kenis, *J. Power Sources*, 2011, **196**, 1762.

287 (a) M. Stoukides, *J. Appl. Electrochem.*, 1995, **25**, 899; (b) Y. Amenomiya, V. Birss, M. Goledzinowski, J. Galuszka and A. Sanger, *Catal. Rev.: Sci. Eng.*, 1990, **32**, 163.

288 J. S. Spendelow, J. D. Goodpaster, P. J. A. Kenis and A. Wieckowski, *J. Phys. Chem. B*, 2006, **110**, 9545.

289 (a) S. Mafé and P. Ramírez, *Acta Polym.*, 1997, **48**, 234; (b) P. Ramírez, S. Mafé, J. A. Manzanares and J. Pellicer, *J. Electroanal. Chem.*, 1996, **404**, 187; (c) R. Simons, *J. Membr. Sci.*, 1993, **78**, 13; (d) P. Ramírez, V. M. Aguilera, J. A. Manzanares and S. Mafé, *J. Membr. Sci.*, 1992, **73**, 191; (e) R. Simons, *Electrochim. Acta*, 1985, **30**, 275; (f) R. Simons and G. Khanarian, *J. Membr. Biol.*, 1978, **38**, 11.

290 (a) A. Iizuka, K. Hashimoto, H. Nagasawa, Y. Yanagisawa and A. Yamasaki, *Sep. Purif. Technol.*, 2012, **101**, 49; (b) M. D. Eisaman, L. Alvarado, D. Larner, P. Wang and K. A. Littau, *Energy Environ. Sci.*, 2011, **4**, 4031; (c) M. D. Eisaman, L. Alvarado, D. Larner, P. Wang, B. Garg and K. A. Littau, *Energy Environ. Sci.*, 2011, **4**, 1319.

291 (a) M. Ünlü, J. Zhou and P. A. Kohl, *Angew. Chem., Int. Ed.*, 2010, **49**, 1299; (b) M. Ünlü, J. Zhou and P. A. Kohl, *J. Electrochem. Soc.*, 2010, **157**, B1391; (c) M. Ünlü, J. Zhou and P. A. Kohl, *J. Phys. Chem. C*, 2009, **113**, 11416.

292 M. Ünlü, J. Zhou and P. A. Kohl, *Fuel Cells*, 2010, **10**, 54.

293 (a) I. D. Raistrick, *Electrochim. Acta*, 1990, **35**, 1579; (b) T. E. Springer, T. A. Zawodzinski, M. S. Wilson and S. Gottesfeld, *J. Electrochem. Soc.*, 1996, **143**, 587.

294 J. M. Spurgeon, M. G. Walter, J. Zhou, P. A. Kohl and N. S. Lewis, *Energy Environ. Sci.*, 2011, **4**, 1172.

295 (a) A. Heller, H. J. Lewerenz and B. Miller, *J. Am. Chem. Soc.*, 1981, **103**, 200; (b) M. Szkłarczyk and J. O. M. Bockris, *J. Phys. Chem.*, 1984, **88**, 1808.

296 B. D. Alexander, P. J. Kulesza, L. Rutkowska and J. Augustynski, *J. Mater. Chem.*, 2008, **18**, 2298.

297 A. L. Dicks, *J. Power Sources*, 2006, **156**, 128.

298 (a) J. P. Meyers and R. M. Darling, *J. Electrochem. Soc.*, 2006, **153**, A1432; (b) C. A. Reiser, L. Bregoli, T. W. Patterson, J. S. Yi, J. D. L. Yang, M. L. Perry and T. D. Jarvi, *Electrochim. Solid-State Lett.*, 2005, **8**, A273.

299 W. W. Jacques, *US Pat.*, 555511, 1896.

300 M. L. Perry and T. F. Fuller, *J. Electrochem. Soc.*, 2002, **149**, S59.

301 (a) D. Cao, Y. Sun and G. Wang, *J. Power Sources*, 2007, **167**, 250; (b) S. Zecevic, E. M. Patton and P. Parhami, *Carbon*, 2004, **42**, 1983.

302 K. Tomantschger, R. Findlay, M. Hanson, K. Kordesch and S. Srinivasan, *J. Power Sources*, 1992, **39**, 21.

303 B. K. Kakati, D. Sathiyamoorthy and A. Verma, *Int. J. Hydrogen Energy*, 2010, **35**, 4185.

304 H. Kinoshita, S. Yonezawa, J.-H. Kim, M. Kawai, M. Takashima and T. Tsukatani, *J. Power Sources*, 2008, **183**, 464.

305 (a) F. Bidault, D. J. L. Brett, P. H. Middleton, N. Abson and N. P. Brandon, *Int. J. Hydrogen Energy*, 2010, **35**, 1783; (b) F. Bidault, D. J. L. Brett, P. H. Middleton, N. Abson and N. P. Brandon, *Int. J. Hydrogen Energy*, 2009, **34**, 6799.

306 F. Bidault and A. Kucernak, *J. Power Sources*, 2010, **195**, 2549.



307 (a) A. Kucernak, F. Bidault and G. Smith, *Electrochim. Acta*, 2012, **82**, 284; (b) F. Bidault and A. Kucernak, *J. Power Sources*, 2011, **196**, 4950.

308 S. M. Alia, K. Duong, T. Liu, K. Jensen and Y. Yan, *ChemSusChem*, 2012, **5**, 1619.

309 A. Luzzi, L. Bonadio and M. McCann, in *Pursuit of the Future. 25 years of IEA research towards the realisation of Hydrogen Energy Systems, IEA-HIA Report*, 2004, ISBN 0-9752270-0-9.

310 W. Kreuter and H. Hofmann, *Int. J. Hydrogen Energy*, 1998, **23**, 661.

311 Electrochemical hydrogen technologies, *Electrochemical production and combustion of hydrogen*, ed. H. Wendt, Elsevier, Amsterdam, 1990.

312 S.-E. Jang and H. Kim, *J. Am. Chem. Soc.*, 2010, **132**, 14700.

313 J. R. McKone, S. C. Marinescu, B. S. Brunschwig, J. R. Winkler and H. B. Gray, *Chem. Sci.*, 2014, **5**, 865.

314 P. Millet, F. Andolfatto and R. Durand, *Int. J. Hydrogen Energy*, 1996, **21**, 87.

315 J. W. Vogt, *Materials for electrochemical cell separators*, NASA Report NAS CR72493, NASA Lewis Research Center, 1968.

316 L. H. Baetsle and D. Huys, *J. Inorg. Nucl. Chem.*, 1968, **30**, 639.

317 P. Vermeiren, W. Adriansens, J. P. Moreels and R. Leysen, Hydrogen Power: Theoretical and Engineering Solutions, in *Proceedings of the HYPOTHESIS II Symposium*, ed. T. O. Saetre, Grimstad (Norway), 1997, p. 179.

318 J. Xu, G.-P. Sheng, H.-W. Luo, W.-W. Li, L.-F. Wang and H.-Q. Yu, *Water Res.*, 2012, **46**, 1817.

319 M. B. Rodrigues, A. S. Paleta, J. A. R. Marquez and O. Soalorza, *Int. J. Electrochem. Sci.*, 2009, **4**, 43.

320 D. Pletcher and X. Li, *Int. J. Hydrogen Energy*, 2011, **36**, 15089.

321 V. Bambagioni, M. Bevilacqua, C. Bianchini, J. Filippi, A. Lavacchi, A. Marchionni, F. Vizza and P. K. Shen, *ChemSusChem*, 2010, **3**, 851.

322 S. H. Ahn, B.-S. Lee, I. Choi, S. J. Yoo, H.-J. Kim, E. Cho, D. Henkensmeier, S. W. Nam, S.-K. Kim and J. H. Jang, *Appl. Catal., B*, 2014, **154–155**, 197.

323 Y. Leng, G. Chen, A. J. Mendoza, T. B. Tighe, M. A. Hickner and C.-Y. Wang, *J. Am. Chem. Soc.*, 2012, **134**, 9054.

324 X. Li, F. C. Walsh and D. Pletcher, *Phys. Chem. Chem. Phys.*, 2011, **13**, 1162.

325 D. Pletcher, X. Li and S. Wang, *Int. J. Hydrogen Energy*, 2012, **37**, 7429.

326 X. Wu and K. Scott, *J. Mater. Chem.*, 2011, **21**, 12344.

327 X. Wu and K. Scott, *J. Power Sources*, 2012, **214**, 124.

328 X. Wu and K. Scott, *J. Power Sources*, 2012, **206**, 14.

329 C. C. Pavel, F. Cecconi, C. Emiliani, S. Santiccioli, A. Scaffidi, S. Catanorchi and M. Comotti, *Angew. Chem., Int. Ed.*, 2014, **53**, 1378.

330 L. Xiao, S. Zhang, J. Pan, C. Yan, M. He, L. Zhuang and J. Lu, *Energy Environ. Sci.*, 2012, **5**, 7869.

331 J. Parrondo, C. G. Argos, M. Niedzwiecki, E. B. Anderson, K. E. Ayres and V. Ramani, *RSC Adv.*, 2014, **4**, 9875.

332 F. Miltitsky, B. Myers and A. H. Weisberg, *Energy & Fuels*, 1998, **12**, 56.

333 T. Ioroi, N. Kitazawa, K. Yasuda, Y. Yamamoto and H. Takenaka, *J. Appl. Electrochem.*, 2001, **31**, 1179.

334 P. Hosseini Benhangi, A. Alfantazi and E. Gyenge, *Electrochim. Acta*, 2014, **123**, 42.

335 X. Wu, K. Scott, F. Xie and N. Alford, *J. Power Sources*, 2014, **246**, 225.

336 H. B. Suffredini, J. L. Cerne, F. C. Crnkovic, S. A. S. Machado and L. A. Avaca, *Int. J. Hydrogen Energy*, 2000, **25**, 415.

337 X. Tang, L. Xiao, C. Yang, J. Lu and L. Zhuang, *Int. J. Hydrogen Energy*, 2014, **39**, 3055.

338 W. Hu and J.-Y. Lee, *Int. J. Hydrogen Energy*, 1998, **23**, 253.

339 W.-X. Chen, *Int. J. Hydrogen Energy*, 2001, **26**, 603.

340 A. C. Tavares and S. Trasatti, *Electrochim. Acta*, 2000, **45**, 4195.

341 H. Obayashi and T. Kudo, *Mater. Res. Bull.*, 1978, **13**, 1409.

342 London Metal Exchange, <https://www.lme.com/metals/non-ferrous/nickel/>, accessed 22 November 2013.

343 G. E. Stoner and P. J. Moran, *Proceedings of the Symposium on Industrial Water Electrolysis*, Vancouver, Canada, 1978, p. 169.

344 C. Ballieux, A. Damien and A. Montet, *Int. J. Hydrogen Energy*, 1983, **8**, 529.

345 Batelle Geneva Research Centre Technical Note: Plasma-sprayed inorganic membranes as diaphragms for electrolysis, 1978.

346 A. C. C. Tseung and S. Jasem, *Electrochim. Acta*, 1977, **22**, 31.

347 P. Rasiyah and A. C. C. Tseung, *Adv. Hydrogen Energy*, 1982, **1982(3)**, 383.

348 M. Prigent, L. J. Mas and F. C. Verillon, *Proceedings of the Symposium on Industrial Water Electrolysis*, Vancouver, Canada, 1978, p. 234.

349 V. K. V. P. Srirapu, C. S. Sharma, R. Awasthi, R. N. Singh and A. S. K. Sinha, *Phys. Chem. Chem. Phys.*, 2014, **16**, 7385.

350 H. S. Horowitz, J. M. Longo and H. H. Horowitz, *J. Electrochem. Soc.*, 1983, **130**, 1851.

351 A. Simon, T. Fujioka, W. E. Price and L. D. Nghiem, *Sep. Purif. Technol.*, 2014, **127**, 70.

352 W. E. Mustain, N. S. Spinner and J. A. Vega, WIPO Pat. Application WO/2012/061728, submitted November 2011.

353 (a) M. Aresta, A. Dibenedetto and A. Angelini, *Chem. Rev.*, 2014, **114**, 1709; (b) A. Goeppert, M. Czaun, G. K. S. Prakash and G. A. Olah, *Energy Environ. Sci.*, 2012, **5**, 7833; (c) M. Mikkelsen, M. Jørgensen and F. C. Krebs, *Energy Environ. Sci.*, 2010, **3**, 43; (d) <http://co2chem.co.uk/>, accessed 4 October 2013.

354 H. He, W. Li, M. Zhong, D. Konkolewicz, D. Wu, K. Yaccato, T. Rappold, G. Sugar, N. E. David and K. Matyjaszewski, *Energy Environ. Sci.*, 2013, **6**, 488.

355 (a) E. V. Kondratenko, G. Mul, J. Baltrusaitis, G. O. Larrazábal and J. Pérez-Ramírez, *Energy Environ. Sci.*, 2013, **6**, 3112; (b) C. Coestentin, M. Robert and J.-M. Savéant, *Chem. Soc. Rev.*, 2013, **42**, 2423; N. S. Spinner, J. A. Vega and W. E. Mustain, *Catal. Sci. Technol.*, 2012, **2**, 19.

356 <http://www.eon.com/en/media/news-detail.jsp?id=10738&year=2011>.



357 <http://theotcinvestor.com/mantra-venture-group-mvtg-moves-to-commercialize-carbon-dioxide-reduction-technology-1196/>.

358 H.-R. Jhong, S. Ma and P. J. A. Kenis, *Curr. Opin. Chem. Eng.*, 2013, **2**, 191.

359 K. P. Kuhl, E. R. Cave, D. N. Abram and T. F. Jamamillo, *Energy Environ. Sci.*, 2012, **5**, 7050.

360 C. W. Li, J. Ciston and M. W. Kanan, *Nature*, 2014, **508**, 504.

361 (a) E. Ruiz-Trejo and J. T. S. Irvine, *Solid State Ionics*, 2013, **252**, 157; (b) K. Xie, Y. Zhang, G. Meng and J. T. S. Irvine, *Energy Environ. Sci.*, 2011, **4**, 2218.

362 M. A. Rahman, X. Wang and C. Wen, *J. Electrochem. Soc.*, 2013, **160**, A1759.

363 Q. Wu, L. Jiang, L. Qi, L. Yuan, E. Wang and G. Sun, *Electrochim. Acta*, 2014, **123**, 167.

364 A. A. Mohamad, N. S. Mohamed, M. Z. A. Yahya, R. Othman, S. Ramesh, Y. Alias and A. K. Arof, *Solid State Ionics*, 2003, **156**, 171.

365 http://bestar.lbl.gov/bli5/files/2012/06/Imanishi_session3.pdf, accessed 22 January 2014.

366 (a) N. Vassal, E. Salmon and J. F. Fauvarque, *Electrochim. Acta*, 2000, **45**, 1527; (b) S. Guinot, E. Salmon, J. F. Penneau and J. F. Fauvarque, *Electrochim. Acta*, 1998, **43**, 1163; (c) J. F. Fauvarque, S. Guinot, N. Bouzir, E. Salmon and J. F. Penneau, *Electrochim. Acta*, 1995, **40**, 2449.

367 (a) C.-C. Yang, S.-J. Lin and S.-T. Hsu, *J. Power Sources*, 2003, **122**, 210; (b) C.-C. Yang, *J. Power Sources*, 2002, **109**, 22.

368 Z. Zhang, C. Zuo, Z. Liu, Y. Yu, Y. Zuo and Y. Song, *J. Power Sources*, 2014, **251**, 470.

369 N. Fujiwara, M. Yao, Z. Siroma, H. Senoh, T. Ioroi and K. Yasuda, *J. Power Sources*, 2011, **196**, 808.

370 P. Alotto, M. Guarnieri and F. Moro, *Renewable Sustainable Energy Rev.*, 2014, **29**, 325.

371 A. Z. Weber, M. M. Mench, J. P. Meyers, P. N. Ross, J. T. Gostick and Q. H. Liu, *J. Appl. Electrochem.*, 2011, **41**, 1137.

372 S. C. Chieng, M. Kazacos and M. Skyllas-Kazacos, *J. Membr. Sci.*, 1992, **75**, 81.

373 (a) D.-H. Kim, S.-J. Seo, M.-J. Lee, J.-S. Park, S.-H. Moon, Y. S. Kang, Y.-W. Choi and M.-S. Kang, *J. Membr. Sci.*, 2014, **454**, 44; (b) S. Maurya, S.-H. Shin, K.-W. Sung and S.-H. Moon, *J. Power Sources*, 2014, **255**, 325; (c) A. A. Shinkle, A. E. S. Sleightholme, L. D. Griffith, L. T. Thompson and C. W. Monroe, *J. Power Sources*, 2012, **206**, 490.

374 Q. Luo, L. Li, W. Wang, Z. Nie, X. Wei, B. Li, B. Chen, Z. Yang and V. Sprenkle, *ChemSusChem*, 2013, **6**, 268.

375 (a) D. Chen and M. A. Hickner, *Phys. Chem. Chem. Phys.*, 2013, **15**, 11299; (b) S. Kim, T. Tighe, B. Schwenzler, J. Yan, J. Zhang, J. Liu, Z. Yang and M. A. Hickner, *J. Appl. Electrochem.*, 2011, **41**, 1201.

376 D. Chen, S. Kim, L. Li, G. Yang and M. A. Hickner, *RSC Adv.*, 2012, **2**, 8087.

377 M. S. J. Jung, J. Parrondo, C. G. Arges and V. Ramani, *J. Mater. Chem. A*, 2013, **1**, 10458.

378 K. D. Kreuer, *J. Membr. Sci.*, 2001, **185**, 29.

379 (a) B. Pivovar, Y. Yang and E. L. Cussler, *J. Membr. Sci.*, 1999, **154**, 155; (b) M. A. Hickner and B. Pivovar, *Fuel Cells*, 2005, **5**, 213.

380 D. Chen, S. Kim, V. Sprenkle and M. A. Hickner, *J. Power Sources*, 2013, **231**, 301.

381 D. Chen, M. A. Hickner, E. Agar and E. C. Kumbur, *Electrochim. Commun.*, 2013, **26**, 37.

382 S.-G. Park, N.-S. Kwak, C. W. Hwang, H.-M. Park and T. S. Hwang, *J. Membr. Sci.*, 2012, **423**, 429.

383 S.-J. Seo, B.-C. Kim, K.-W. Sung, J. Shim, J.-D. Jeon, K.-H. Shin, S.-H. Shin, S.-H. Yun, J.-Y. Lee and S.-H. Moon, *J. Membr. Sci.*, 2013, **428**, 17.

384 D. Chen, M. A. Hickner, E. Agar and E. C. Kumbur, *ACS Appl. Mater. Interfaces*, 2013, **5**, 7559.

385 D. Chen, M. A. Hickner, E. Agar and E. C. Kumbur, *J. Membr. Sci.*, 2013, **437**, 108.

386 (a) C. W. Hwang, H.-M. Park, C. M. Oh, T. S. Hwang, J. Shim and C.-S. Jin, *J. Membr. Sci.*, 2014, **468**, 98; (b) F. Zhang, H. Zhang and C. Qu, *ChemSusChem*, 2013, **6**, 2290; (c) S. H. Zhang, B. G. Zhang, D. B. Xing and X. G. Jian, *J. Mater. Chem. A*, 2013, **1**, 12246; (d) J. Y. Qiu, M. Y. Li, J. F. Ni, M. L. Zhai, J. Peng, L. Xu, H. H. Zhou, J. Q. Li and G. S. Wei, *J. Membr. Sci.*, 2007, **297**, 174; (e) G. J. Hwang and H. Ohya, *J. Membr. Sci.*, 1997, **132**, 55; (f) T. Mohammadi and M. Skyllas-Kazacos, *J. Power Sources*, 1996, **63**, 179.

387 (a) J. Fang, H. Xu, X. Wei, M. Guo, X. Lu, C. Lan, Y. Zhang, Y. Liu and T. Peng, *Polym. Adv. Technol.*, 2013, **24**, 168; (b) Y. Wang, J. Qiu, J. Peng, L. Xu, J. Li and M. Zhai, *J. Membr. Sci.*, 2011, **376**, 70.

388 (a) S. Zhang, B. Zhang, G. Zhao and X. Jian, *J. Mater. Chem. A*, 2014, **2**, 3083; (b) S.-G. Park, N.-S. Kwak, C. W. Hwang, H.-M. Park and T. S. Hwang, *J. Membr. Sci.*, 2012, **423**, 429; (c) F. Zhang, H. Zhang and C. Qu, *J. Phys. Chem. B*, 2012, **116**, 9016; (d) S. Zhang, C. Yin, D. Xing, D. Yang and X. Kiang, *J. Membr. Sci.*, 2010, **363**, 243.

389 D. S. Aaron, Q. Liu, Z. Tang, G. M. Grim, A. B. Papandrew, A. Turhan, T. A. Zawodzinski and M. M. Mench, *J. Power Sources*, 2012, **206**, 450.

390 S. Yun, J. Parrondo and V. Ramani, *J. Mater. Chem. A*, 2014, **2**, 6605.

391 G. L. Wick and W. R. Schmitt, *Mar. Technol. Soc. J.*, 1977, **11**, 16.

392 J. W. Post, J. Veerman, H. V. M. Hamelers, G. J. W. Euverink, S. J. Metz, K. Nijmeijer and C. J. N. Buisman, *J. Membr. Sci.*, 2007, **288**, 218.

393 S. Loeb, *J. Membr. Sci.*, 1976, **1**, 49.

394 R. E. Pattle, *Nature*, 1954, **174**, 660.

395 D. A. Vermaas, S. Bajracharya, B. B. Sales, M. Saakes, B. Hamelers and K. Nijmeijer, *Energy Environ. Sci.*, 2013, **6**, 643.

396 J. N. Wiesenfeld and F. B. Leitz, *Science*, 1976, **191**, 557.

397 R. E. Lacey, *Ocean Eng.*, 1980, **7**, 1.

398 R. Audino, *J. Power Sources*, 1983, **10**, 203.

399 P. Długołęcki, A. Gambier, K. Nijmeijer and M. Wessling, *Environ. Sci. Technol.*, 2009, **43**, 6888.





400 J. W. Post, H. V. M. Hamelers and C. J. N. Buisman, *Environ. Sci. Technol.*, 2008, **42**, 5785.

401 J. Veerman, M. Saakes, S. J. Metz and G. J. Harmsen, *J. Membr. Sci.*, 2009, **327**, 136.

402 M. Turek and B. Bandura, *Desalination*, 2007, **205**, 67.

403 (a) G. M. Geise, M. A. Hickner and B. E. Logan, *ACS Macro Lett.*, 2013, **2**, 814; (b) M. C. Hatzell and B. E. Logan, *J. Membr. Sci.*, 2013, **446**, 449; (c) X. Luo, X. Cao, Y. Mo, K. Xiao, X. Zhang, P. Liang and X. Huang, *Electrochem. Commun.*, 2012, **19**, 25.

404 E. Brauns, *Desalin. Water Treat.*, 2010, **13**, 53.

405 W. Li, B. Krantz, E. R. Cornelissen, J. W. Post, A. R. D. Verliefde and C. Y. Tang, *Appl. Energ.*, 2013, **104**, 592.

406 J. Veerman, R. M. de Jong, M. Saakes, S. J. Metz and G. J. Harmsen, *J. Membr. Sci.*, 2009, **343**, 7.

407 M. C. Hatzell, I. Ivanov, R. D. Cusick, X. Zhu and B. E. Logan, *Phys. Chem. Chem. Phys.*, 2014, **16**, 1632.

408 P. Długołęcki, K. Nijmeijer, S. Metz and M. Wessling, *J. Membr. Sci.*, 2008, **319**, 214.

409 E. Güler, R. Elizen, D. Vermaas, M. Saakes and K. Nijmeijer, *J. Membr. Sci.*, 2013, **446**, 266.

410 E. Güler, Y. Zhang, M. Saakes and K. Nijmeijer, *ChemSusChem*, 2012, **5**, 2262.

411 G. M. Geise, M. A. Hickner and B. E. Logan, *ACS Appl. Mater. Interf.*, 2013, **5**, 10294.

412 K. Kwon, S. J. Lee, L. Li, C. Han and D. Kim, *Int. J. Energ. Res.*, 2013, **38**, 530.

413 P. Długołęcki, J. Dąbrowska, K. Nijmeijer and M. Wessling, *J. Membr. Sci.*, 2010, **347**, 101.

414 D. A. Vermaas, M. Saakes and K. Nijmeijer, *J. Membr. Sci.*, 2011, **385–386**, 234.

415 E. Güler, R. Elizen, M. Saakes and K. Nijmeijer, *J. Membr. Sci.*, 2014, **455**, 254.

416 E. Güler, R. Elizen, M. Saakes and K. Nijmeijer, *J. Membr. Sci.*, 2014, **458**, 136.

417 J. W. Post, H. V. M. Hamelers and C. J. N. Buisman, *J. Membr. Sci.*, 2009, **330**, 65.

418 D. A. Vermaas, J. Veerman, M. Saakes and K. Nijmeijer, *Energy Environ. Sci.*, 2014, **7**, 1434.

419 D. A. Vermaas, D. Kunteng, M. Saakes and K. Nijmeijer, *Water Res.*, 2013, **47**, 1289.

420 D. A. Vermaas, D. Kunteng, J. Veerman, M. Saakes and K. Nijmeijer, *Environ. Sci. Technol.*, 2014, **48**, 3065.

421 E. Guler, W. van Baak, M. Saakes and K. Nijmeijer, *J. Membr. Sci.*, 2014, **455**, 254.

422 (a) X. Zhang, F. Zhu, L. Chen, Q. Zhao and G. Tao, *Bioresour. Technol.*, 2013, **146**, 161; (b) I. Singh and A. Chandra, *Bioresour. Technol.*, 2013, **142**, 77; (c) X. Xia, J. C. Tokash, F. Zhang, P. Liang, X. Huang and B. E. Logan, *Environ. Sci. Technol.*, 2013, **47**, 2085; (d) X. Zhang, J. Shi, P. Liang, J. Wei, X. Huang, C. Zhang and B. E. Logan, *Bioresour. Technol.*, 2013, **142**, 109; (e) J. M. Gohil and D. G. Karamanov, *J. Power Sources*, 2013, **243**, 603; (f) Y. Ahn and B. E. Logan, *Bioresour. Technol.*, 2013, **132**, 436; (g) S. Haddadi, E. Elbeshbishi and H.-S. Lee, *Bioresour. Technol.*, 2013, **142**, 562; (h) E. Mahendiravarman and D. Sangeetha, *Int. J. Hydrogen Energy*, 2013, **38**, 2471; (i) S. Pandit, S. Ghosh, M. M. Ghangrekar and D. Das, *Int. J. Hydrogen Energy*, 2012, **37**, 9383; (j) S. Pandit, A. Sengupta, S. Kale and D. Das, *Bioresour. Technol.*, 2011, **102**, 2736; (k) E. Ji, H. Moon, J. Piao, P. T. Ha, J. An, D. Kim, J.-J. Woo, Y. Lee, S.-H. Moon, B. E. Rittmann and I. S. Chang, *Biosens. Bioelectron.*, 2011, **26**, 3266; (l) X. Zhang, S. Cheng, X. Huang and B. E. Logan, *Biosens. Bioelectron.*, 2010, **25**, 1825; (m) L. Zhuang, C. Feng, S. Zhou, Y. Li and Y. Wang, *Process Biochem.*, 2010, **45**, 929; (n) Y. Mo, P. Liang, X. Huang, H. Wang and X. Cao, *J. Chem. Technol. Biotechnol.*, 2009, **84**, 1767; (o) G. la O'gerardo, J. J. Walish and E. J. Crumlin, US Pat. Application 2009/0087690 A1, 2009; (p) Y. Zuo, S. Cheng and B. E. Logan, *Environ. Sci. Technol.*, 2008, **42**, 6967; (q) J. R. Kim, S. Cheng, S.-E. Oh and B. E. Logan, *Environ. Sci. Technol.*, 2007, **41**, 1004; also reviews in ref. 6 above.

423 H. Wang and Z. J. Ren, *Biotechnol. Adv.*, 2013, **31**, 1796.

424 (a) B. E. Logan and K. Rabaey, *Science*, 2012, **337**, 686; (b) O. Lefebvre, A. Uzabiaga, I. S. Chang, B.-H. Kim and H. Y. Ng, *Appl. Microbiol. Biotechnol.*, 2011, **89**, 259; (c) Y. Qiao, S.-J. Bao and C. M. Li, *Energy Environ. Sci.*, 2010, **3**, 544; (d) D. R. Lovley, *Nat. Rev. Microbiol.*, 2006, **4**, 497.

425 K. B. Liew, W. R. W. Daud, M. Ghasemi, J. X. Leong, S. S. Lim and M. Ismail, *Int. J. Hydrogen Energy*, 2014, **39**, 4870.

426 (a) E. Martin, B. Tartakovsky and O. Savadogo, *Electrochim. Acta*, 2011, **58**, 58; (b) M. Lu, S. Kharkwal, H. Y. Ng and S. F. Y. Li, *Biosens. Bioelectron.*, 2011, **26**, 4728; (c) I. Roche and K. Scott, *J. Appl. Electrochem.*, 2009, **39**, 197.

427 (a) X. Shi, Y. Feng, X. Wang, H. Lee, J. Liu, Y. Qu, W. He, S. M. S. Kumar and N. Ren, *Bioresour. Technol.*, 2012, **108**, 89; (b) B. Erable, N. Duteanu, S. M. S. Kumar, Y. Feng, M. M. Ghangrekar and K. Scott, *Electrochim. Commun.*, 2009, **11**, 1547.

428 (a) C. Wu, X. Liu, W. Li, G. Sheng, G. Zang, Y. Cheng, N. Shen, Y. Yang and H. Yu, *Appl. Energy*, 2012, **98**, 594; (b) O. Schaetzle, F. Barrière and U. Schröder, *Energy Environ. Sci.*, 2009, **2**, 96.

429 X. Cao, X. Huang, P. Liang, N. Boon, M. Fan, L. Zhang and X. Zhang, *Energy Environ. Sci.*, 2009, **2**, 498.

430 Y. Zhang and I. Angelidaki, *Water Res.*, 2014, **56**, 11.

431 (a) J. An and H.-S. Lee, *RSC Adv.*, 2013, **3**, 14021; (b) E. Ribot-Llobet, J.-Y. Nam, J. C. Tokash, A. Guisasola and B. E. Logan, *Int. J. Hydrogen Energy*, 2013, **38**, 2951; (c) T. H. J. A. Sleutels, H. V. M. Hamelers, R. A. Rozendal and C. J. N. Buisman, *Int. J. Hydrogen Energy*, 2009, **34**, 3612; (d) S. Cheng and B. E. Logan, *Proc. Natl. Acad. Sci. U. S. A.*, 2007, **104**, 18871.

432 Y. Kim and B. E. Logan, *Desalination*, 2013, **308**, 122.

433 (a) K. Zuo, L. Yuan, J. Wei, P. Liang and X. Huang, *Bioresour. Technol.*, 2013, **146**, 637; (b) Y. Qu, Y. Feng, J. Liu, X. Shi, Q. Yang, J. Lv and B. E. Logan, *Desalination*, 2013, **317**, 17; (c) Q. Ping and Z. He, *Bioresour. Technol.*, 2013, **144**, 304; (d) Q. Ping, B. Cohen, C. Dosoretz and Z. He, *Desalination*, 2013, **325**, 48; (e) B. Zhang and Z. He, *J. Membr. Sci.*, 2013, **441**, 18; (f) K. S. Brastad and Z. He,

Desalination, 2013, **309**, 32; (g) H. Luo, P. Xu, P. E. Jenkins and Z. Ren, *J. Membr. Sci.*, 2012, **409–410**, 16; (h) K. S. Jacobson, D. M. Drew and Z. He, *Environ. Sci. Technol.*, 2011, **45**, 4652; (i) S. Chen, G. Liu, R. Zhang, B. Qin and Y. Luo, *Environ. Sci. Technol.*, 2012, **46**, 2467; (j) Y. Qu, Y. Feng, X. Wang, J. Liu, J. Lv, W. He and B. E. Logan, *Bioresour. Technol.*, 2012, **106**, 89; (k) X. Chen, X. Xia, P. Liang, X. Cao, H. Sun and X. Huang, *Environ. Sci. Technol.*, 2011, **45**, 2465; (l) M. Mehanna, P. D. Kiely, D. F. Call and B. E. Logan, *Environ. Sci. Technol.*, 2010, **44**, 9578; (m) M. Mehanna, T. Saito, J. Yan, M. Hickner, X. Cao, X. Huang and B. E. Logan, *Energy Environ. Sci.*, 2010, **3**, 1114; (n) X. Cao, X. Huang, P. Liang, K. Xiao, Y. Zhou, X. Zhang and B. E. Logan, *Environ. Sci. Technol.*, 2009, **43**, 7148; also ref. 5a above.

434 C. M. Werner, B. E. Logan, P. E. Saikaly and G. L. Amy, *J. Membr. Sci.*, 2013, **428**, 116.

435 (a) R. D. Cusick, M. Hatzell, F. Zhang and B. E. Logan, *Environ. Sci. Technol.*, 2013, **47**, 14518; (b) X. Luo, J.-Y. Nam, F. Zhang, X. Zhang, P. Liang, X. Huang and B. E. Logan, *Bioresour. Technol.*, 2013, **140**, 399; (c) X. Zhu, M. C. Hatzell, R. D. Cusick and B. E. Logan, *Electrochem. Commun.*, 2013, **31**, 52; (d) R. D. Cusick, Y. Kim and B. E. Logan, *Science*, 2012, **335**, 1474; (e) Y. Kim and B. E. Logan, *Environ. Sci. Technol.*, 2011, **45**, 5834; (f) Y. Kim and B. E. Logan, *Proc. Natl. Acad. Sci. U. S. A.*, 2011, **108**, 16176; also ref. 5a above.

436 (a) T. Zhang, H. Nie, T. S. Bain, H. Lu, M. Cui, O. L. Snoeyenbos-West, A. E. Franks, K. P. Nevin, T. P. Russell and D. R. Lovley, *Energy Environ. Sci.*, 2013, **6**, 217; (b) Y. Gong, A. Ebrahim, A. M. Feist, M. Embree, T. Zhang, D. Lovley and K. Zengler, *Environ. Sci. Technol.*, 2013, **47**, 568; (c) S. Pandit, B. K. Nayak and D. Das, *Bioresour. Technol.*, 2012, **107**, 97.

437 H. Li and J. C. Liao, *Energy Environ. Sci.*, 2013, **6**, 2892.

438 (a) X. Zhu and B. E. Logan, *Bioresour. Technol.*, 2014, **159**, 24; (b) X. Zhu, M. C. Hatzell and B. E. Logan, *Environ. Sci. Technol. Lett.*, 2014, **1**, 231.

